PROCEEDINGS OF THE 24TH INTERNATIONAL APPLIED GEOCHEMISTRY SYMPOSIUM

FREDERICTON, NEW BRUNSWICK, CANADA

JUNE 1ST-4TH, 2009

EDITED BY

DAVID R. LENTZ, KATHLEEN G. THORNE, & KRISTY-LEE BEAL

VOLUME II

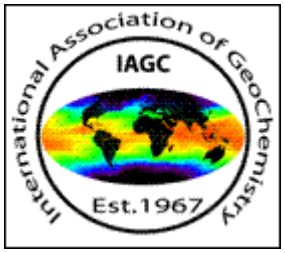

ISBN 978-1-55131-137-1 (Volume 2)

PROCEEDINGS OF THE 24TH INTERNATIONAL APPLIED GEOCHEMISTRY SYMPOSIUM

FREDERICTON, NEW BRUNSWICK
CANADA
JUNE 1ST-4TH, 2009

EDITED BY

DAVID R. LENTZ
KATHLEEN G. THORNE
KRISTY-LEE BEAL

VOLUME II

TABLE OF CONTENTS (VOLUME II)

TECHNICAL EDITORS

(Listed in alphabetical order)

Mark Arundell
U. Aswathanarayana
Roger Beckie
Chris Benn
Robert Bowell
Charles Butt
Bill Coker
Hugh deSouza
Sara Fortner
David Gladwell
Wayne Goodfellow
Eric Grunsky
William Gunter
Gwendy Hall
Jacob Hanley
Russell Harmon
David Heberlein
Brian Hitchon
Andrew Kerr
Dan Kontak
Kurt Kyser
David Lentz
Ray Lett
Matthew Leybourne
Steven McCutcheon
Beth McClenaghan
Nancy McMillan
Paul Morris
Lee Ann Munk
Dogan Paktunc
Roger Paulen
Ernie Perkins
David Quirt
Andy Rencz
David Smith
Cliff Stanley
Gerry Stanley
Nick Susak
Bruce Taylor
Ed Van Hees
James Walker
Lawrence Winter

APPLIED AQUEOUS GEOCHEMISTRY

EDITED BY:

DAVE GLADWELL
RAY LETT
ROGER BECKIE

Application of calcite precipitation rate in predicting the utilization period of calcite scale affected wells, Philippines

Gabriel M. Aragon[1], Benson G. Sambrano[1], & James B. Nogara[1]
[1]*Energy Development Corporation, Merritt Road, Fort Bonifacio, Makati City, Taguig PHILIPPINES*
(e-mail: aragon.gm@energy.com.ph)

ABSTRACT: The empirically determined precipitation rate law was applied to calculate the utilization period of calcite scale affected wells where pipe geometry and varying boiling temperatures were considered. The results using the empirical precipitation rate law method showed extended utilization periods for saturation ratio (Q/K) less than or equal to 1.72, and shorter utilization periods for saturation ratios above 1.72 compared to the direct deposition of excess calcite method. The applicability of the calcite precipitation rate law method in predicting the utilization period of the calciting wells depends on the determination of the actual flash point temperature and calibration of the empirical equation to the field observations. The empirical equation was derived under laboratory conditions using stirred reactor tanks at 100°C and extrapolated to higher temperatures. The laboratory test set-up is perceived to be an approximation and does not mimic the complexity of the flow regime observed in geothermal wells. Information on the utilization period of calciting wells derived from the modified rate law method will assist in a refined evaluation of steam availability from geothermal fields as well as providing a well maintenance schedule.

KEYWORDS: *precipitation rate, calciting, saturation ratio, boiling temperatures, Mindanao Geothermal Production field*

INTRODUCTION

The majority of available speciation software only reveals the characteristics of the geothermal fluids in terms of degree of saturation with respect to calcite. This does not directly translate into the duration during which the well will sustain the discharge. The utilization period of calciting wells can be derived from the discharge history, assuming that the well has had stable chemistry. Variations of the utilization period through time is expected because of geothermal reservoirs are very dynamic due to the effects of mass extraction and injection, which particularly affects the fluid chemistry.

The initial methodology used assumed that all excess calcite from the solution would be deposited in a predetermined volume of the geothermal pipe. This approach is conservative considering that calcite deposition is an instantaneous process. However, the literature frequently states that calcite deposition is kinetically-controlled where the process of deposition could either be slower or faster (Sjöberg & Rickard 1984; Compton & Unwin 1990; Lebron 1996; Shiraki & Brantley 1995) developed a precipitation rate equation for high salinity fluid in laboratory conditions at a temperature of 100°C using a reactor tank. This was modified through extrapolation to extend the application up to 300°C and currently used in the program code of *FRACHEM* (Andre *et al*. 2006).

This paper evaluates the applicability of the modified precipitation rate equation in predicting the discharge duration of a calciting well compared to the observed utilization history and the results of the conservative method from direct deposition of excess calcite. Three wells in Mindanao Geothermal Production Field (MGPF) with documented output decline due to calcite deposition were studied, namely APO1D, SP4D, and MD1D.

THE GEOTHERMAL FIELD

The Mindanao Geothermal Production Field (MGPF), with an area of ~30 sq km, is situated on the northwest flanks of Mt.

Apo volcano located in the southwestern part of Mindanao Island (Fig. 1). Commercial exploitation of the field started in March 1997 with commissioning of the 52-MWe Mindanao-1 geothermal power plant (M1). An additional 52-MWe power plant (M2) commissioned in June 1999 increased the total capacity to 104 MWe. Each power plant requires a minimum energy off-take at the end of the year. This necessitates an updated total steam availability of the field and realistic forecast to ensure realization of steam production. The unexpected drop in output in the calcite-affected wells upset the steam availability of the field and required immediate well intervention utilizing a drilling rig to regain the initial capacity.

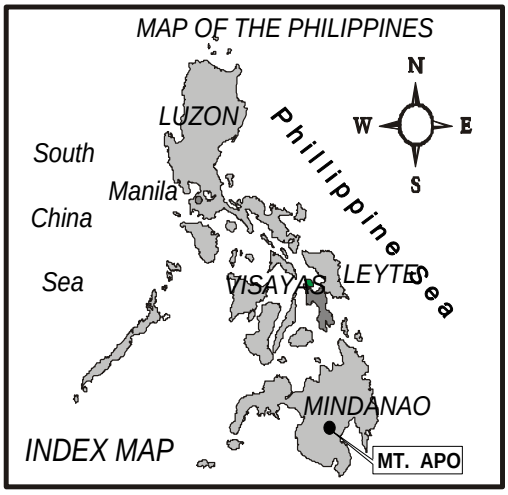

Fig. 1. Philippine map showing the location of the project sites

PRECIPITATION RATE

The general rate law equation is given by:

$$Rate = Kp(\Omega - 1)^n A_{kgw} \quad (1)$$

where:

- Rate – precipitation rate, mole/kgw-s
- Kp – rate contant, mole/m^2-s
- Ω - saturation ratio (Q/K)
- A_{kgw} – surface area for deposition per kilogram water
- n – empirically determined

The following equations are derived from Eq. 1 depending on the saturation levels (Q/K) which is modified to include higher temperature range:

For Q/K < 1.72:

$$R_p = 1.927x10^{-2} T \exp^{\left(\frac{-41840}{RT}\right)} A_{kgw}\left(\frac{Q}{K} - 1\right)^{1.93} \quad (2)$$

For Q/K > 1.72:

$$R_p = 1.011T \exp^{\left(\frac{-41840}{RT}\right)} A_{kgw} \exp\left(\frac{-2.36}{\ln\left(\frac{Q}{K}\right)}\right) \quad (3)$$

where:

- R – 8.315 J/mol-K
- T – Temperature in Kelvin
- Q/K – Saturation ratio taken from *WATCHWORKS*
- A_{kgw} – Surface area for deposition per kilogram water in m2
- R_p – Precipitation rate, mole/Kgw-s

The following are the assumptions made in applying the precipitation rate equation:

- Deposition occurred at boiling point
- The fluid is supersaturated with calcite mineral
- Complete adhesion of the calcite mineral on the inner wall of the pipe
- Moderate flow in the pipe to mimic the stirring experiment

The last two assumptions may not be true under actual well conditions, where instantaneous boiling and turbulent flow in the pipe occur. However, these conditions do not allow certain calcite crystals to deposit immediately and fractions may be removed by the fluid.

RESULTS AND DISCUSSION

Fluid Chemistry

The Ca^{2+} concentration of the wells range between 87 to 211 mg/L at different boiling temperatures and near neutral to slightly alkaline pH is comparable to the quartz reservoir temperature. For instance, APO1D had the lowest reservoir temperature at 228°C had the highest calcium value of 211 mg/L among the three. This is followed by SP4D with a temperature of 236°C and Ca^{2+} value of 139 mg/L while the hottest well MD1D with reservoir temperature of 270°C has the lowest Ca^{2+} value of 87 mg/L. Except for MD1D, the wells at reservoir condition are almost saturated with respect to calcite, while the residual liquid becomes oversaturated following boiling as the

liquid flows to the well bore due to the pressure difference. This boiling process as a triggering mechanism for calcite formation is proven in the depths of the calcite minerals. The majority of the calcite blockages were found at flash point depths of the production wells.

Utilization Rate

Well APO1D

The utilization periods for APO1D given by the direct deposition of the excess calcite method has a minimum of 1 month and maximum of 6 months as shown in Fig. 2. It should be noted that the calcite precipitation rate equation at a saturation ratio above 1.72 provided shorter utilization time than the direct deposition method, indicating that the rate law overestimated the amount of calcite deposited. At a saturation ratio below 1.72, however, the rate law indicated a longer utilization period, which was expected since the calcite deposition is kinetically controlled rather than instantaneous deposition of the excess calcite.

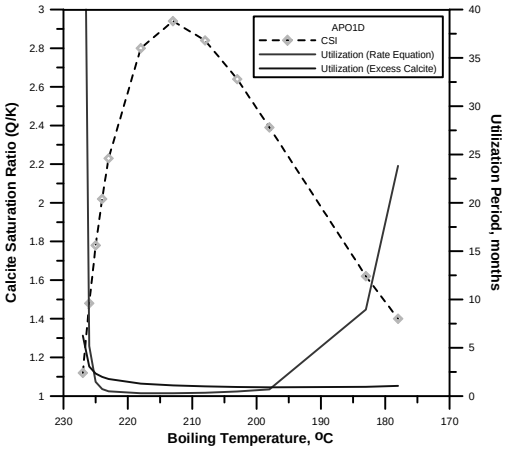

Fig. 2. APO1D saturation radio and utilization periods at different boiling temperatures.

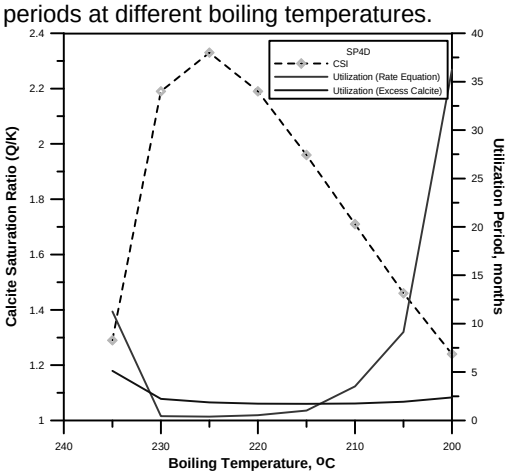

Fig. 3. SP4D saturation ratio and utilization periods at different boiling temperatures.

Well SP4D

The actual utilization period of the well prior to maintenance ranged from 10 to 15 months. Using the calcite precipitation rate equation, the utilization period indicated 235°C as the first boiling temperature coinciding to a period of 11 months (Fig. 3). Again the 205°C was not considered here since it occurred at the surface pipeline and the calcite blockages were found in the production liner. The equivalent utilization period for the direct deposition of excess calcite at this condition is only 5 months. The simulated flash temperature of SP4D is 234°C which is comparable to actual and calculated utilization periods. Similar to APO1D, the calculated utilization periods for saturation ratio above 1.72 indicated shorter duration than the direct deposition of excess calcite.

Well MD1D

This well has no saturation values obtained below 1.72. Thus the utilization period based on precipitation rate (Eq. 1) consistently resulted in a short utilization (maximum of 15 days) compared to the utilization from direct deposition of excess calcite (maximum 6 months). Based on the last maintenance, the actual utilization period of the well is almost 6 months. This actual utilization period corresponded to the value from the direct deposition of excess calcite at the boiling temperature of 270°C.

Notably, well MD1D has high calcite saturation values and yet produces for longer than the calculated utilization periods than APO1D and SP4D using the direct deposition method (Fig. 4). This can be attributed to the lower equilibrium constant of calcite at higher temperatures. Thus, despite the inherently lower calcium

concentration of MD1D, the well has a high degree of saturation.

CONCLUSIONS

(1) The precipitation rate (Eq. 1) indicates comparable values for utilization period at calcite saturation ratio below 1.72 since the results are closer to the observed

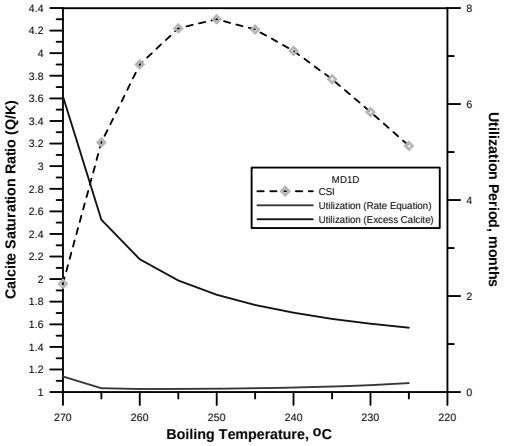

Fig. 4. MD1D saturation ratio and utilization periods at different boiling temperatures.

utilization period.

(2) The calcite precipitation rate (Eq. 1) should be further refined by calibrating the equation to the field condition particularly for saturation ratio above 1.72.

(3) The calcite saturation ratio is more responsive with regards to detecting the onset of calcite deposition through the sudden shift of the saturation ratio from consistently > 1 to < 1.

(4) The direct deposition of excess calcite method should be used in predicting the utilization period in cases where the flash point temperature of the well is known and the saturation ratio at this condition is above 1.72.

ACKNOWLEDGMENTS

The authors wish to thank EDC for allowing the presentation and publication of this paper.

REFERENCES

ANDRE, L., SPYCHER, N., XU T., VUATAZ, F.D., & PRUESS, K. 2006. Modelling brine-rock interactions in an enhanced geothermal system deep fractured reservoir at Soultz-Sous-Forets (France): a joint approach using two geochemical codes: frachem and toughreact. *Lawrence Berkley National Laboratory, University of California.*

BERNER, R.A. & MORSE, J.M. 1974. Dissolution kinetics of calcium carbonate in seawater. IV. Theory of calcite dissolution, *American Journal of Science,* **274**,108-134.

BUSENBERG, E. & PLUMMER, L.N. 1986. A comparative study of the dissolution and crystal growth kinetics of calcite and aragonite. *U.S. Geological Survey Bulletin,* **1578**, 139-168.

COMPTON R. G. & UNWIN P. R. 1990. The dissolution of calcite in aqueous solution at pH < 4: Kinetics and mechanism. *Philisophical Transactions of the Royal Society, London Series A,* **330**, I-46.

DULCE, R.G., NOGARA, J.B., & SAMBRANO, B.G. 2000. Calcite scale deposition in production wells in Mindanao Geothermal Production Field, Philippines. *PNOC-EDC Internal Report*. **2000**.

KLEIN, C. & CHAPPELL, N. 1998. WATCHWORKS V 1.0. GeothermEx, Inc., 5221 Central Ave., Suite 201, Richmond, CA 94804, USA .

LEBRON, I. & SUAREZ, D.L. 1996. Calcite nucleation and precipitation kinetics as affected by dissolved organic matter at 25°C and pH > 7.5. *Geochimica et Cosmochimica Acta,* **60**(15), 2765-2776.

MORSE, J.W. 1978. Dissolution kinetics of calcium carbonate in sea water; VI, The near-equilibrium dissolution kinetics of calcium carbonate-rich deep sea sediments. *American Journal of Science,* **278***,* 344-353.

PLUMMER L.N., WIGLEY T.M.L., & PARKHURST, D.L. 1978. The kinetics of calcite dissolution in CO_2-water systems at 5° to 60°C and 0.0 to 1.0 atm CO_2. *American Journal of Science,* **278**, 179-216.

SHIRAKI, R. & BRANTLEY, S.L. 1995. Kinetics of near-equilibrium calcite precipitation at 100°C: An evaluation of elementary reaction-based and affinity-based rate laws. *Geochemica et Cosmochimica Acta,* **59***,* 1457-1471.

SJÖBERG, E.L. & RICKARD, D.T. 1984. Calcite dissolution kinetics: surface speciation and the origin of the variable pH dependence, *Chemical Geology,* ***42***, 119-136.

Sources of arsenic contamination and remediation of mine water at the historical Glen Wills mining area in Northeast Victoria, Australia

Dennis Arne[1], Andrew Nelson[2], & John Webb[2]
[1]*ioGlobal, 469 Glen Huntley Road, Elsternwick, Victoria, 3185 AUSTRALIA*
(email: dennis.arne@ioGlobal.net)
[2]*Department of Environmental Geoscience, La Trobe University, Bundoora, 3086, Victoria AUSTRALIA*

ABSTRACT: Arsenic in Glen Wills Creek is seasonally elevated to levels exceeding Australian drinking water guidelines and environmental trigger values of 7 μg/L and 13 μg/L, respectively. Arsenic enters the creek from both surface and groundwater drainage from sulfidic mine tailings in and adjacent to Glen Wills Creek. Arsenic was also previously contributed to the creek by natural outflow from the Maude Mine No. 5 adit, but this water is now retained in a storage dam on site. Mine waters are reduced, contain between 2.8 and 3.5 mg/L Fe and an average of 1.87 mg/L As, mainly as As^{3+}. This water becomes progressively oxidised as it flows from a sump at the adit mouth down to the storage dam. Up to 98% of the As is removed through passive oxidation and the precipitation of ferrihydrite. The remaining As can be removed through the use of coagulating agents, such as poly-aluminium chloride and ferric chloride.

KEYWORDS: *arsenic, mine water, tailings, Glen Wills, Australia*

INTRODUCTION

Glen Wills is a historical gold mining area located in the headwaters of the Mitta Mitta River in the highlands region of eastern Victoria (Fig. 1). Mining involved the processing of arsenical gold ore and the production of ~200,000 t of waste rock and tailings, mainly prior to 1970. Most of the tailings were deposited either directly in or adjacent to Glen Wills Creek. A long-term water quality monitoring program for Glen Wills Creek was initiated by Australian Gold Mines in late 2003 to establish baseline data for future development of the mine. Analysis of the data collected between 2003 and 2005 has revealed arsenic levels downstream of historical mine workings and tailings deposits generally exceed the maximum allowable guideline value for Australian drinking water of 7 μg/L and are often in excess of the Australian and New Zealand Environment and Conservation Council trigger value for the protection of 95% of species in freshwater aquatic ecosystems of 13 μg/L. Possible arsenic sources include natural discharge water from the No. 5 adit of the Maude Mine, both ground and surface water discharging from the Yellow Girl tailings (~20,000 t), and groundwater discharging from the combined Maude/Yellow Girl tailings (~85,000 t).

GEOLOGICAL SETTING

The Glen Wills area occurs within Ordovician sedimentary rocks the Omeo Zone (Pinnak Sandstone), which underwent medium grade metamorphism during the Silurian Benambran Orogeny (Morand *et al*. 2005). The rocks in the immediate vicinity of Glen Wills consist largely of corderite- and andalusite- or sillimanite-bearing schists intruded by the

Fig.1. Location of Glen Wills in eastern Victoria, Australia.

Silurian Mt. Wills Granite. Gold mineralisation is structurally-hosted and accompanied by the presence of pyrite, arsenopyrite, sphalerite, aurostibite, and a variety of sulfosalts (Crohn 1958). Gangue phases include quartz and ferroan dolomite.

METHODOLOGY

Water from Glen Wills Creek was sampled monthly over a two-year period from eight monitoring sites. These samples were not filtered or acid-stabilised in the field. However, the samples were chilled and shipped overnight to the laboratory for analysis. Surface waters emanating from the No. 5 adit of the Maude Mine and the Yellow Girl tailings, as well as discharge waters from the No. 5 adit that are stored in a sump and dam near the adit entrance were sampled less frequently. Groundwater within the Yellow Girl tailings was sampled from a diamond drill exploration hole, and mine water from the internal shaft in the Maude Mine was sampled using a 1L stainless steel sampling bomb. Both filtered (<0.45 μm) and unfiltered samples were collected from contaminated sources, and samples for heavy metal analysis were acidified with HNO_3 in the field. No special preservation for Hg was undertaken. Samples for arsenic speciation were stabilised with HCl. Heavy metals (As, Se, Zn, Pb, Ni, Cu, Cr, Cd, Mn, Fe, Hg) were determined using ICP-MS. Arsenic speciation was determined using High Performance Liquid Chromatography-Inductively Coupled Plasma-Mass Spectrometry (HPLC-ICP-MS).

Net acidity of tailings was determined using a modification of the procedure described by Ahern *et al.* (2000). Potential sulfidic acidity was determined from XRF S determinations. Net acidity was taken as the sum of the potential sulfidic acidity and titratable actual acidity, less the acid neutralisation capacity.

GLEN WILLS CREEK

Average As levels measured in Glen Wills Creek between 2003 and 2005 increase downstream, beginning from where mine waters from the No. 5 adit discharge into the creek (Fig. 2). A clear positive correlation also exists between As and total Fe in solution (Fig. 3) because As is present in the form of arsenopyrite in the deposit.

Arsenic levels in the creek show a seasonal variation with the highest levels occurring during the summer and autumn months when water flow levels in the creek are at their lowest. Major cations and anions for the water samples are illustrated in Figure 4. Group 1 samples are relatively fresh surface water samples, whereas Group 4 samples are highly contaminated waters. Groups 2 and 3 represent varying degrees of mixing between these two end members.

MINE WATER

Mine water from a depth of up to 80 m from the internal shaft has a total Fe content of between 2.8 to 3.5 mg/L, an average As content of 1.87 mg/L, an average pH of 6.63 and a negative Eh.

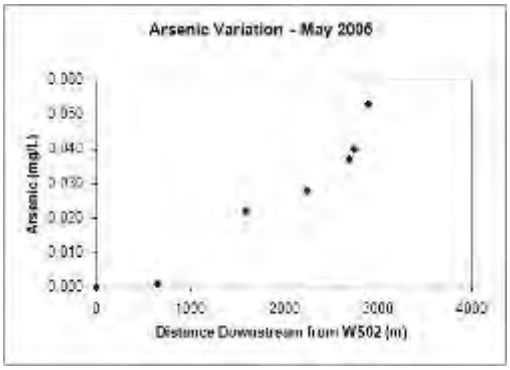

Fig. 2. Average As levels in Glen Wills Creek during May, 2005.

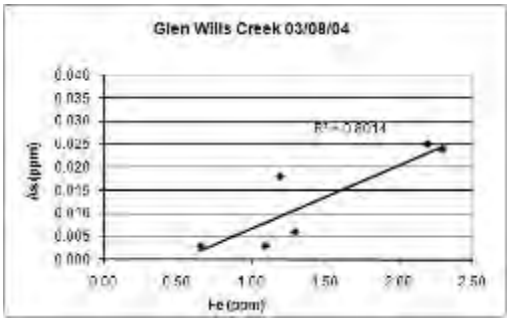

Fig.3. Relationship between As and Fe in Glen Wills Creek.

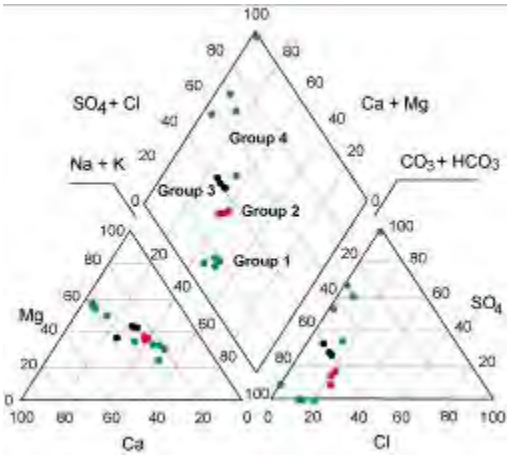

Fig. 4. Piper diagram comparing water monitoring data (Groups 1-3) and contaminated samples (Group 4). From Arne (2005).

The majority of the As in mine water from the internal shaft occurs as As^{3+}, with only a minor component of As^{5+} (Fig. 5). Iron and As are predominantly in solution in these waters. Water from the internal shaft oxidises as it flows from the sump to the storage dam, and the amount of Fe and As in solution drops sharply as As is absorbed onto precipitating ferrihydrite (Fig. 6). The dominant As species in the sump and dam is As^{5+}. Natural attenuation through passive oxidation removes ~98% of the As in solution from the mine waters.

WATER TREATMENT

To determine the most practical and cost effective method of treatment to remove the remaining As in the dam water, a number of bench-scale trials have been performed, testing commercial products which utilise the enhanced coagulation, fixed-bed adsorption, and ion exchange methods of arsenic removal. Fixed-bed adsorbents (activated alumina and granular ferric oxyhydroxide) and ion exchange resin displayed a relatively poor efficiency for arsenic removal. However, the coagulating agents poly-aluminium chloride and ferric chloride reduced arsenic concentrations to ≤13 ppb; achieving near 100 percent arsenic removal efficiencies at minimum dose rates of 7.1 mg/L and 16.3 mg/L,

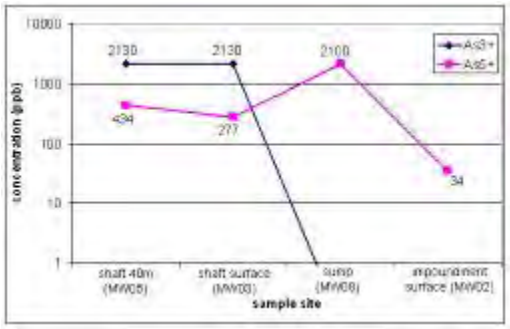

Fig. 5. Variation in As species during oxidation of mine waters from the internal shaft, Maude Mine. Measured values are indicated. From Nelson (2008).

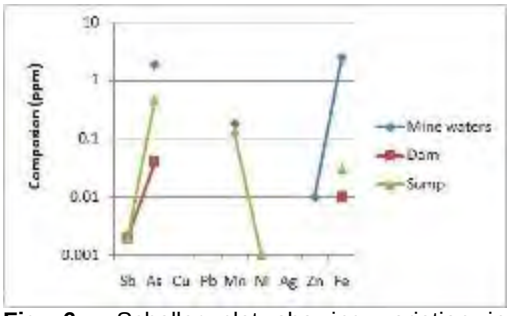

Fig. 6. Scholler plot showing variation in dissolved metals during oxidation of Maude Mine water.

respectively.

TAILINGS

Analyses of six sulfidic tailings samples indicate a range of net acidities ranging between 294 mole H^+/tonne in un-oxidized tailings and -115 mole H^+/tonne in oxidised tailings. The wide range of net acidities reflects both the effects of historic sulfide oxidation and the presence of carbonate gangue phases. Groundwater from the Yellow Girl tailings is sulfate-rich, with a lower pH (5.9) than mine water and contains elevated Ca, Mg and Fe, as well as dissolved As, Mn, Hg, Ni and Zn.

CONCLUSIONS

Arsenic and Fe are being released from mine water emanating from the No. 5 adit of the Maude Mine, and from surface and ground water draining from variably oxidized sulfidic tailings. From both a rinking water and ecosystem perspective this As contaminates Glen Wills Creek.

Passive oxidation of mine water from the Maude Mine removes up to 98% of the contained As through precipitation of ferrihydrite and scavenging of As from solution. The remaining arsenic in the water can be removed by the use of the coagulating agents poly-aluminium chloride or ferric chloride.

ACKNOWLEDGEMENTS

This project would not have been possible without the support of Australian Gold Mines and, more recently, Synergy Metals Ltd.

REFERENCES

ARNE, D.C. 2005. *Groundwater Management at the Glen Wills Historic Mining Area, Victoria.* Unpublished Graduate Diploma Thesis, University of Technology, Sydney.

AHERN, C.R., MCELNEA, A.E., LATHAM, N.P., & DENNY, S.L. 2000. A modified acid sulfate soil method for comparing net acid generation and potential sulfide oxidation - POCASm. In: AHERN, C. R., HEY, K. M., WATLING, K. M., & ELDERSHAW, V. J. (eds.), *Acid sulfate soils: Environmental issues, assessment and management.* Department of Natural Resources, Brisbane, 21/21 - 22/12.

CROHN, P.W. 1958. Geology of the Glen Wills and Sunnyside Goldfields, northeastern Victoria. *Bulletin of the Geological Survey of Victoria,* **56.**

MORAND, V.J., SIMONS, B.A., TAYLOR, D.H., CAYLEY, R.A., MAHER, S., WOHIT, K.E., & RADOJKOVIC, A.M. 2005. Bogong 1:100,000 map area geological report, *Geological Survey of Victoria Report* **125**.

NELSON, A. 2008. *Geochemical Characterization and Arsenic Remediation of Mine Discharge Water at the Glen Wills Historic Mining Area, Victoria.* Unpublished Honours Thesis, La Trobe University, Bundoora.

Geochemical and hydrogeological controls on naturally occurring arsenic in groundwater at a field site in West Bengal, India

Roger D. Beckie[1], Alexandre J. Desbarats[2], Tarak Pal[3], Cassandra E. M. Koenig[1], Pradip K. Mukherjee[3], Andrew Rencz[2], & Gwendy Hall[2]

[1]Department of Earth and Ocean Sciences, University of British Columbia, Vancouver, BC, V6T 1Z4 CANADA (e-mail: rbeckie@eos.ubc.ca)
[2]Geological Survey of Canada, Ottawa, ON, K1A 0E8 CANADA
[3]Central Petrological Laboratories, Geological Survey of India, Kolkata-700016 INDIA

ABSTRACT: Since 2004, the Geological Surveys of India and Canada in collaboration with the University of British Columbia have been investigating naturally occurring arsenic in groundwater at a field site near the village of Gotra, West Bengal, India. At the field site, high (> 50 ppb) and low arsenic groundwater zones are separated by a transition zone less than 30 m wide. There is no clear distinction in major-element chemistry between high-dissolved-arsenic and low-dissolved-arsenic zones. Sediment cores show arsenic values between 1 ppm As in sandy zones up to 20 ppm As in finer-grained material. The distinguishing feature of the site is that groundwater with high concentrations of arsenic (> 50 ppb) is found in the aquifer below and proximal to an in-filled channel. Shallow wells completed in the low-permeability soft, gray clayey-silt channel fill within 5 m from the edge of a pond provide strong evidence for near surface arsenic release. Water proximal to another pond away from the channel is not associated with high arsenic. All geochemical indicators point to organic-matter driven reductive release processes. Indeed, groundwater with high arsenic is associated with high phosphate, low sulfate, high ammonia, high alkalinity, abundant methane, high dissolved organic carbon and PCO_2 between $10^{-1.2}$ and $10^{-0.7}$ bars. The degree of super-saturation with respect to vivianite and siderite increases with arsenic concentration. Sediments contained solid-phase arsenic concentrations of 1 to several ppm As in sandy zones up to 20 ppm As in finer-grained channel material.

KEYWORDS: *arsenic, groundwater, Bengal Basin*

INTRODUCTION

Since its initial discovery in 1978 in West Bengal, India, arsenic has been found in groundwater at concentrations above World Health Organization (WHO) recommended threshold for human consumption in a large area of the Bengal Basin. It is now well-accepted that the groundwater arsenic is naturally occurring, derived from the Himalayan sediments in the basin, and that arsenic release into the groundwater is related to reduction processes driven by organic matter (Acharyya *et al.* 1999; Nickson *et al.* 2000; Harvey *et al.* 2002). However, the location and detailed mechanism of arsenic release into groundwater has yet to be clearly defined by any of the numerous groups working in the Bengal Basin. While arsenic is found in groundwater in many regions of the Bengal Basin, locally the arsenic distribution is very patchy. Wells separated by 10's of meters can produce groundwater with arsenic concentrations that differ by 100's of parts per billion. In addition, the source of the organic matter driving reduction is unclear, with both subsurface peat and pond-derived organic matter proposed. In this paper we present results from detail characterization of the site established by the Geological Surveys of India and Canada (GSI/GSC) where low and high arsenic concentrations are found in close proximity.

SITE

The study site is located approximately 56 km northeast of Kolkata India in the village of Gotra in Nadia District, West Bengal, (2546396N 662938E UTM, 88.59 N,

23.018 E). The village is approximately 1 km long and 500 m wide, oriented on a south-east to north-west trend. The village is bounded to the south west by a line of south-east to north-west trending ponds that mark the trace of an abandoned channel. The north-east limit of the village is defined by four ponds that trend on a similar orientation, but it is less clear if these ponds were dug or are abandoned channels.

SAMPLING

Groundwater samples were collected from approximately 50 domestic wells in and surrounding the village of Gotra and from approximately 15 monitoring piezometers and multilevel wells installed by the GSI/GSC. Sediments were collected in 2004 from two continuous 40 – m and from finer grained units during drilling of monitoring piezometers by the indigenous hand-flapper method.

RESULTS

The water chemistry results from the shallow aquifer at the site reveal a zone of low arsenic concentrations (<50 ppb) adjacent to high arsenic concentrations. These zones are separated by a 10 – 30 m transition.

Arsenic concentrations vary from below detection to above 500 parts per billion (ppb) (Fig. 1). The highest dissolved arsenic concentrations in the aquifer occur below the in-filled abandoned channel. Groundwater flow data provides strong evidence for near surface arsenic release.

Sequential extractions carried out by the Geological Survey of Canada show that arsenic is distributed among a number of

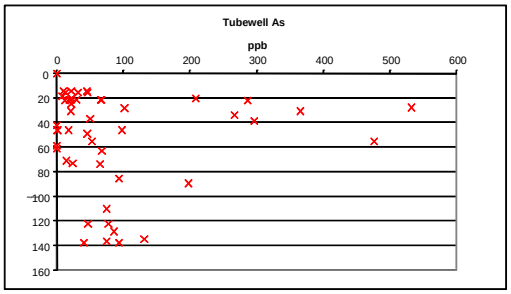

Fig. 1. Arsenic concentration in ppb versus depth in m for all wells in Gotra area, 2004 sampling event.

pools: weakly absorbed, amorphous and crystalline iron oxides and in sulfides and silicates. The dominant solid phase arsenic pools are iron oxides and sulfides and silicates. From 30 % - 50 % of the arsenic is in a form that can be considered easily releasable. The release of 1 ppm solid-phase arsenic can result in approximately 5 ppm aqueous - phase arsenic.

Solid – phase arsenic concentrations are low in aquifer sands in both high and low arsenic zones – generally 2 parts per million (ppm) or less. In fine grain sediments, arsenic levels are typically 5 – 10 ppm in both the low and high arsenic zones, peaking at 20 ppm near the surface in the channel-fill silts (borehole 20, Fig. 2).

The groundwater is dominantly calcium-

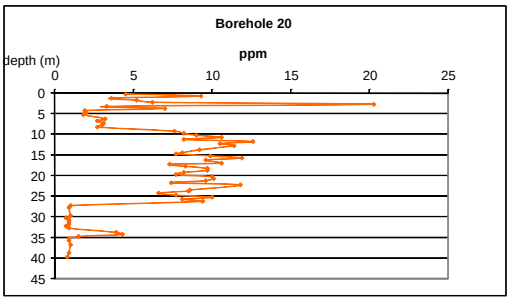

Fig. 2. Solid-phase arsenic in ppm versus depth in m from a continuous core. The core consists of clayey silt to depth of 28 m, and fine sand thereafter with a silt horizon at 34 m depth. As was measured by digestion with an HCl-HNO_3-H_2O aqua regia solution followed by inductively coupled plasma mass spectrometry and inductively coupled plasma atomic emission spectroscopy analysis.

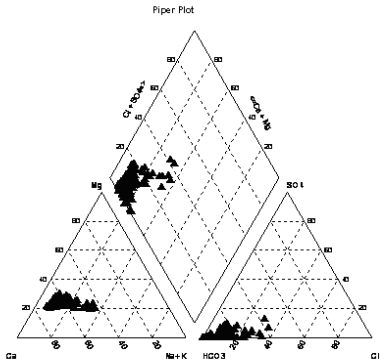

Fig. 3. Piper plot of Gotra – area groundwater.

bicarbonate type, with remarkably little variation in proportions of major elements between low and high arsenic zones (Fig. 3). Specific conductance ranges from a low of ~300 µS/cm in locations with sand to the surface to ~1800 µS/cm in fine-grained sediments. The groundwaters are almost all anoxic, with iron concentrations up to 21 mg/L. Sulfate concentrations are generally less than a few mg/L, and are typically below detection in high arsenic zones and the highest in low arsenic zones.

Dissolved arsenic is correlated with ammonia (Fig. 4), consistent with a release mechanism associated with the oxidation of organic carbon. Other chemical data not shown here provide clear evidence of iron, manganese and sulfate reduction and abundant methane in some samples indicates that methanogenesis is also occurring. It is not clear however if arsenic is released primarily by a desorption process associated with reduction of sorbed arsenic or by release after the reductive dissolution of the iron oxide sorbent. Phreeqc analysis shows PCO_2 between $10^{-1.2}$ and $10^{-0.7}$ bars and that high arsenic waters are supersaturated with both siderite and vivianite.

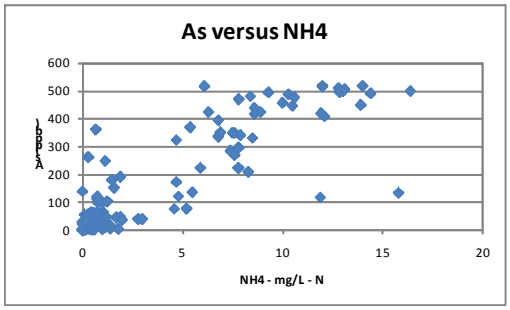

Fig. 4. Solid phase arsenic in ppm versus depth in m. The core consists of silty clay to depth of 28 m, and fine sand thereafter.

REFERENCES

ACHARYYA, S.K., CHAKRABORTY, P., LAHIRI, S., RAYMAHASHAY, B.C., GUHA, S., & BHOWMIK, A. 1999. Arsenic poisoning in the Ganges delta. *Nature*, ***401***, 545-545.

HARVEY, C.F., SWARTZ, C.H., BADRUZZAMAN, A. *et al.* 2002. Arsenic mobility and groundwater extraction in Bangladesh. *Science*, ***298***, 1602-1606.

NICKSON, R.T., MCARTHUR, J.M., RAVENSCROFT, P., BURGESS, W.G., & AHMED, K.M. 2000. Mechanism of arsenic release to groundwater, Bangladesh and West Bengal. *Applied Geochemistry*, ***15***, 403-413.

Flux of river active material flowing into the sea from Chinese continent: preliminary results

Sun Binbin[1,2,3], Zhou Guohua[1,2], Wei Hualing[1,2], Liu Zhanyuan[1,2], & Zeng Daoming[1,2]

[1] Institute of Geophysical and Geochemical Exploration, CAGS, Langfang 065000, Hebei CHINA (e-mail: sunbinbin@igge.cn)

[2] Laboratory for Applied Geochemistry, CAGS, Langfang, 065000, Hebei CHINA

[3] School of Earth Sciences and Resources, China University of Geosciences, Beijing 100083 CHINA

ABSTRACT: It's one of the key tasks for current regional eco-geochemical assessments proceeding in China to find out the flux flowing into the sea through rivers, especially for dissolved and suspended particulate matter (SPM) forms, which are active parts in water body and of high eco-environmental significance. This paper presents the method of the survey and gives the approximately primary heavy metal and nutritious elements' flux and proportion of water-soluble and SPM forms when the elements migrate to the sea for the whole Chinese continent, which bases on the actual SPM, filtering water and bed mud sampling, analysis and rivers' runoff data of main 35 rivers eastern coastline of China.

KEYWORDS: *element flux, filtering water, suspended particulate matter (SPM), active mass, transport way.*

INTRODUCTION

River is the most consanguineous natural water body to human being and is the channel between terrene and ocean. The length of Chinese coastline is over 18000km. There are over 1500 and 80 rivers flowing into the sea that watershed area respectively exceed 1000km^2 and 10000km^2. Furthermore, the rivers included like Yangtze River, Yellow River and Pearl River are all world-class. These rivers span wide latitude, various climate-landscape and different geological setting, and many of them have been polluted seriously. Research of inorganic and organic chemical components, flux flowing into the sea and transport form for great rivers like Yangtze, Yellow and Pearl River has been doing systemically since 1990s, and plenty of fruits in theory, mechanism and methodology have been showed (Zhang *et al*.1995; Ye 2001; Pan *et al*. 2005; Ying *et al*. 2005; Wu *et al*. 2006; Zhou *et al*. 2008). Few rivers, limited index (most studies give just the content of total heavy metal) and hydrologic data in different terms are the same points of these studies. This survey designed to trace the source and transport form of heavy metals in shallow sea environment, and then to make forecast and precaution through evaluating its potential ecological effect. This work includes systemic survey of 35 main rivers flowing into the sea in China.

METHOD

In this survey, we collected SPM and filtering water samples respectively in wet and dry seasons and bottom mud in dry. Water was collected by plastic bucket below 30cm of the river surface at the place where the river is wide and lowly velocity relatively. In addition, we did this in the middle of the river. Conductivity, water temperature, pH and salinity were determined in field. Water samples were pumped through 0.45μm nylon membranes at stationed place. Then both membranes and filtering water samples were preserved. Membranes were folded, then put into sealing plastic envelop. Two bottles of filtering water were collected to 250ml plastic bottle. One was infused 2.5ml HNO_3(1:1) for common elements analysis. Another was infused 2.5ml HNO_3(1:1) and 12.5ml $K_2Cr_2O_7$(5%) for mercury. Nylon membranes' drying and

weighting were proceeded before field work and after both for calculating the quality of SPM.

ANALYSIS

The membrane is put into 30ml quartz crucible after drying and weighting. Add 15ml aqua regia and 10ml distilled water into crucible. Then put it to platen heater for 1 hour, use 5ml distilled water to rinse the crucible and heat up for another hour. Displace the liquid to 25ml polythene pipe by water and add water to the calibration. Finally, determine the contents by ICP-MS, ICP-OES and AFS after shaking up and clarify. Insert 2 pieces of nothingness membranes to SPM samples for background value evaluation. All membrane samples are analyzed in duplicate for no reference material monitoring.

RESULTS

We calculate the flux by the formula blow:

$$T_i=C_{SPM\text{-}F}\times C_{SPM\text{-}Fi}\times Q_F+C_{SPM\text{-}K}\times C_{SPM\text{-}Ki}\times Q_K+C_{W\text{-}Fi}\times Q_F+C_{W\text{-}Ki}\times Q_K$$

where T_i is the flux of one or other element(i) flowing into the sea, $C_{SPM\text{-}F}$ and $C_{SPM\text{-}K}$ are concentrations of SPM in wet and dry season respectively, $C_{SPM\text{-}Fi}$ and $C_{SPM\text{-}Ki}$ are contents of element "i" in SPM respectively, $C_{W\text{-}Fi}$ and $C_{W\text{-}Ki}$ are contents of element "i" in filtering water respectively, Q_F and Q_K are runoffs respectively. Base on the publications, ratios of Q_F and Q_K in whole runoff are approximately determined to 8:2 and 6:4 for north and south (Yellow river is concluded) of Yellow river respectively. Sum of 32 (we get only 32 rivers runoff data as yet) main rivers' runoff is 1526.97 billion m^3, while the runoff of Chinese continent is 1592.3 billon m^3. Ratio between former and later is 95.90%. Flux of Chinese continent flowing into the sea is calculated blow:

$$T_t = \frac{\sum T_i}{95.90\%}$$

where T_t is the flux of the whole Chinese continent flowing into the sea, $\sum T_i$ is the flux of 32 rivers flowing into the sea.

Table 4 shows the flux of main heavy metals and nutritious elements for 32 rivers (R-Flux) and Chinese continent (T-Flux) flowing into the sea. Furthermore, it shows the average ratio of SPM and dissolved forms (SPM-rate and Water-rate) when rivers reach to shallow sea. From it, variation of flux is very large among different elements, flux of major elements like as Ca, Fe, K, Mg, Na can get to a few or decades million tons, while trace elements including Cd and Hg have only decades to one hundred tons. In the same boat, transport forms of different elements vary largely too. Ratio of dissolved form for Ca, K, Mg and Na when river water migrates to sea takes up over 90%, while for Fe and Pb SPM form takes up domination.

PROBLEMS AND DISCUSSION

Flux showed in this paper exist some problems that:

Runoff, which changes greatly in different seasons and years, is one of the key factors influencing flux's calculation. So, exact calculation needs long-term, dynamic and synchronic hydrologic data.

Hydrological characters are very complex in estuary. Flocculation, agglomeration, deposition and resuspension occur together. Element in river water is in condition of dynamic changes. Therefore, sample site plays a key role in flux survey. Near to downriver more, it should be affected by ocean

Table 4. Total flux of elements flowing into the sea and main transport forms for Chinese continental rivers(flux units: ton)

Element	R-Flux	T-flux	SPM-rate	Water-rate
As	4301	4494	27.5	72.5
Ca	69089129	72181089	3.3	96.7
Cd	110.9	115.8	64.5	35.5
Cu	10221	10678	62.9	37.1
Fe	4029673	4210014	97.5	2.5
Hg	24.7	25.8	42.9	57.1
K	5476964	5722075	7.8	92.2
Mg	17145829	17913160	6.2	93.8
Na	35814027	37416819	0.2	99.8
P	246259	257279	42.3	57.7
Pb	7309	7636	89.1	10.9
Zn	66834	69825	24.7	75.3

more, whereas influence aroused by violent industrial activities couldn't be displayed at estuary area. Furthermore, it's in estuary where many branches' afflux into the main river. To consider these branches we should add sample sites, in other words, we have to increase survey cost.

Besides, publications of rivers' runoff and ratio in wet and dry season are usually out of data or average values, which have been changed greatly by human in past decades. To this day, we can't get exact runoff data for different departments' data share difficulty.

On the other hand, this survey is mainly about active material flux, which is less affected by hydrological conditions than coarse particles. Accordingly, flux of this can provide reference data in some respects.

REFERENCES

PAN, Y.J. GUO, Z.G., YANG, Z.S., FAN, D.J., & SUN, X.G. 2005. Comparative Study on the Composition of Grain Size of Suspended Sediments from the Yangtze and Yellow Rivers. *Journal of Ocean University of Qingdao*, **35(3)**, 417-422 (in Chinese).

WU, H.L., SHEN, H.T., YAN, Y.X., & WANG, Y.H. 2006. Preliminary study on sediment flux into the sea from Yangtze Estuary. *Journal of Sediment Research*, **6**, 75-81(in Chinese).

YE, L.Q. 2001. Discussion on the Flux of Heavy Meatals into the sea from the Pearl River. *Environment and Exploitation*, **16**(2), 52-54(in Chinese).

YING, M., LI, J.F., WAN, X.N., & SHEN, H.T. 2005. Study on Time Series of Sediment Discharge at Datong Station in the Yangtze River. *Resources and Environment in the Yangtze Basin,* **14**(1), 83-87(in Chinese).

ZHANG, C.S., WANG, L.J., & ZHANG, S. 1995. Metal speciation in sediments and suspended matter in the middle-lower reaches of the Changjiang River. *China Environmental Science,* **15**(5), 342-347 (in Chinese).

ZHOU, G.H., SUN, B.B., LIU, Z.Y., WEI, H.L., & ZENG, D.M. 2008. Flux of River Active Material Flowing into the Sea:Concept and Methodology. *Geological Bulletin of China*, **27**(2), 182-187 (in Chinese).

Methods for obtaining a national-scale overview of groundwater quality in New Zealand

Christopher J. Daughney, Uwe Morgenstern, Rob van der Raaij, Robert Reeves, Matthias Raiber, & Mark Randall

GNS Science, 1 Fairway Drive, Avalon NEW ZEALAND (e-mail: c.daughney@gns.cri.nz)

ABSTRACT: This study presents methods developed to summarise groundwater quality in New Zealand, based on data collected since 1990 from over 100 monitoring sites comprising the National Groundwater Monitoring Programme (NGMP). Site-specific groundwater age determinations based on measured concentrations of tritium, CFCs and SF_6 range from less than one year to more than 100 years, with the 25th, 50th and 75th percentiles (across the entire NGMP) being approximately 10, 40 and 100 years, respectively. Hierarchical cluster analysis based on median concentrations of 15 major and minor constituents reveals three dominant water types across the NGMP. At 42% of the monitoring sites, groundwater quality shows some level of human influence, with nitrate, chloride and/or sulphate concentrations in excess of natural background levels. At 32% of the monitoring sites, groundwater quality shows little or no evidence of human influence, but due to high levels of oxygen in the aquifer, any introduced nitrate or sulphate will persist and accumulate. At the remaining 26% of the monitoring sites, the groundwater is oxygen-poor and is not likely to accumulate significant nitrate, but due to natural processes, it commonly accumulates concentrations of iron, manganese, arsenic and/or ammonia.

KEYWORDS: *hydrochemistry, groundwater age, multivariate statistics, New Zealand*

INTRODUCTION

The objective of this study is to provide an overview of groundwater quality across all of New Zealand (NZ). This is achieved by analysis of data collected through the NZ National Groundwater Monitoring Programme (NGMP). The NGMP, established in 1990, is a long-term research programme that aims to identify spatial and temporal trends in NZ groundwater quality and relate them to specific causes. The data analysis methods of interest in this study include hierarchical classification of monitoring sites from hydrochemistry (Daughney & Reeves 2005, 2006), and groundwater age determination based on measured concentrations of tritium, CFCs (*chlorofluorocarbons)* and SF_6 (Daughney *et al*. 2009).

Hierarchical Cluster Analysis (HCA) is a multivariate statistical method that can be used assign groundwater samples or monitoring sites to distinct categories (hydrochemical facies). HCA offers several advantages over other methods of grouping or categorising groundwaters. HCA does not require *a priori* assumptions about the number of groups or the criteria that control the groupings, such as aquifer lithology or confinement. HCA can be based on any number of variables, and these variables can be of any type (chemical, physical, biological; distributed or non-distributed). HCA can thus provide a more holistic approach to sample comparison than most other methods, which are limited in terms of the number of variables that can be simultaneously presented clearly. HCA produces a set of average parameter values (a centroid) for each cluster in the original units of the input variables, and hence the results of HCA can be more readily interpreted in the geological or hydrochemical context than multivariate methods based on transformation, e.g. Principal Components Analysis. The output of HCA can be displayed as a membership table, where each site or sample is unambiguously assigned to a single group. By contrast, for most graphical methods (e.g. Piper

diagrams), it is difficult to determine exactly where the boundaries of each group should be placed, how many groups there should be, or which samples should be assigned to each group.

Determination of groundwater age is valuable for a variety of reasons covering the spectrum from applied resource management to fundamental scientific research. Groundwater dating relies on measurement of one or more tracer substances, followed by fitting of the tracer concentration data with a lumped-parameter model (Zuber *et al*. 2005). Tritium, CFCs and SF_6 are the tracers most commonly used for dating young groundwater (less than about 100 years old).

It is often useful to estimate groundwater age independently of the tracer method in order to overcome ambiguities that can arise in age determinations based on limited tracer data at some sites and in some hydrogeological conditions. Ambiguity in groundwater age can be overcome by fitting the convolution integral to time series tracer data, but it may not be practical to make several measurements over perhaps several years, as might be necessary to permit detection of significant change in the tracer concentrations relative to analytical uncertainty. Major ion hydrochemistry and well depth can be used to estimate groundwater age independently from the direct method of measuring tracer concentrations.

Discriminant Analysis (DA) is a multivariate statistical method that generates a set of classification functions that can be used to predict into which of two or more categories an observation is most likely to fall, based on a certain combination of input variables. DA may be more effective than regression for relating groundwater age to major ion hydrochemistry and well construction because it can account for complex, non-continuous relationships between age and each individual variable used in the algorithm while inherently coping with uncertainty in the age values used for calibration, and there is no need to assume that the sites involved are within the same aquifer or even within the same catchment.

METHODS

The NGMP includes 112 long-term monitoring sites across New Zealand; four sites that are no longer included in the NGMP were also considered as part of this study. NGMP sites are situated in discrete aquifers (or on discrete flow lines in large aquifer systems) and are selected to encompass a range of aquifer lithology, confinement and surrounding land use that is representative of New Zealand aquifers in general. Median well depth is 26 m below ground surface (b.g.s.), and the minimum, lower quartile, upper quartile and maximum well depths across all NGMP sites are 3, 10, 55 and 337 m b.g.s., respectively.

Samples are collected quarterly on an on-going basis from each NGMP site according to a standardized protocol. Electrical conductivity, pH and temperature are measured in the field using portable meters, and three different types of samples are collected for laboratory analysis of various parameters. An unfiltered, unpreserved sample is analysed in the laboratory for alkalinity, conductivity and pH using an autotitrator. A filtered (0.45 µm) unpreserved sample is analyzed for Cl, Br, F, SO_4, NO_3-N and PO_4-P by ion chromatography, and for NH_4-N by automated phenohypochlorite method. A filtered, acid-preserved (HNO_3) sample is analyzed for Na, K, Ca, Mg, Fe, Mn and SiO_2 by inductively coupled plasma optical emission spectrometry. The length of the historical record differs for each NGMP site but on average covers a period of seven years.

Groundwater age at each NGMP site has been assessed using multiple tracers. Tritium was analyzed in a 1 L unfiltered unpreserved sample using 70-fold electrolytic enrichment prior to ultra-low level liquid scintillation spectrometry (Morgenstern & Taylor 2005). Samples for analysis of CFCs and SF_6 (125 ml and 1 L, respectively) were collected in strict

isolation from the atmosphere and analysed by gas chromatography using an electron capture detector (Busenberg & Plummer 1992; van der Raaij 2003). Dissolved Ar and N_2 concentrations were used to estimate the temperature at the time of recharge and the excess air concentration, which allowed calculation of the atmospheric partial pressure of CFCs and SF_6 at the time of recharge.

The convolution integral and the Exponential Piston Flow Model (EPM) were used to relate measured tracer concentrations to historical tracer input. The tritium input function is based on tritium concentrations measured monthly since the 1960s near Wellington, New Zealand. CFC and SF_6 input functions are based on measured and reconstructed data from southern hemisphere sites. The EPM was applied consistently in this study because statistical justification for selection of some other response function requires a substantial record of time-series tracer data which is not yet available for the majority of NGMP sites, and for those NGMP sites with the required time-series data, the EPM and other response functions yield similar results for groundwater age.

HCA and DA were conducted using log-transformed site-specific median concentrations of various parameters as described by Daughney & Reeves (2005) and Daughney *et al*. (2009). HCA was conducted with median concentrations of Br, Ca, Cl, F, Fe, HCO_3, K, Mg, Mn, Na, NH_4-N, NO_3-N, PO_4-P, SiO_2 and SO_4 using the Nearest-Neighbour and Wards linkage rules. DA was conducted using electrical conductivity, well depth, and the median concentrations of Ca, Mg, Na, K, HCO_3, Cl and SO_4.

SUMMARY OF RESULTS

The range of hydrochemistry encountered across the NGMP can be summarized by assigning each site to one of three categories (hydrochemical facies) defined via HCA. 32% of the NGMP monitoring sites are assigned to the *natural-fresh* category and are typified by oxic groundwater showing little or no evidence of human or agricultural impact. 42% of the NGMP sites are assigned to the *impacted* category, and are also typified by oxic groundwater, but with evidence of some degree of human or agricultural impact in the form of above-background concentrations of NO_3-N, often co-occurring with elevated concentrations of Cl and/or SO_4. The level of impact observed at these sites is variable, with 15% of sites having median NO_3-N concentration above the guideline for safe human consumption (11.3 mg/L). The remaining 26% of the NGMP sites are assigned to the *natural-evolved* category and are typified by reduced (anoxic) groundwater, often with measurable concentrations of NH_4-N, dissolved Fe and/or dissolved Mn, and relatively high total dissolved solids concentrations.

Site-specific groundwater age values ranged from less than one year to more than 100 years, with the 25th, 50th and 75th percentiles being approximately 10, 40 and 100 years, respectively, across the entire NGMP. Classification functions derived from DA allowed assignment of 71% of the sites to the correct of four age categories (mean residence time ten years or less, 11 to 40 years, 41 to 100 years, or more than 100 years).

Groundwater age displays a generally expected relationship to well depth, but the age category cannot be predicted from well depth alone. In line with expectation, over all NGMP sites, well depth has a weak positive correlation to groundwater age, with the youngest and oldest age categories generally being associated with shallow and deep bores, respectively. However, shallow wells do not always tap young groundwater: there were a small number of NGMP sites at which groundwater from the oldest age category was found in a well less than 10 m deep. This situation occurred in both confined and unconfined aquifers, corresponding to upward-moving groundwater at the discharge end of a flow system.

Likewise, despite certain expected relationships between groundwater age and hydrochemistry, a particular site's groundwater age category cannot be

predicted from its hydrochemistry alone. For example, the older the groundwater is, the more likely it is to be assigned to the natural-evolved hydrochemical category. This is expected because the longer the groundwater is in the aquifer and isolated from the atmosphere, the more likely it is to become anoxic and to accumulate dissolved substances through water-rock interaction. However, only 85% of the NGMP sites assigned to the oldest age category display the natural-evolved hydrochemical signature, indicating that groundwater can remain oxic in some New Zealand aquifers for more than 100 years. Conversely, the natural-evolved hydrochemical signature is found at a small proportion (5%) of NGMP sites in the youngest age category, indicating that in some situations groundwater can become anoxic in less than a decade. Not surprisingly, this confirms that the rates of hydrochemical reactions are variable, as would be expected for aquifers with varied or mixed lithologies.

There is no significant partitioning of the different age categories between the natural-fresh and impacted hydrochemical categories. In other words, the number of sites having oxic impacted groundwater is always roughly equal to the number of sites with oxic unimpacted groundwater, regardless of groundwater age category. This implies that the impact of human and agricultural activity on New Zealand's groundwater quality is of similar extent over the last ten years as over the previous century.

ACKNOWLEDGEMENTS

The authors thank personnel from New Zealand regional councils for assistance with sample collection. This research was funded by the New Zealand Foundation for Research, Science and Technology (Contract C05X0706).

REFERENCES

BUSENBERG, E. & PLUMMER, L.N. 1992. Use of chlorofluorocarbons (CCl_3F and CCl_2F_2) as hydrologic tracers and age dating tools: the alluvium and terrace system of Central Oklahoma. *Water Resources Research*, **28**, 2257-2283

DAUGHNEY, C.J., MORGENSTERN, U., VAN DER RAAIJ, R., & REEVES, R.R. 2009. Groundwater age in New Zealand aquifers: Tracer measurements and age estimation from hydrochemistry. *Hydrogeology Journal*, in press.

DAUGHNEY, C.J. & REEVES, R.R. 2005. Definition of hydrochemical facies in the New Zealand National Groundwater Monitoring Programme. *Journal of Hydrogeology New Zealand,* **44**, 105-130.

MORGENSTERN, U. & TAYLOR, C.B. 2005. Low-level tritium measurement using electrolytic enrichment and LSC. *Proc. Int. Symp. Quality Assurance for Analytical Methods in Isotope Hydrology.* International Atomic Energy Agency.

VAN DER RAAIJ, R.W. 2003. *Age dating of New Zealand groundwaters using sulphur hexafluoride.* M.Sc. thesis, School of Earth Sciences, Victoria University of Wellington, New Zealand.

ZUBER, A., WITCZAK, S., RÓZAŃSKI, K. *et al*. 2005. Groundwater dating with ^3H and SF_6 in relation to mixing patterns, transport modelling and hydrochemistry. *Hydrological Processes,* **19**, 2247-2275.

Genesis of smectite scales in Mindanao geothermal production field, Philippines

Rosella G. Dulce[1], Gabriel M. Aragon[2], Benson G. Sambrano[3], & Lauro F. Bayrante[4]

[1]*Energy Development Corporation, Merritt Road, Fort Bonifacio, Taguig City 1634 PHILIPPINES*
(e-mail: dulce.rg@energy.com.ph)

ABSTRACT: Smectite [$Al_4Si_8O_{20}(OH)_4n•H_2O$], a hydrated expanding clay mineral is present in significant amounts in the surface facilities of the Mindanao Geothermal Production Field. It is the dominant constituent of total deposits in the low-pressure flash vessel station, and Separator Vessels (SV) 100 and 101. It is found in minor quantities of total deposits downstream of these vessels. The fragmental clay deposits cause recurrent operational problems, such as flooding of brine surge tank and flash vessel, clogging of pump at the LP station, and subsequent power plant trip. Petrologic and scanning electron microscopy analyses of clay samples reveal micro-textural features and mineral association suggesting that they deposited directly from the brine in the surface facilities, and are not hydrothermal alteration minerals transported from production wells. Moreover, simulation using SV-100 brine chemistry gives a high saturation index of smectite (log Q/K of 10-24) indicating high potential for depositing smectite. Very high saturation index is due to the brine's elevated aluminum content of 640 ppb. Since aluminum is the major parameter that controls smectite saturation index, clay scaling may be controlled by brine treatment with Al-sequestering or complexing agent (Gallup, 1997).

KEYWORDS: *smectite, scale, saturation index, deposits, brine*

INTRODUCTION

Smectite refers to a hydrated expanding clay mineral with a general chemical formula of $Al_4Si_8O_{20}(OH)_4n•H_2O$ (Read 1970). Aside from being commonly observed as a hydrothermal alteration of rock cuttings from geothermal wells, this clay mineral is noticeably present in the surface facilities of the Mindanao Geothermal Production Field (MGPF). It is abundant in the Low-Pressure (LP) Flash Vessel Station, particularly in the brine surge tank, flash vessel, bypass line and valve, and pump. It occurs in lesser amounts upstream of this station: in the solid trap, main brine line 1 (MBL-1), brine line sampling points after SV-100/101 and SV-602, and at the bases of SV-100 and SV-101. The huge amounts of fragmental clay deposits cause recurrent operational problems such as flooding of brine surge tank and flash vessel, clogging of pump at the LP station, and subsequent power plant trip.

This study attempts to determine the probable origin of abundant smectite in the LP station of MGPF. Samples were collected and analyzed using polarizing microscope and scanning electron microscope (SEM), and energy dispersive x-ray (EDX). Brine chemistry at selected sampling locations was also studied, and simulation using WATCH speciation software was done to determine the potential of the brine to directly deposit smectite. The conduct of this study will focus on the root cause of the problem, *i.e.*, the formation of huge amounts of smectite scales.

SMECTITE CHARACTERIZATION

Petrologic Analysis

Abundant fragmental sand- to pebble-sized deposits at several Fluid Collection and Recycling System (FCRS) locations in MGPF (Fig. 1 and Table 1) were collected and analyzed using a polarizing microscope.

The abundant dark brown to black soft minerals in the collected samples are identified as smectite, based on optical properties under a polarizing microscope.

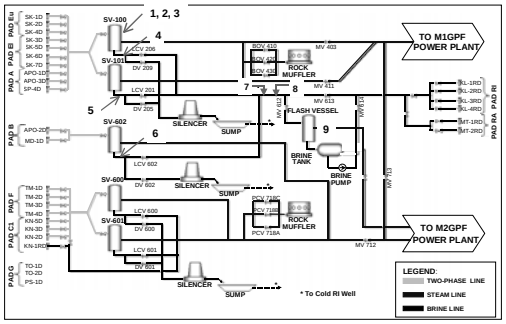

Fig. 1. Process flow diagram of MGPF.

Sampling Location	Smectite	Amorphous Silica	Corrosion Products	Rock Cuttings	Calcite
1. SV100 sidewall	5	80	15	-	-
2. SV100 stand pipe	10	70	20	-	-
3. SV100 base	5	85	10	-	-
4. SV100 brine line	80	6	7	5	2
5. SV101 brine line	55	15	10	15	5
6. SV602 brine line	3	70	15	5	7
7. MBL-1 (main brine line)	83	2	7	5	3
8. Solid trap	20	40	35	5	-
9. Low Pressure Flash Vessel station					
Brine surge tank	85	5	2	7	1
Flash vessel wall	-	97	1	1	-
Flash vessel base	3	85	5	7	-
Bypass valve	80	8	2	10	-
Bypass line	80	15	-	3	2
Brine line pump	4	90	6	-	-

Table 1. Sampling locations in MGPF.

Under the microscope, smectite is light to dark brown, or greenish to yellowish brown mineral. It has a grain size range of 0.07-7.00 mm. Smectite is present together with other fine-sized fragmental amorphous silica, corrosion products and rocks. Smectite comprises from 5% to 85% of the total deposits in MGPF FCRS.

Smectite occurs commonly as rounded

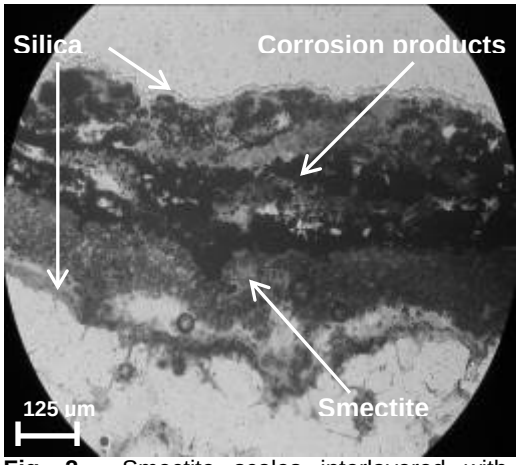

Fig. 2. Smectite scales interlayered with amorphous silica and corrosion products.

birefringent crystalline masses. Occasionally, it exists as amorphous to microcrystalline materials. Smectite exhibits fibrous, radiated, or daisy-like textures, very typical of smectite scales, but not observed in smectite as hydrothermal alteration mineral. It also shows very fine ripple marks which are displayed by amorphous silica scales in geothermal brine lines. In addition, smectite also has wavy extinction like amorphous silica. Smectite is occasionally thinly (1-2 mm) interlayered with amorphous silica and corrosion products (Fig. 2). It is embedded with abundant minute dendritic opaque minerals.

Determination of the Chemical Formulae of Clay Samples using EDX Analysis

The elemental compositions in weight percent of the four samples coded Brine Surge 1, Brine Surge 2, MBL-1A and MBL-1B collected from brine surge tank and MBL-1 sampling points were determined by EDX analysis. The clays are composed dominantly of O_2 (~70-80 wt. %) and Si (~10-15 wt. %), and minor amounts of Na, Mg, and Al (below 5 wt.%). Trace to nil K, Ca, Fe, Mn, Zn, and Cl are also present. In MBL-1B, however, significant amounts of Fe (~6.5 wt. %) is present in the sample. These elemental compositions are consistent with the general formula of smectite as will be discussed later.

All four clay samples have been identified as smectite on a polarizing microscope. Deciphering their chemical formulae can be done using the atomic percentages (Aragon 2006). Smectite has a general chemical formula of $\mathbf{Al_4Si_8O_{20}(OH)_4.nH_2O}$ (Read 1970), with substitution of Mg for part of the Al. As a result of this substitution, positive ions such as Na^+ or Ca^{2+} are attached to the surfaces or edges of the minute crystals, thus balancing the negative charges, which result when Mg^{2+} takes the place of Al^{3+}. In this way, variants known as sodium-smectite and calcium-smectite are formed. The positive ions (Na^+, Ca^{2+}) are

exchangeable bases, and their presence accounts for the high base-exchange capacity of the mineral.

Table 2 gives the compositions of the same four clay samples in atomic percent. The atomic percent is defined as the number of atoms of an element per unit volume divided by the number of atoms per unit volume of the substance containing the element. This is similar to mole fraction when the atomic percent is converted to fractional value.

Thus, the chemical formula of smectite (Table 3) is slightly complex since deficiency in Al^{3+} will be directly sufficed by Mg^{2+} and indirectly by Na^{+} and Ca^{2+}.

The chemical formula may be in the form of $Al_wMg_xNa_yCa_zSi_8O_{20}(OH)4.nH_2O$ where w, x, y, and z are the subscripts for each cation. The subscript is variable and highly dependent on the availability of the cations when the clay mineral was formed.

CLAY FORMATION SIMULATION USING SV-100 BRINE CHEMISTRY

Simulation of clay formation using SV-100 fluid was done using WATCH speciation program. Table 4 shows the data (Urbino & Lam, 2005) used for the clay simulation study. The speciation program calculates the saturation index in terms of log Q/K of the four clay minerals: Ca-smectite, Mg-smectite, K-smectite, and Na-smectite. Based on simulation, the log Q/K values at separator temperature of 170°C are **23.8**, **22.6**, **9.6,** and **10.8** for Ca-smectite, Mg-smectite, K-smectite, and Na-smectite, respectively. Thus, the brine fluid from the separator vessel is super saturated with respect to all clay minerals due to its very high aluminum content of 640 ppb. The inherently high potential for smectite deposition of the SV-100 separated brine fluid explains the presence of abundant clay minerals in the FCRS, most particularly in the second flash separator (LP station) where the separated brine from SV-100, SV-101, and SV-602 is further flashed at low pressure (120°C) to produce steam for the power plant.

CONCLUSIONS

(1) Abundant fragmental smectite deposits in the low-pressure flash vessel station and other surface facilities in the Mindanao geothermal production field cause recurrent operational problems.

(2) Petrologic and SEM analyses of these clay samples reveal micro-textural and structural features and mineral association suggesting that they deposited directly from the brine in the surface facilities, and are not hydrothermal alteration minerals transported from production wells.

(3) The chemical formulae of the clays based on atomic % are: $Al_{1.5}Mg_{2.5}Na_{2.3}Ca_{0.2}Si_8O_{20}(OH)_4 \bullet 69H_2O$ in brine surge tank, and

Element	Brine Surge 1	Brine Surge 2	MBL-1A	MBL-1B
O	79.39	85.07	83.49	82.69
Na	2.08	2.08	0.83	2.37
Mg	1.79	2.30	5.34	3.31
Al	2.16	1.33	0.41	0.94
Si	13.86	8.78	8.47	7.71
K	0.26	0.07	0.09	0.15
Ca	0.28	0.15	0.15	0.23
Fe	0.19	0.16	0.75	2.15
Mn	---	0.05	0.30	0.27
Zn	---	---	0.17	0.03
Cl	---	---	---	0.14
Total	100.00	100.00	100.00	100.00

Table 2. Compositions in atomic % based on EDX analysis.

Sample Code	Chemical Formulae for Smectite
Brine Surge 1	$Al_{2.0}Mg_{1.7}Na_{2.0}Ca_{0.3}Si_8O_{20}(OH)_4.51H_2O$
Brine Surge 2	$Al_{1.5}Mg_{2.5}Na_{2.3}Ca_{0.2}$ $Si_8O_{20}(OH)_4.69H_2O$
MBL-1A	$Al_{0.4}Mg_{4.9}Na_{0.8}Ca_{0.1}Si_8O_{20}(OH)_4.53H_2O$
MBL-1B	$Al_{0.9}Mg_{2.9}Na_{2.3}Ca_{0.2}$ $Si_8O_{20}(OH)_4.57H_2O$

Table 3. Chemical formulae of clay samples.

	SV-100	SV-602	MBL-1	LPBL*
Date	4/21/2005	4/18/2005	4/18/2005	4/7/2005
Sampling Pressure (MPaa)	0.79	0.83	0.74	0.89
Temp. (°C)	172	172	167	175
pH (@20°C)	6.92	7.02	6.92	6.95
Na	3462	3378	3821	3549
Mg	0.20	0.07	0.28	0.12
Al	0.64	0.58	---	0.64
K	549	674	546	531
Ca	165	137	93.5	182
Fe	1.53	0.72	---	0.06
Zn	0.0246	0.0212	---	0.0188
Cl	6063	6095	6220	6167
SO_4	47.9	88.2	33.5	37.6
B	117	61.9	61.1	120
SiO_2	541	688	566	574
H_2S	---	3.7	---	4.11
SSI		0.91	0.78	0.742

Table 4. Brine chemistry at SV-100, SV-602, MBL-1 & LPBL (*low pressure brine line).

$Al_{0.9}Mg_{2.9}Na_{2.3}Ca_{0.2}Si_8O_{20}(OH)_4 \bullet 57H_2O$ in MBL-1.

(4) Simulation using SV-100 brine chemistry gives a tremendously high saturation index of smectite (log Q/K of 10-24) indicating high potential for depositing smectite. Very high saturation index is due to the brine's elevated aluminum content of 640 ppb. Thus, abundant smectite scales likely form in LP station where separated brine from SV-100/101/602 is further flashed at 120°C. These soft clay deposits are easily removed from the vessels and transported as fragmental materials downstream of these facilities.

REFERENCES

ARAGON, G.M. 2006. Determining the chemical formulae of clay samples from the Mindanao geothermal production field, Philippines. *PNOC-EDC internal report*.

GALLUP, D.L. 1997. Aluminum silicate scale formation and inhibition: scale characterization and laboratory experiments. *Geothermics*, **26**, 483-499.

READ, H.H. 1970. Rutley's elements of mineralogy. *c.George Allen & Unwin (Publishers) Ltd*.

URBINO, G.A. & LAM, J.C. 2005. Mindanao geothermal production field water test report. *PNOC-EDC internal report.*

Adding Value to Kinetic Testing Data I – Interpretation of Tailings Humidity Cell Data from the Perspectives of Aqueous Geochemistry and Mineralogy at the Crowflight Minerals, Bucko Lake Nickel Project

David R. Gladwell[1] & Catherine T. Ziten[1]

[1]*Wardrop Engineering Inc., 900 – 330 Bay Street,Toronto, ON, M5H 2S8 (e-mail david.gladwell@wardrop.com)*

ABSTRACT: Kinetic testing of tailings is often focused on issues of acid mine drainage or metal leaching from an environmental perspective. Data is presented from 76 weeks of kinetic testing of bench test rougher tailings from the Crowflight Minerals, Bucko Lake Nickel Project. Statistical examination of the kinetic test data indicates that the data set is highly auto-correlated, a common feature of kinetic test data. Auto-correlated data is difficult to interpret without a prior knowledge of the dataset, therefore mineralogy determined during metallurgical testing was used to define the sample mineralogy and PHREEQC software was used to compute the equilibrium concentrations of ionic species according to ion pair theory. The sulfide mineral assemblage includes pyrrhotite, pentlandite, pyrite and chalcopyrite. Periods of oxidation of specific sulfide minerals and carbonate phases were identified from leachate chemistry using both ion pair molalities and sliding correlation coefficients. Pentlandite was observed to begin oxidizing first, followed by iron sulfides (pyrite and pyrrhotite) and chalcopyrite. The ability to define reaction products associated with oxidation of specific minerals in kinetic test data facilitates operational tailings management.

KEYWORDS: *Kinetic Testing, AMD, Tailings, Aqueous Speciation, PHREEQC, Nickel Mining.*

INTRODUCTION

Estimation and prediction as to whether waste rock and tailings will produce acid mine drainage (AMD) are precursory to environmental certification, and therefore are a critical step in mine development. Kinetic tests are carried out using a cell or column that are operated over a period of typically 1 year, whereas static tests are a onetime measurement to determine the acid producing potential (AP) and neutralization potential (NP) when exposed to oxidation, but cannot provide information on reaction rates (Morin & Hutt 1997; Jambor *et al.* 2002; Blowes *et al.* 2003). Humidity cell testing is a standard protocol (ASTM, 2001) involving periodic rinsing of tailings samples over time to remove all reaction products that accumulated following the previous rinsing (Morin & Hutt 1997; Price *et al.* 1997) and subsequently analyzing the leachate for relevant parameters (Lapakko & White 2000; Sapsford *et al.* 2009). The results elucidate how tailings/waste rock will behave over time with the onset of oxidation, assist in calculating oxidation rates, mineral reaction rates, and with respect to prediction of acid generation facilitate estimation of the rate of NP depletion and the period when AMD commences (*Day et al.* 1997; Morin & Hutt 1997; Price *et al.* 1997; Frostan *et al.* 2002; Bowell & Parshley 2005; Ardau *et al.* 2008).

This paper outlines a novel approach to maximising the value of kinetic data by combining mineralogy (from petrological studies) and aqueous geochemistry to reveal oxidation of relevant mineral assemblages based on changes in unique element suites. PHREEQCi was used to calculate equilibrium ion pair concentrations. PHREEQCi and its precursors have been used extensively for sensitive acid precipitation studies (Meranger *et al.* 1986) and for AMD projects (Morin 1985).

GEOLOGICAL SETTING

The Bucko Lake Nickel Project is located in north-central Manitoba and owned by

Crowflight Minerals Inc. The ore deposit consists of Aphebian ultramafic sills intruded into Archean gneisses (Wardrop 2008). Rougher tails were produced from lock cycle testing of bulked drill core samples.

KINETIC TEST DATA

Kinetic testing of the rougher tails sample was carried out in accordance with standard ASTM, 2001. Leachate samples were collected each week for 76 weeks and analyzed for a range of parameters including: conductivity, pH, acidity, total alkalinity, sulfate and a suite of dissolved metals. Dissolved metals and metalloids were determined by ICP-MS, other parameters by titration or selective ion electrode methods.

Data such as that generated by the Bucko kinetic testing (and most other kinetic testing) is difficult to interpret due to its highly auto-correlated content (Cerioli & Riani 2005). The high degree of auto-correlation frustrates the extraction of meaningful information from the data and may be part of the reason why most interpretations of kinetic data are restricted to prediction of potential AMD or metal leaching. Prior knowledge of sample mineralogy is necessary to untangle the complex web of inter-correlated data. Based on metallurgical studies the Bucko rougher tails samples are known to contain several sulfide phases including Pentlandite $(Fe,Ni)_9S_8$, Pyrrhotite (Fe_7S_8 to FeS), Chalcopyrite ($CuFeS_2$), and Pyrite (FeS_2). Calcite ($CaCO_3$) and Magnesite ($MgCO_3$) are also present and the balance of the sample is composed of varieties of talc ($Mg_6[Si_8O_{20}](OH)_4$).

The most likely mineral phases to oxidize under the kinetic testing conditions are the sulfides. Acidity generated from their oxidation is likely to react with calcite and to a lesser extent magnesite. Talc minerals are unlikely to react with leachate. Expected reactions are therefore of the forms:

$$Fe_{(1-x)}S_{(s)} + \left(2 - \left(\frac{x}{2}\right)\right)O_{2(g)} + xH_2O = SO_{4(aq)}^{2-} + (1-x)Fe^{2+} + 2xH^+$$

(1)

$$\left(\frac{Mg}{Ca}\right)CO_{3(s)} + SO_4^{2-} - H^+ = \frac{Mg^{2+}}{Ca_{(aq)}}SO_{4(aq)}^{2-} + H_2O + CO_{2(g)}$$

(2)

CALCULATION OF ION PAIR CONCENTRATION

PHREEQC version 2.15 was used to calculate equilibrium concentrations of ion pairs from the leachate chemistry. PHREEQCi was initially developed by the United States Geological Survey and a substantial library of thermodynamic constants has built up over the ongoing development period (Appelo & Postma 2005).

Considering the other sulfides present as well, likely ion pairs present in the leachate include $FeSO_4$, $CaSO_4$, $NiSO_4$, $CuSO_4$ and $MgSO_4$.

The distributions of $CuSO_4$ and $NiSO_4$ molality (m), determined using PHREEQC, are presented as Figure 1. $NiSO_4$ m is maximum at week 15 and decreases thereafter with peaks at week 34 and around week 60.

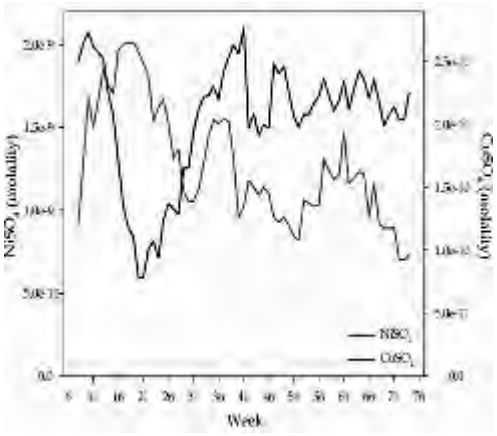

Fig. 1. Distribution of Ni and Cu Sulfate Ion Pair Molality (5 point boxcar filtered).

Table 1. Mean dissolved concentrations for chalcopyrite and pentlandite periods of kinetic tests

	Acidity	Alkalinity	SO_4^{2-}	B	Mg	Ni	K	Si	Na	Sr	$NiCO_3$*	$NiHCO_3$ *
Pentlandite (weeks 10-29)	0.96	28	37	0.086	4.5	0.0027	16	0.95	0.87	0.059	1.80E-09	1.70E-09
Chalcopyrite (weeks 31-47)	0.89	20	40	0.025	3.9	0.0012	14	0.8	0.68	0.044	7.50E-10	6.40E-10

*All concentrations in mg/L except * denotes molality*

$CuSO_4$ shows minimum concentrations around weeks 10 through 29 after which it increases and appears to approach a steady state concentration. The distribution of $FeSO_4$ molality (not shown) is less variable, which is expected since Fe is present in all sulfide phases. The distributions of $NiSO_4$ and $CuSO_4$ suggest that Pentlandite oxidizes before Chalcopyrite since the molality of the sulfates are the products of these reactions. The products of each oxidation reaction are linked by the oxidation reaction of type (*Eq.1*). Correlation in the analytical data for these parameters should be higher when these reactions are occurring. Correlation coefficients for the Ni/SO_4 and Cu/SO_4 ion pairs are presented in Figure 2. The coefficients are calculated using an un-weighted seven point sliding window and the results are smoothed using an un-weighted three point window.

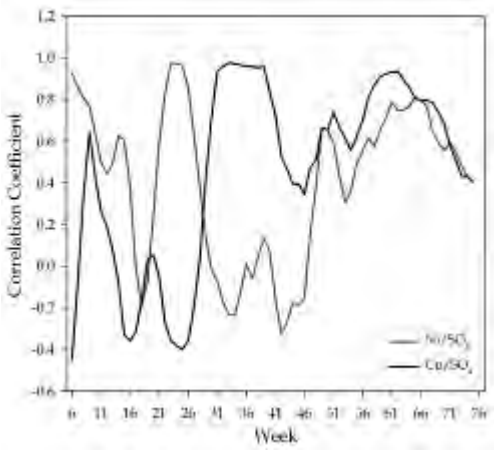

Fig. 2. Smoothed 7-point Sliding Correlation Coefficients for Ni/SO_4 and Cu/SO_4.

High values of $NiSO_4$ and $CuSO_4$ correspond to high values of the appropriate correlation coefficients, confirming the interpretation that pentlandite oxidizes first, around weeks 10 through 29, but also from weeks 50 through 70. Chalcopyrite appears to be actively oxidizing from approximately week 31 through the end of the kinetic test. The ability to identify periods of the tailings kinetic testing when individual sulfide minerals are oxidizing makes the testing data much more useful for design of the tailings management strategy, especially regarding potential changes in ore composition or metallurgical processing. For example, for the Bucko test, during weeks 10 through 29 there is minimal chalcopyrite oxidation and during weeks 31 through 47 there is minimal pentlandite oxidation. Table 1 compares leachate chemistry for the periods of pentlandite and chalcopyrite oxidation. Periods of pyrrhotite and pyrite oxidation cannot be discriminated using the above methodology since iron is present in all sulfides, therefore pyrrhotite and pyrite may also be oxidizing during the two periods compared.

The most significant differences are for B and Ni, which are both over twice the concentrations when pentlandite is oxidizing compared to the period of chalcopyrite oxidation. Ni carbonate and bicarbonate species show the greatest increases in concentration. Leachate generated during periods of increased chalcopyrite oxidation does not show increases in any parameters. Clearly, changes in pentlandite content of the tailings, either from changes in ore, metallurgical processes or sulfide segregation at deposition potentially present a higher environmental concern than changes in chalcopyrite content. The ability to characterize differences of this nature is of significant benefit in management of tailings facility and deposition design and also provides

valuable input into metallurgical process design criteria.

CONCLUSIONS

Periods of kinetic testing of tailings where individual sulfide phases are oxidizing were identified in highly auto-correlated data from the Crowflight Minerals Bucko Lake Nickel Project using PHREEQC modelling and sliding correlation coefficients in tandem with mineralogical data. This capability provides significant added value to kinetic testing data through the increased ability to utilize the data in tailings management.

ACKNOWLEDGEMENTS

The authors acknowledge and thank Crowflight Mineral Inc for permission to use the case study and Wardrop Engineering Inc. for support and reviews.

REFERENCES

APELLO, C.A.J. & POSTMA, D. 2005. *Geochemistry, Groundwater and Pollution, 2nd Edition*. CRC Press; Boca Raton.

ARDAU, C., BLOWES, D.W. & PTACEK, C.J. 2009. Comparison of laboratory testing protocols to field observations of the weathering of sulfide-bearing mine tailings. *Journal of Geochemical Exploration*, **100**, 182-191.

ASTM. 2001. Standard test method for accelerated weathering of solid materials using a modified humidity cell. **Method D5744–96**.

BLOWES, D.W., PTACEK, C.J., JAMBOR, J.L., & WEISENER, C.G. 2003. The geochemistry of acid mine drainage. In: LOLLAR, B.S. (ed.) *Environmental Geochemistry, Treatise on Geochemistry* (eds. HOLLAND, H.D.; TUREKIAN, K.K.) Elsevier-Pergamon, Oxford. **9**, 149-204.

BOWELL, R.J. & PARSHLEY, J.V. 2005. Mineralogical controls on Pit Lake geochemistry, summer Camp Pit, Nevada. *Chemical Geology*, **215**, 373-385.

CERIOLI, A. & RIANI, M. 2005. Studies in Classification, Data Analysis, and Knowledge Organization. *Data and Information Analysis to Knowledge Engineering. The 29th Annual Conference of the German Classification Society.* University of Magdeburg.

DAY, S.J., HOPE, G., & KUIT, W. 1997. Waste rock management planning for the Kudz Ze Kayah project, Yukon Territory: 1. Predictive Static and Kinetic Test Work. *Proceedings of the 4th International Conference on Acid Rock Drainage*. Vancouver, **I**, 81-98.

FROSTAD, S., KLEIN, B., & LAWRENCE, R.W. 2002. Evaluation of laboratory kinetic test methods for measuring rates of weathering. *Mine Water and the Environment,* **21**, 183-192.

JAMBOR, J.L., DUTRIZAC, J.E., GROAT, L.A., & RAUDSEPP, M. 2002. Static tests of neutralization potentials of silicate and aluminosilicate minerals. *Environmental Geology*, **43**, 1-17.

LAPAKKO, K.A. & WHITE, W.W.III. 2000. Modification of the ASTM 5744-96 kinetic test. *Proceedings from the 5th International Conference on Acid Rock Drainage*. Littleton, 631-639.

MERANGER, J.C., GLADWELL, D.R., & LETT, R.E. 1986. Application of a conceptual model to assessing the impact of acid rain on drinking water quality. *WHO Water Quality Bulletin*, **11**, 179-186.

MORIN, K. 1985. Simplified explanations and examples of computerized methods for calculating chemical equilibria in water. *Computers and Geoscience*, **11**, 409-416.

MORIN, K.A. & HUTT, N.M. 1997. *Environmental Geochemistry of Minesite Drainage: Practical Theory and Case Studies*. MDAG Publishing, Vancouver.

PRICE, W.A., MORIN, K.A., & HUTT, N.M. 1997. Guidelines for the prediction of acid rock drainage and metal leaching for mines in British Columbia: Part II. Recommended procedures for static and kinetic testing. In: *Proceedings of the 4th International Conference on Acid Rock Drainage.* Vancouver, **I**, 15-30.

SAPSFORD, D.J., BOWELL, R.J., DEY, M., & WILLIAMS, K.P. 2009. Humidity cell tests for the prediction of acid rock drainage. *Minerals Engineering*, **22**, 25-36.

Large-scale hydrogeochemical mapping - insight into alteration processes and prospectivity mapping

David J Gray, Ryan R.P. Noble, & Nathan Reid
CSIRO Exploration and Mining, 26 Dick Perry Ave, Kensington, WA, 6117 AUSTRALIA
(e-mail: david.gray@csiro.au)

ABSTRACT: The hydrogeochemistry of the northern Yilgarn Craton of Western Australia has been examined to assess the utility of groundwater for regional exploration for Ni, Au, Zn and U mineralization. The objective was to develop reliable regional hydrogeochemical vectors to mineralization in the study area, as well as establish size of geochemical haloes from various systems, and determine regional background concentrations for environmental and exploration purposes. Approximately 1400 samples were collected across and area of 500 x 300 km with additional samples from selected sites near differing mineralisation styles. Results corroborate established geochemical weathering models around sulfide mineralisation, clearly depict major U systems, and have been valuable for understanding background concentrations of elements, particularly those of environmental importance such Cr, As and NO_3. Regional groundwater chemistry shows potential for discovering large mineralised systems in deeply covered terrains that are often uneconomical to explore with more traditional methods.

KEYWORDS: *groundwater, Yilgarn, Western Australia, sulfide weathering, exploration*

INTRODUCTION

Following on from a successful groundwater sampling study along the Leonora-Wiluna Belt (Gray & Noble 2007), a hydrogeochemical mapping project for the northern Yilgarn was established as a proof of concept for broad scale hydrogeochemistry, with potential for mapping, environmental background establishment and mineral exploration across many other areas of Western Australia, especially outside recognized mineralisation belts.

GEOLOGICAL SETTING

The Archaean Yilgarn Craton is composed mainly of granite, with mafic, volcanic and sedimentary “greenstone” rocks. It is one of the world's principal mineral provinces, with considerable resources of primary and supergene Au, sulfide-hosted and lateritic nickel, bauxite, as well as a wide range of other commodities.

Much of the Yilgarn (~70%) is under transported cover and exploration has relied heavily on geochemical sampling either at surface or from depth (drilling). Two broad regions (north and south) are identified based on their regolith history, vegetation, rainfall pattern and groundwater characteristics. The boundary between these regions is quite sharp, approximately coincident with latitude 30ºS – commonly called the *Menzies Line*. In the north, groundwaters are fresh and neutral, trending more saline in the valley axes, whereas in the south, groundwaters are commonly neutral to acid, saline to hyper-saline and reducing. These regional variations have major effects on the dispersion of many elements and their distribution in the regolith.

METHODS AND MATERIALS

Approximately 1400 samples were collected from predominantly farm wells and bores, although dewatering bores and groundwater monitoring bores were also sampled. Water was collected from the outflow pipe when the bore or well was operational, or bailed using a flow-though system with one-way valves. Additional samples were added to the assessment from previous work to enhance the study around key mineralised sites such as

those shown in Figures 1 and 2.

Field measurements included pH, Eh, EC, temperature, depth of water table and depth of sample collection. Separate, field preserved sub-samples were collected for cation (ICP-MS/OES), anion (IC), alkalinity (titration), DOC, PO_4 and Au and PGE analysis (using carbon sorption).

One litre of unfiltered water was rolled with a carbon sachet and 10g NaCl for 7 days. The carbon was then dried, ashed, digested in aqua regia and analysed by ICP-MS, for Ag, Au, Pd, and Pt. Field and analytical blanks, as well as duplicates were used in all analyses to ensure accuracy (Gray *et al.* 2001).

GROUNDWATER CHARACTERISTICS OF DIFFERING DEPOSIT TYPES

Orogenic Gold

South of the Menzies Line, gold dissolves as Au halide (Gray *et al.* 2001). Dissolved Au concentrations reach µg/L levels, with groundwater anomalies greater than 200 m spatial extent. To the north, anomalous Au concentrations are much lower (> 5 ng/L is anomalous), though the spatial extent is similar.

In the northern Yilgarn and surrounding areas, such as the Baxter deposit) chalcophile elements are enriched in groundwaters contacting with weathering sulfides (e.g., As, Mo, Ag, Sb, W, Tl, and Bi) and these may be more useful regional exploration tools than dissolved Au itself (Fig. 1).

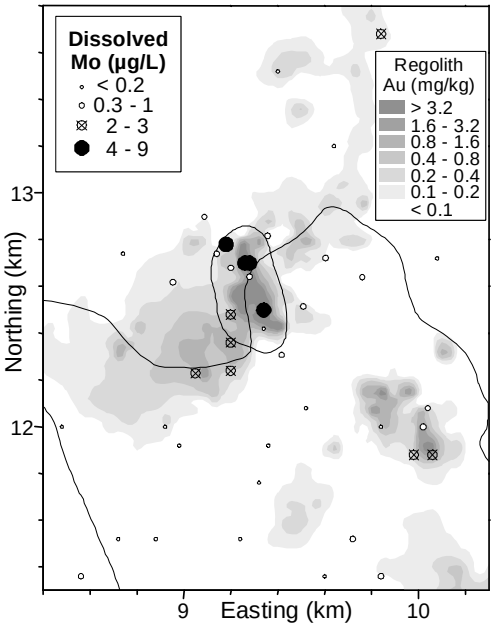

Fig. 1. Dissolved Mo distribution at the Baxter deposit in Western Australia has a much greater and consistent anomaly compared to dissolved Au (not shown). The results are superimposed on maximum Au contents in the regolith to show the extent of mineralisation.

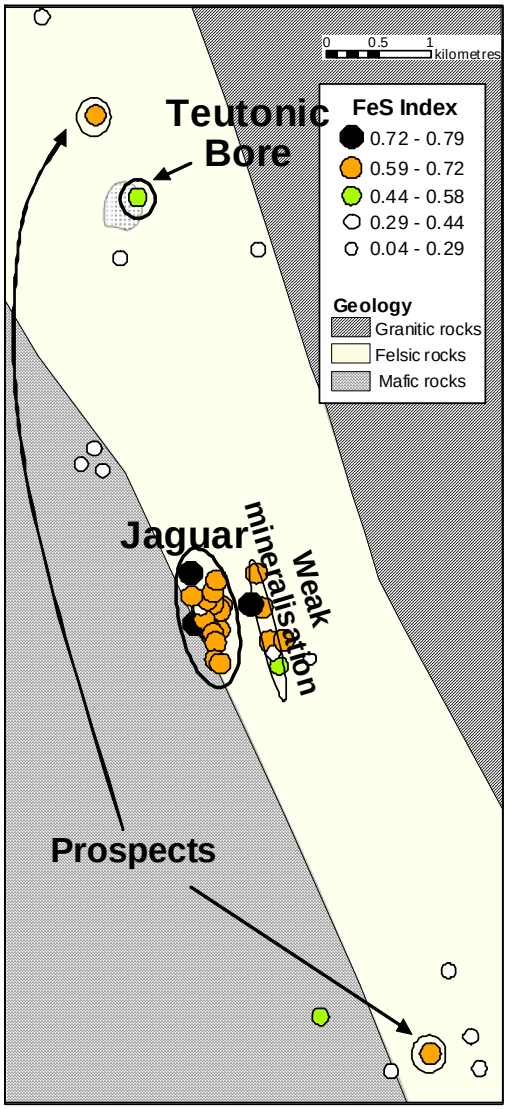

Fig. 2. The distribution of the calculated FeS index from groundwater results at the Teutonic Bore / Jaguar VMS camp. Results correlate closely with known ore bodies and prospects.

Nickel Sulfides

The development of reliable regional and smaller-scale hydrogeochemical vectors to Ni sulfide mineralisation in weathered terrains requires understanding of controls on Ni-S weathering.

The first alteration phase is the partial sulfide oxidation: pyrrhotite → pyrite and pentlandite → violarite, which can utilise either sulfate or bicarbonate as oxidants:

This causes sulfate and bicarbonate depletion in deep groundwaters around mineralisation.

In shallow groundwaters, dissolved nitrate is a strong oxidant in high concentrations (> 100 mg/L) across much of central Australia, and is possibly derived from "leakage" from nitrogen

$$5FeS + SO_4^{2-} + 4H2O \rightarrow 3FeS_2 + 2Fe(OH)_3 + 2OH^- \quad (1)$$

fixing nodules in *Acacia* sp. roots. The reduction of nitrate and the oxidation of pyrite and violarite results in nitrate depletion and sulfate enrichment in groundwater:

$$2FeS_2 + 6NO_3^- + 4H2O \rightarrow 2Fe(OH)_3 + 4SO_4^{2-} + 3N_2 + 2H^+ \quad (2)$$

Thus use of sulfate and nitrate is effective at detecting the presence of sulfides. Other indices, consistent with the model for groundwater evolution around weathering sulfides, delineate the sulfide signature independent of the type of water i.e. varied Eh and pH. The better performing indices for mineralization targeting are:

Mineralised (Ni+Co+W+Pt)
Acid Sulfides (Mo+Ba+Li+Al) and
FeS (pH-Eh+Fe+Mn)

Combined indices use the *mineralised* signature and take away the *acid sulfides* or the *FeS index*. Massive NiS gave stronger groundwater signatures than disseminated mineralisation, which commonly were only clearly delineated using these combined indices.

Volcanic Massive Sulfides

VMS exploration using groundwaters uses similar principles to NiS exploration using a combination of parameters for finding sulfides (Fig. 2), then distinguishing VMS using other parameters including Ag, Pt, W. Metals such as Cu or Zn can give very high (>> mg/L) anomalism, although the spatial distribution is highly variable.

Palaeochannel Uranium

Secondary uranium (carnotite; $K_2(UO_2)_2(VO_4)_2 \cdot 3H_2O$) commonly shows a strong groundwater signature (Fig. 3), and hydrogeochemical exploration is likely to be successful, particularly in the northern parts of the Yilgarn Craton (Gray & Noble 2007; Fig. 3) and elsewhere in central Australia. Uranium mineral saturation indices are also valuable for exploration targeting.

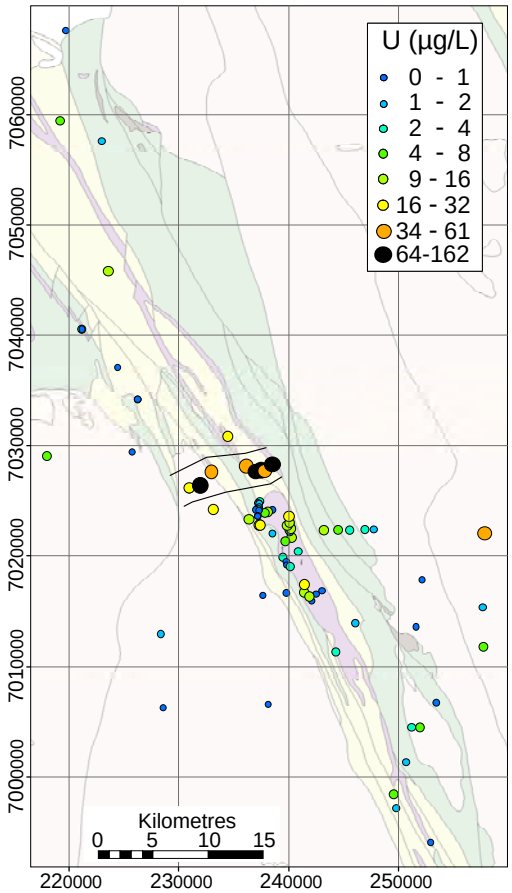

Fig. 3. Dissolved uranium at Honeymoon Well. The Centripede Palaeochannel uranium deposit is clearly deliniated.

Another area for research is how groundwater fluxes of vanadium (critical for carnotite precipitation) and phosphate (enhances uranium mobility) are controlled by geology and geomorphology. This may assist in targeting economic from sub-economic targets.

HYDROGEOCHEMICAL MAPPING

Large-scale groundwater results from the regional mapping show patterns stretching 10s of kms. Mineralisation signatures are also evident, particularly for U systems. Nitrate, Cr and As are also found in large concentrations and are valuable for assessing water resources for human and agricultural purposes. Other lithological changes between granites and greenstones, and different types of granites are also evident on the regional scale. Numerous underexplored regions have also been highlighted that, based on their groundwater signature, may warrant further exploration.

CONCLUSIONS

Results which corroborate established geochemical weathering models around sulfide mineralisation, clearly depict major U systems, and have been valuable for understanding background concentrations of elements, particularly those of environmental importance such Cr, As and NO_3. The use of NO_3 and SO_4 for exploration is an important new development for exploration targeting of sulfide systems. Regional groundwater chemistry shows good potential for discovering large mineralised systems in deeply covered terrains that are often uneconomical to explore with more traditional methods.

ACKNOWLEDGEMENTS

We thank CSIRO and the Minerals Down Under Flagship, as well as a number of companies for the support for this research. The most recent regional study was supported by the exploration industry, GSWA, MERIWA, WA DoW, and GA.

REFERENCES

GRAY, D.J. 2001. Hydrogeochemistry in the Yilgarn Craton. *Geochemistry: Exploration, Environment, Analysis*, **1**, 253–264.

GRAY D.J. & NOBLE R.R.P. 2007. Nickel hydrogeochemistry of the NE Yilgarn Craton, Western Australia. CSIRO Division of Exploration and Mining Restricted Report P2006/524. CRC LEME *Open File Report* **243R**, 133 p.

Ontario's ambient groundwater geochemistry project

Stewart M. Hamilton[1]
[1]*Ontario Geological Survey, 933 Ramsey Lake Road, Sudbury, ON CANADA*
(e-mail: stew.hamilton@ontario.ca)

ABSTRACT: The Ontario Geological Survey has recently completed the second year of a multi-year groundwater sampling project that is intended to cover all the accessible areas of the one million square kilometre province of Ontario. The project will provide baseline groundwater quality for policy makers and other stakeholders. Areas of natural groundwater quality hazards are being outlined and the chemistry of groundwater will be established with a specific focus on the effect of geology on water quality. Samples are being collected from domestic wells on a regular 10x10 km grid with one sample being collected from an overburden well and another from bedrock in each node. The study is helping to establish 'normal' levels of over 80 parameters in groundwater, many of which have poorly understood range and distribution in natural groundwaters. Preliminary results demonstrate that geology indeed plays an important role in the distribution of dissolved constituents. Concentrations of natural hazards such as fluoride are controlled by the nature and distribution of the host rock.

KEYWORDS: *groundwater geochemistry, background concentrations, well sampling*

INTRODUCTION

Ontario encompasses approximately one million km^2 and is Canada's 2nd largest province. Across Ontario, natural water quality variations exist in groundwater-sourced water supplies that have the potential to impact human health and limit the usability of the resource. Most of these variations, including well-known regional water quality problems, can be attributed to easily definable geological conditions. Until recently no detailed province-wide groundwater geochemical study had ever been carried out that delineates areas of poor water quality and attempts to relate them to variations in rock and soil type despite very large amounts of geochemical data that exist in the public domain. Part of the reason for this is that the available data were collected in myriad studies by different groups and, as such, sampling was carried out over limited areas at various scales, with analysis being done to various standards of precision and accuracy. In addition, many analyses did not determine a wide enough range of parameters to allow comparison of any one parameter across the province as a whole or even within particular geological units. This project was initiated by the OGS initiated in part to address these knowledge gaps.

THE RELATIONSHIP BETWEEN GEOLOGY AND WATER GEOCHEMISTRY

The OGS regularly receives requests from the public, other government agencies and private sector companies for data that show 'normal' levels of dissolved constituents in waters. Since the geochemistry of groundwater is strongly influenced by the nature of aquifer materials, a 'normal' level for parameters in groundwater such as mercury, arsenic or nitrate is meaningless outside its geological context.

Rainwater is the ultimate source of recharge and resupply of all terrestrial waters. The total dissolved solids (TDS) content of rainwater rarely exceeds 10 parts per million (ppm) but is much higher for groundwater, river water and lake water (Fig. 1).

The increased solute-loading in terrestrial waters is due to dissolution of minerals in rock, soil and overburden materials as rainwater infiltrates them. Groundwater experiences the largest degree of water-rock interaction and consequently has the highest average

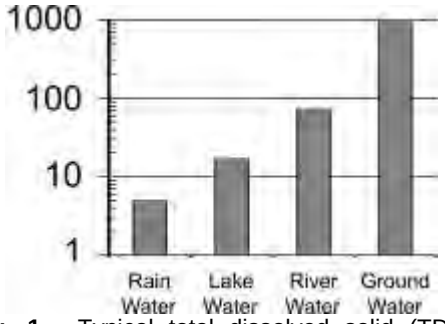

Fig. 1. Typical total dissolved solid (TDS) concentrations (mg/L) in terrestrial waters (from various sources listed in Hamilton *et al.* 2007).

TDS loading; lake-water experiences the least and has correspondingly lower loading. River water is a mixture of rainwater runoff and groundwater base flow and has intermediate amounts of TDS. This project seeks to collect representative numbers of groundwater samples in the major rock and overburden units in the province. This will help to establish background levels in an appropriate geological context and to understand the sources of minerals, nutrients and potential hazards in groundwater.

SAMPLING APPROACH

Groundwater samples are collected from domestic wells on a regular 10x10 km grid. One sample within each grid node is collected from a well finished in bedrock and another from overburden.

Only untreated water is collected and samples are taken from the point in the domestic plumbing that is closest to the well. Information on the pump, plumbing and well are also collected from the homeowner or from Ontario Ministry of Environment water well records database.

Wells are purged until stable readings are obtained for field chemical parameters including pH, temperature, dissolved oxygen, redox and electrical conductivity. Samples are then collected for a wide variety of chemical parameters. Time sensitive parameters are analyzed within specific holding times. For example, alkalinity and hydrogen sulphide are measured at the time of sampling, iodide within 24 hours and nitrogen parameters and bacteria within 48 hours.

Good quality control procedures are crucial to allowing the results of this project to integrated year upon year. More than 10% of all samples analyzed are for quality control. About half of these are duplicates; the others are blanks, certified or internal reference standards and spiked samples.

RESULTS TO DATE

The 2007 and 2008 study areas covered 9,700 and 12,000 km2 respectively and collected close to 500 groundwater samples (Fig. 2). The results of analyses for the second year are complete and are currently being processed. Results for the first year and preliminary results for 2008 demonstrate the remarkable effect that geology has on groundwater geochemistry. Most of the more than 80 geochemical parameters show correlation with at least one of the 10 major rock units in the study areas. For example F^-, a health related parameter, and H_2S are elevated in the Hamilton Group shales. Light rare earth elements also show enrichment in this unit but the heavy rare earth elements are more enriched in the stratigraphically higher Kettle Point shales.

CONCLUSIONS

The results from the first 2 years of the Ambient Groundwater Geochemistry project demonstrate very clearly that:
(1) anthropogenic contaminants only occur locally in isolated areas and very rarely in bedrock wells;
(2) geology is the ultimate source of most chemical constituents in groundwater; and
(3) the geological context must be considered when determining the 'normal' level of any parameter.

This project will be an ongoing part of the OGS program for the foreseeable future. In addition to maintaining high sampling and analytical standards, a key challenge will be the seamless integration of the data year upon year as analytical methods improve. This and related problems are the subject of ongoing research at the OGS.

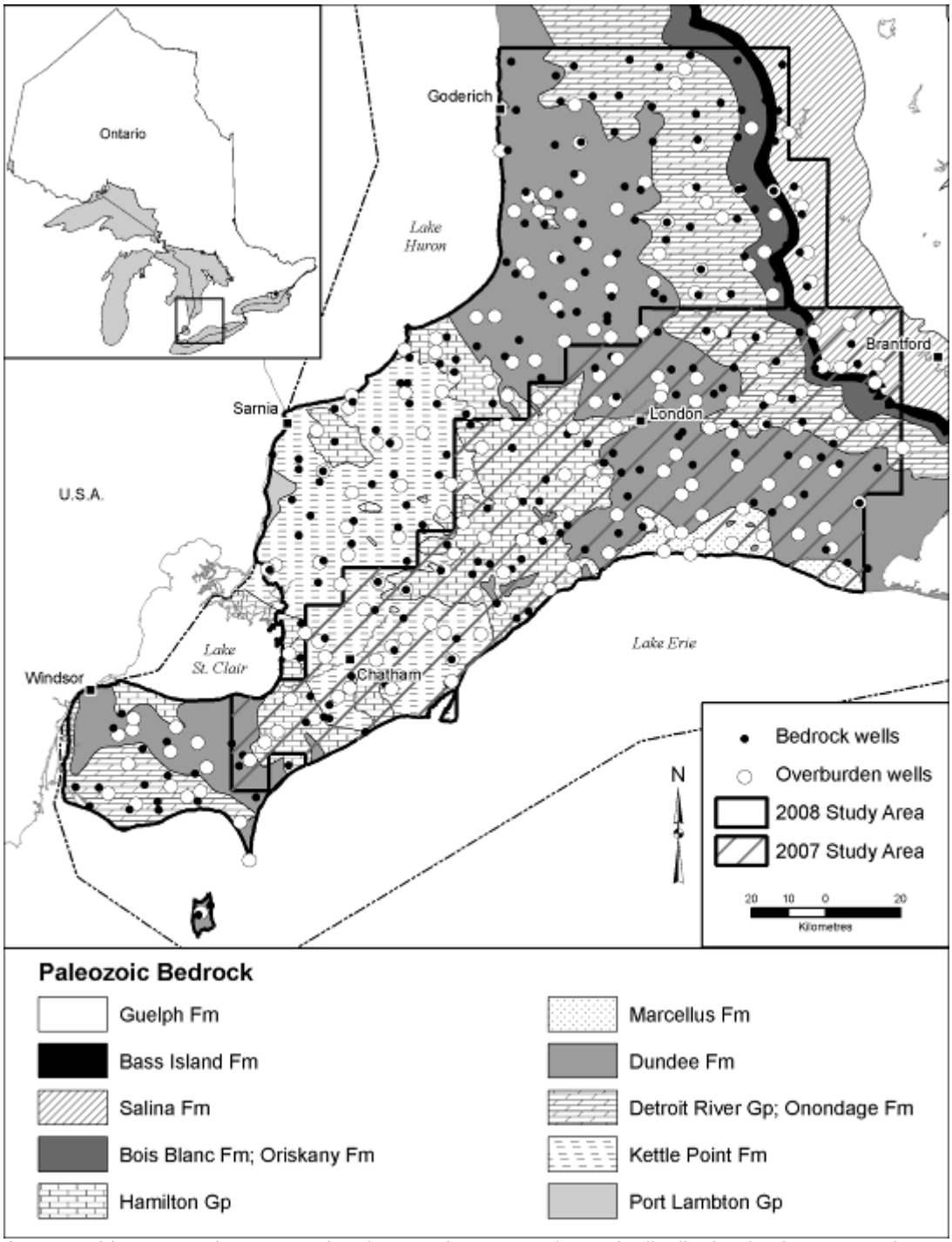

Fig. 2. Ambient Groundwater Geochemistry study areas and sample distribution for the 2007 and 2008 seasons (from Hamilton & Brauneder 2008).

REFERENCES

HAMILTON, S.M. & BRAUNEDER, K. 2008. The Ambient Groundwater Geochemistry Project: Year 2; in *Summary of Fieldwork and Other Activities*, Ontario Geological Survey Open File Report **6226**, 34-1 to 34-7.

HAMILTON, S.M., BRAUNEDER, K., & MELLOR, K.J. 2007. The Ambient Groundwater Geochemistry Project – Southwestern Ontario; in *Summary of Fieldwork and Other Activities*, Ontario Geological Survey Open File Report **6213**, 23-1 to 23-5.

Distribution of cadmium forms and their correlation with organic matters in acid soils

Wei Hualing[1,2] & Zhou Guohua[1,2]

[1] *Institute of Geophysical and Geochemical Exploration,Langfang, CO, 065000,Hebei China*
(e-mail: weihualing@igge.cn)
[2]*Key Laboratory of Applied Geochemistry, CAGS, Langfang, CO, 065000,Hebei China*

ABSTRACT: The activation, migration, transformation of heavy metals in soils can have environmental impact on human being and animals. Cadmium forms in soil can be classified into water-extractable, adsorbed and exchangeable, carbonate bounded, humic acid bounded, occluded metals onto Fe-Mn oxides, organically bounded and residual metals. This study focused on the distribution of Cd forms and their correlation with organic matters in the acid soils of Zhejiang, eastern China. The results show that Cadmium in soils mainly occurs as adsorbed and exchangeable forms and carbonate bounded forms in the acid soils, and its contents are relatively low as other forms. Organic matter is one of major factors controlling Cd forms.

KEYWORDS: *Cadmium forms, organic matter, acid soils*

INTRODUCTION

Heavy metals in the environment, especially their accumulation in soils, is a serious environmental problem which the whole world faces (Du *et al.* 2005). The farmland soils are an important media of the ecological cycle of Cadmium, and its harm to human health can't be neglected (Wu *et al.* 2004). Heavy metal migration, transformation and toxicity to plants in soil are directly influenced by the quantity proportions of various forms (Zhu *et al.* 2002). The toxicity of water-extractable and adsorbed and exchangeable metals are the greatest, and residual metals is the lowest (Liu *et al.* 2002). Different forms have different bioavailability thus their influences on the environment and human health are different. It is critical to have a good understanding of Cadmium forms in soil. This paper describes the Cadmium forms in the acid soils of eastern China.

SAMPLING AND ANALYSIS

In this study, 30 soil samples from rice farmland in Zhejiang province, in eastern China. We sampled the cultivation layer soils during rice harvest season. The soils are acidified and the average value of pH is 5.82. A sequential extraction procedure with seven steps was used to extract the cadmium forms which was determined by ICP-MS (technical requirements of sample analysis in ecological geochemical assessment (trial Implementation), 2005). Water-extractable forms was extracted by distilled water, adsorbed and exchangeable forms by $MgCl_2$,. carbonate bounded metals by NaAc acid glacial acedic acid,. Humic acid bounded forms by sodium pyrophosphate, occluded forms onto Fe-Mn oxides by hydroxylamine Hydrochloride, organically bounded forms by H_2O_2 and residual forms by hydrofluoric acid acids.

RESULTS AND DISCUSSION

Cd Forms in the Soils

The proportion of various Cd forms in soils are shown in Figure 1. water-extractable forms make up 2.0%, adsorbed and exchangeable forms, 57%, carbonate bounded forms, 10.9%, humic bounded forms, 4.8%, occluded forms onto Fe-Mn oxides, 8.1%, organically bounded forms, 8.1%, and residual forms, 9.0%. Proportions of adsorbed and exchangeable forms >carbonate bounded forms>residual forms> occluded forms onto Fe-Mn oxides =organically bounded forms> Humic acid bounded forms

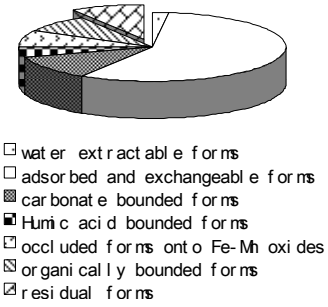

Fig. 1. Pie showing the proportion of Cd forms.

>water-extractable forms. The results show that Cd mainly occurs as non-residual forms in soils, and its proportion accounts for 90% of the total Cd. And among non-residual forms, adsorded and exchangeable forms are dominated, which is bioavailable forms (Tu 1997; Wang 1997).

Correlation Between Cd Forms and Organic Matter

The amount of organic matters not only determines the nutrition of the soils, but also form complex compound with heavy metals to influence metal migration and bioavailability (Liu *et al*. 2002). From table 1, we can found that extractable Cd contents, especially occluded Cd onto Fe-Mn oxides and organically bounded Cd has a prominent positive correlation with organic matters (α =0.05,n =30, F =0.361), (Fig. 2). Organic matters are one of the major factors which influence Cd occurrence forms. Bioavailable Cd increases with the content increase of soil organic matter.

CONCLUSIONS

(1) Cadmium in acid soils mainly occurs as adsorbed and exchangeable forms.

(2) There is a good correlation between organic matters and contents of various Cd forms. Organic matters can make Cadmium activate in the soils and lead to, biological toxicity.

ACKNOWLEDGEMENTS

We thank all the members of Key Laboratory of Applied Geochemistry, who have helped with collecting sampling, analysis and data processing.

Table 1. Correlation coefficient of Cd forms and organic matters.

Cd forms	organic matters
Water-extractable Cd	0.399
adsorbed and exchangeable Cd	0.478
carbonate bounded Cd	0.480
Humic Cd	0.480
occluded Cd onto Fe-Mn oxides	0.559
organically bounded Cd	0.559
residual forms	0.248

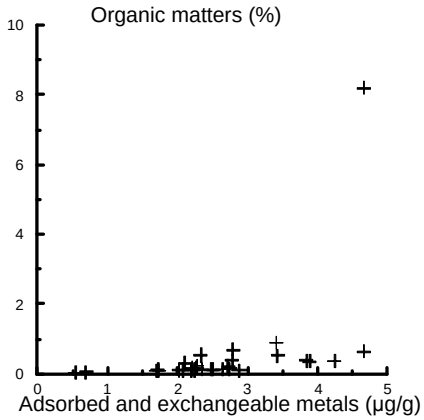

Fig. 2. Plot showing correlation between contents of adsorbed and exchangeable Cd and organic matters.

REFERENCES

CHINA GEOLOGICAL SURVEY. 2005 Technical Requirements of Sample Analysis in Ecological Geochemical Assessment (trial Implementation). DD2005-03 (in Chinese).

DU CAIYAN, ZU YANQUN, & LI YUAN. 2005. Effect of pH and Organic Matteron the Bioavailability Cd and Zn in Soil. *Journal of Yunnan Agricultural University*, **20**(4), 539-543 (in Chinese with English abstract).

LIU XIA, LIU SHUQING, & TANG ZHAOHONG. 2002. The Relationship Between Cd and Pb Forms and Their Availability to Rape in Major Soils of Hebei Province. *Actaecologica Sinica*, **22**(10), 1688-1694 (in Chinese with English abstract).

TU CONG. 1997. Bioavailability of Ni fractions in

soils. *Acta Scientiae Circumstantiae.***17**(2), 179-185.

WANG, P.X., QU, E.F., LI, Z.B., & SHUMAN, L. M. 1997. Fractions and availability of nickel in Loessial soil amended with sewage sludge or sewage. *Environ Qual.,***26**, 795-800. (in Chinese with English abstract).

WU TAO, ZENG YING, & NI SHIJUN. 2004. A Study on Cadmium Forms in Farmland Soil in the Suburb of Chengdu. *Shanghai Environment Sciences,* **23**(6), 236-23.

ZHU BO, QING CHANGLE, & MU SHUSEN. 2002. Bioavailability of exotic zinc and cadmium in purple soil. *Chinese Journal of Applied Ecology*,**13**(5), 555-558 (in Chinese with English abstract).

Adaptation of the OECD T/DP for metals and metal compounds to marine systems

Philippa Huntsman-Mapila[1], Jim Skeaff[1], Marcin Pawlak[1], Hayley Roach[1], & Dave Hardy[1]

[1]CANMET-MMSL, 555 Booth St., Ottawa, Ontario, K1A 0G1 CANADA
(e-mail:phuntsma@nrcan.gc.ca)

ABSTRACT: The transformation/dissolution (T/D) characteristics of metals and alloys in a marine medium in seven- and twenty eight- day tests are being evaluated in this project. The two metals tested to date were selected based on data availability from freshwater T/D testing: cuprous oxide powder (Cu_2O) and nickel metal powder (Ni). Prior to T/D testing, trace metals are initially removed from the marine medium with a Chelex-100 resin, while following T/D testing they are separated from the saltwater matrix by a metal chelation step with flow injection and analysed by ICP-AES. The marine media T/D data yields useful comparisons with data reported earlier for the freshwater OECD 203-based media at pH 6 and 8 and provides insight into the behaviour of metal-bearing substances in commerce under marine transformation/dissolution protocol (T/DP) conditions. Furthermore, the collected data supports an approach directed to the extension of the application of the T/DP to derive hazard classification proposals with respect to the marine environment.

KEYWORDS: *metals, marine systems, transformation/dissolution protocol*

INTRODUCTION

The United Nations Globally Harmonized System of Classification and Labelling of Chemicals (GHS) includes an internationally standardized guidance procedure on Transformation/Dissolution Protocol (T/DP) for metals and sparingly soluble metal compounds (United Nations, 2007), recently validated by the OECD (Organization for Economic Cooperation and Development). To establish the acute aquatic hazard classification level of a metal-bearing substance under the GHS, data from the T/DP are compared with an acute ecotoxicity reference value (ERV) derived under conditions similar to those of the T/DP.

Industry is obligated to submit mandatory dossiers to the REACH (Registration, Evaluation and Authorisation of Chemicals) registry, an environmental protection regulation within the framework of the European Union (EU), and are to include a GHS aquatic hazard classification proposal. Both REACH and the GHS have significant implications for environmental protection and market access for chemicals in commerce.

Freshwater media based on the OECD 203 ecotoxicity testing medium for fish and daphnia have been used in all T/DP testing of metals, metal compounds and alloys in the pH range 6-8.5 to date. However, the composition of a marine medium is also given in the T/DP section of the GHS, and by implication, a method for marine T/D testing is open for development and validation. While not currently required for REACH dossiers, T/D data in marine media and attendant classification proposals may be required in the future for marine shipping.

ANALYTICAL PROCEDURE

We followed the OECD guidance document [United Nations 2007, p. 548] for the preparation of a standardized marine test medium. The document states that trace metals should be removed from the test medium before T/D tests are performed. For this step we used a Chelex-100 resin in a column set-up with a flow rate of 5 ml/min.

Prior to analysis, solutions from seven-day T/D tests on cuprous oxide (Cu_2O) and nickel metal powder (Ni) were passed through a column with iminodiacetate functional groups using an ammonium acetate buffer. The alkali and alkali earth metals are not bound to the column thereby separating the cations associated with the saltwater matrix from the transition metals of interest which are subsequently eluted with nitric acid and analysed by ICP-AES (inductively-coupled plasma-atomic emission spectrometry).

RESULTS

The reactivity and transformation to yield soluble bioavailable species of metal-bearing substances are expected to be significantly affected by the high chloride content and other unique chemical characteristics of marine waters.

Results of the T/DP testing of copper and nickel on freshwater medium can be found in the CANMET-MMSL report (Skeaff & Hardy 2005). At pH 6 and 100 mg/L loadings, the concentrations of copper and nickel dissolved from cuprous oxide and nickel metal powder attained average seven-day concentrations of about 3,250 and 540 μg/L, respectively. The average seven-day concentrations at pH 8 and 100 mg/L loadings of copper and nickel dissolved from cuprous oxide and nickel metal powder were significantly lower than those at pH 6: about 105 and 315 μg/L, respectively. Preliminary results from the pH 8 marine testing suggest that cuprous oxide powder has a greater reactivity in marine water to the pH 8 freshwater, while nickel metal powder is significantly less reactive in the marine media than in the pH 8 freshwater.

CONCLUSIONS

This is an on-going project aimed at examining the T/D characteristics of metals and alloys in a marine medium in seven- and twenty eight-day tests. The data obtained to date on seven-day tests of cuprous oxide (Cu_2O) and nickel metal powder (Ni) provides useful comparisons with those reported earlier for the freshwater OECD 203-based media at pH 6 and 8 (Skeaff & Hardy 2005) and insight into the behaviour of metal-bearing substances used in commerce under marine conditions of the T/DP. The data supports an approach directed to the eventual adaptation, validation and application of the OECD T/DP to marine systems for the purposes of marine hazard classification of metals, metal compounds and alloys.

REFERENCES

UNITED NATIONS. 2007. *Globally Harmonized System of Classification and Labelling of Chemicals*, ST/SG/AC.10/30/Rev.2. http://www.unece.org/trans/danger/publi/ghs/ghs_rev02/02files_e.html

SKEAFF, J.M. & HARDY, D.J. 2005. Validation Study of the Draft OECD Transformation/Dissolution Protocol for Metals and Sparingly Soluble Metal Compounds, Mining and Mineral Sciences Report-MMSL 04-45(CR)/-Contract No. 6028210, Natural Resources Canada, Ottawa K1A 0G1

Ferromanganese nodules in Lake George, New Brunswick

Camilla Melrose[1] & Tom Al[1]
[1]*Department of Geology, University of New Brunswick, 2 Bailey Drive, Fredericton NB E3B 5A3 CANADA*
(e-mail: camilla.melrose@unb.ca)

ABSTRACT: Ferromanganese nodules have been found in temperate freshwater lakes around the world. They form around a central nucleus of detrital rock in concentric iron- and manganese-rich bands. These nodules form when anoxic groundwater carrying dissolved metals seeps into oxygenated lake water, resulting in the formation of oxide minerals. Radiometric dating has shown that the nodules can be as old as the age of the lakes, after the retreat of the last glaciers approximately 10,000 years ago. Transects across nodules from two locations in Lake George, New Brunswick, were analyzed using LA-ICP-MS to determine compositional variations as the nodules grew. The nodules show enrichment in trace metals near the centre that decreases outwards, reflecting changes in groundwater composition over time.

KEYWORDS: *ferromanganese, nodules, lakes, trace metals, LA-ICP-MS*

INTRODUCTION

Ferromanganese nodules have been identified and described in temperate lakes around the world. These nodules were first described by Honeyman (1881) who thought they were fragments of prehistoric pottery. Further investigation showed that the nodules were composed of iron and manganese oxides (Honeyman 1881).

Ferromanganese nodules found in freshwater lakes show concentric, alternating, iron- and manganese-rich bands radiating out from a central nucleus of detrital rock (e.g. Harriss & Troup 1970). The nodules are found primarily in shallow (1-5 meters depth) regions of lakes, in regions with little to no fine-grained sediment accumulation (e.g. Kindle 1935).

GEOGRAPHIC SETTING

Ferromanganese nodules found in Lake George, New Brunswick are the focus of this project. Lake George is situated approximately 35 km southwest of Fredericton (Fig. 1).

Lake George is approximately 2.5 km wide and 3.5 km long, with a maximum depth of approximately 4 meters. Nodules were sampled from two locations on either side of the lake for this study (Fig. 2).

Fig. 1. Map of the Maritime Provinces showing the location of Lake George, to the southwest of Fredericton.

FORMATION OF NODULES

The nodules form when anoxic groundwater carrying dissolved metals seeps up through the ground-water interface (Fig.3). The dissolved oxygen present in the lake water oxidizes the metals, resulting in the precipitation of iron- and manganese-oxides that form coatings on rock fragments.

Iron and manganese oxidize to form insoluble precipitates by the following reactions:

$$Fe^{2+}_{(aq)} + \tfrac{1}{4}O_{2(aq)} + 1\tfrac{1}{2}H_2O \rightarrow FeO(OH)_{(s)} + 2H^{+}_{(aq)} \quad (1)$$

and

$$Mn^{2+}_{(aq)} + \tfrac{1}{2}O_{2(aq)} + H_2O \rightarrow MnO_{2(s)} + 2H^{+}_{(aq)} \quad (2)$$

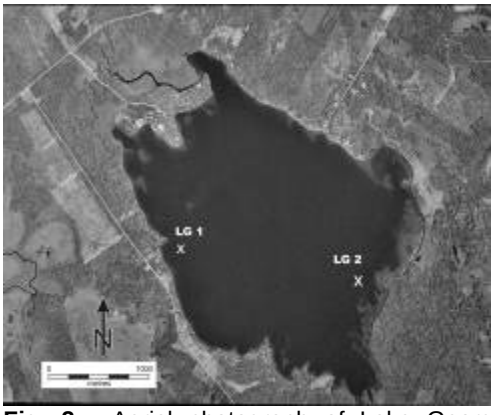

Fig. 2. Aerial photograph of Lake George showing the two sampling locations LG1 and LG2.

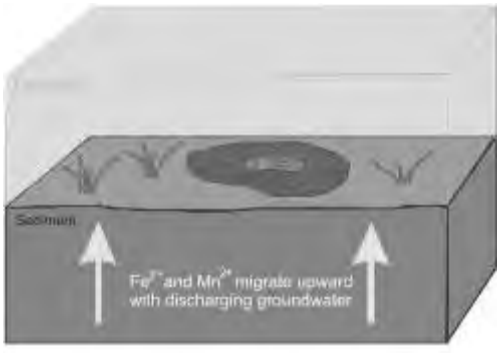

Fig. 3. Diagram illustrating the formation of ferromanganese nodules.

Fe^{2+} will spontaneously oxidize to Fe^{3+} by the process show in reaction 1 under neutral pH conditions in the presence of oxygen (Apello & Postma 1995). Under the same conditions, however, Mn^{2+} will remain as a dissolved ion (Apello & Postma 1995). Manganese oxidizing bacteria are common in freshwater lakes (Gregory & Staley 1982), and have been shown to control manganese cycling in the environment (Chapnick *et al.* 1982). As a result, Fe-oxidation is thought to continue year-round, while Mn-oxidation can only occur during the warmer months, when bacteria populations can flourish (Chapnick *et al.* 1982). This episodic pattern of Mn precipitation may explain the concentric banding observed in the nodules (Fig. 4). Mn-rich bands form during the spring and summer, when the oxidation of manganese is bacterially mediated, and Fe-rich bands would form during the winter, when iron continues to oxidize and precipitate, but Mn-oxidation is arrested (Harriss & Troup 1970).

AGE OF NODULES

Initial estimates of the growth rates of the nodules, and thus the age of the nodules, were based on the idea that one pair of Fe-rich and Mn-rich bands represent one year's growth. Growth rates of 0.1 to 1.5 mm/yr were calculated based on the thicknesses of the concentric bands (Harriss & Troup 1969). Based on this estimation the largest nodules would be approximately 1600 years old (Harriss & Troup 1969).

Radiometric isotope dating provides a more reliable way to estimate the growth rates and ages of the nodules. Moore and Dean (1979) studied nodules from Oneida Lake, USA, and found that, in cross-section, the nodules were characterized by regions showing little change in the amount of ^{226}Ra present, followed by sharp decreases in ^{226}Ra at specific ring boundaries. Such profiles can be explained by a pattern of short periods of concretion growth followed by periods with either no growth or with dissolution of the nodules (Moore & Dean 1979). These measurements give growth rates of 0.009 to 0.016 mm/yr with periods of no growth or dissolution of 500 to 1000 years. At these growth rates the largest nodules would be 10 000 years old (Moore & Dean 1979).

COMPOSITION OF NODULES

Since the nodules form by precipitation of Fe and Mn in groundwater, and other dissolved constituents originating either from the groundwater or the lake water, the composition of the nodules varies according to their location on the lake bed. A comparison of the groundwater and lake

water at Lake George shows that the groundwater contains relatively high concentrations of dissolved ions compared to the lake water. Table 1 compares the elemental composition of representative groundwater and lake water samples collected at LG2 on Sept 11 2008.

The bulk Fe and Mn composition of the nodules is variable and, they contain a variety of trace elements, including significant amounts of P, Ba and As (Table 2).

LA-ICP-MS was used to determine the compositional variation in the nodules along transects from the central rock nucleus toward the outside edge. Analytical transects were conducted across nodules from LG1 and LG2 (Fig. 4). On each sample, one transect followed the shortest axis (from the nucleus to the top of the nodule) and a second followed the longest axis (from the nucleus to the

Table 1. Comparison of the groundwater and lake water composition (µg/L) at LG2 on September 11, 2008.

	Height above lake bed (cm)		
	55	**5**	**-100**
Fe	<2	<2	64
Mn	0.6	0.8	616
As	0.14	0.1	89
P	<5	1.5	411
Ca	803	1048	25553
Na	1450	1420	34600
Mg	211	249	3417
B	2.9	3.2	26
Pb	0.19	0.04	0.06

Table 2. Bulk composition of four nodules, two from location LG1 and two from location LG2, determined by XRF analysis.

	LG1		LG2	
Wt %	**A**	**B**	**A**	**B**
Fe_2O_3	70.24	53.49	35.63	47.47
MnO	16.56	29.75	36.47	35.96
P_2O_5	0.49	0.33	0.37	0.32
Ba (ppm)	5680	5138	11412	11437
As (ppm)	664.7	287.7	645.5	645.5

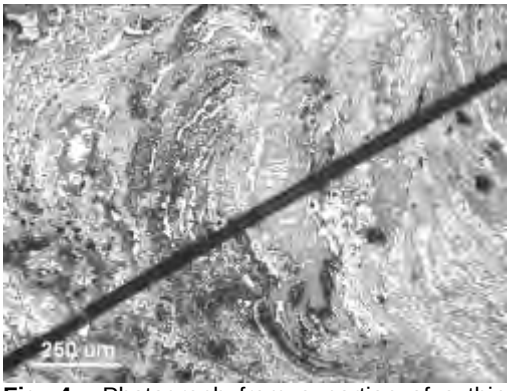

Fig. 4. Photograph from a portion of a thin section of a nodule from LG2. The dark line crossing the section shows the path of the laser used during LA-ICP-MS.

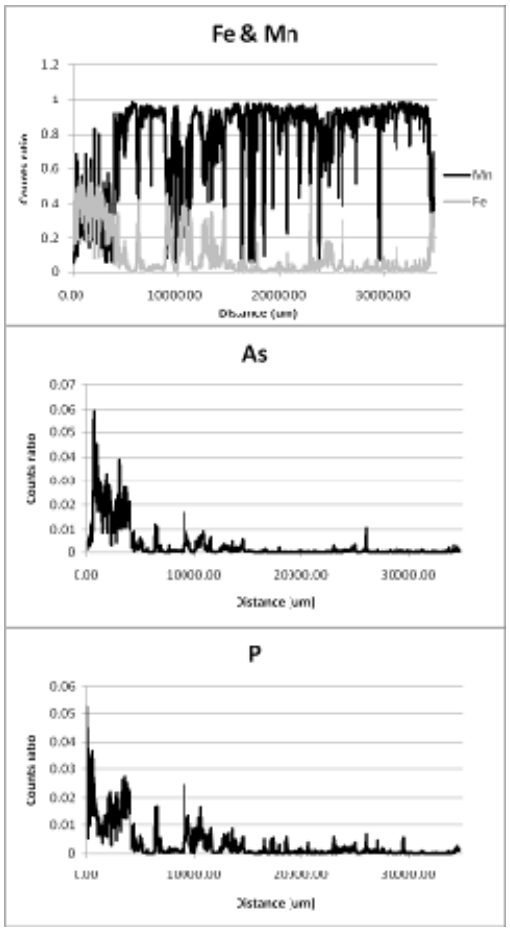

Fig. 5. Compositional variation along a transect across a nodule from LG1 analysed by LA-ICP-

MS. The data are presented as count ratios where the counts for each element are normalized to the total counts.

outer rim).

Figure 5 shows the analytical results for Fe, Mn, As and P along a transect across a nodule from LG1. This nodule is enriched in Fe, As and P at the centre. The As and P enrichment are spatially correlated with the Fe-rich areas of the nodule, indicating co-precipitation of these trace elements with the Fe oxyhydroxide minerals. This compositional variation isassumed to reflect changes in the groundwater chemistry over time, potentially since the lake formed.

CONCLUSIONS

Ferromanganese nodules have formed in temperate lakes around the world. The nodules form by the oxidation of dissolved Fe and Mn in regions of groundwater discharge. Radiometric dating has shown that the nodules grow slowly (Moore & Dean 1979), and can be as old as the lakes in which they are found. LA-ICP-MS transects across the nodules show variable enrichment in trace metals that reflect changes in the groundwater chemistry over time. This characteristic presents significant opportunities for investigations of paleoclimate and hydrology.

REFERENCES

APPELO, C.A.J. & POSTMA, D. 1995. *Geochemistry, groundwater and pollution.* A.A. Balkema Publishers, United States of America.

CHAPNICK, S.D., MOORE, W.S., & NEALSON, K.H. 1982. Microbially Mediated Manganese Oxidation in a Freshwater Lake. *Limnology and Oceanography*, **27**, 1004-1014.

GREGORY, E. & STALEY, J.T. 1982. Widespread Distribution of Ability to Oxidize Manganese Among Freshwater Bacteria. *Applied and Environmental Microbiology*, **44**, 509-511.

HARRISS, R.C. & TROUP, A.G. 1969. Freshwater Ferromanganese Concretions: Chemistry and Internal Structure. *Science*, **166**, 604-606.

HARRISS, R.C. & TROUP, A.G. 1970. Chemistry and Origin of Freshwater Ferromanganese Concretions. *Limnology and Oceanography*, **15**, 702-712.

HONEYMAN, D. 1881. Nova Scotia Geology (Superficial). *Proceedings and Transactions of the Nova Scotian Institute of Natural Science*, **5**, 319-331.

KINDLE, E.M. 1935. Manganese Concretions in Nova Scotia Lakes. *Transactions of the Royal Society of Canada*, **29**, 163-180.

MOORE, W.S. & DEAN, W.E. 1979. Growth Rates of Manganese Nodules in Oneida Lake, New York. *Earth and Planetary Science Letters*, **46**, 191-200.

Application of stable hydrogen isotope models to the evaluation of groundwater and geothermal water resources: case of the Padurea Craiului limestone aquifers system

Delia Cristina Papp[1] & Ioan Cociuba[1]

[1] *Geological Institute of Romania, Cluj-Napoca Branch, P.O. Box 181, 400750, Cluj-Napoca ROMANIA*
(email: deliapapp@yahoo.com)

ABSTRACT: The case of the present free waters system from the Padurea Craiului Mountains and the north-eastern extremity of the Pannonian Basin (Oradea – Felix) is investigated based on the correlation between deuterium, global salt content, and major solutes. All types of groundwaters (springs, drillings, wells) display δD values (-76.1 to -62.3‰) similar to the surface running waters (-76.5‰ to -50.7‰), suggesting that they are meteoric in origin. The global salt content ranges from 48.9mg/l to 1299.9mg/l for the groundwaters and from 47.5mg/l to 665.0mg/l for the surface waters. From the co-variation between the δD values, the global salt content, and the major solutes, as well as from the seasonal variation of these parameters, genetic links could be established. The mineralization of the groundwaters took place by means of an intense underground circulation, markedly on the karst system developed within the Mesozoic deposits of the Padurea Craiului Mountains.

KEYWORDS: *deuterium, global salt content, groundwater, Padurea Craiului, Oradea*

INTRODUCTION

Application of integrated stable hydrogen isotope and hydrogeochemical models to the present free waters systems provides important information on their sources, mixing phenomena and underground dynamics that can be profitably used in problems of groundwater resources management, as well as in environmental protection.

Our work represents an extension of previous studies made by a research team from the Institute of Isotopic and Molecular Technology, Cluj-Napoca (Blaga *et al.* 1981) on the present free waters system from Padurea Craiului - Oradea area (Romania), that includes different sources of groundwaters, surface waters, as well as geothermal waters.

GEOLOGICAL SETTING

The area under study comprises the western part of the Padurea Craiului Mountains in conjunction with the north eastern extremity of the Pannonian Basin (Oradea – Felix zone). The Padurea Craiului Massif had a long-lasting evolution with a pre-Hercynian start, being mainly shaped during alpine orogenesis. Most of its formations belong to the Bihor tectonic unit (Ianovici *et al*. 1976).

The basement is made up of crystalline schists of the meso-metamorphic Somes Series. Sedimentation started during Permian with detritic deposits interbedded with rhyolites. The overlying Triassic deposits are unconformable and include detritic formations (Lower Triassic) and massive layers of carbonate rocks (Middle Triassic). The absence of the Upper Triassic is due to the uplift of the region during the Kimmeric tectonic phase.

The Lower Jurrasic deposits include the detritic formation (Hettangian – Lower Sinemurian), the limestone formation (Upper Sinemurian – Pliensbachian) and the marl formation with ammonites and belemnites (Toarcian).

The Middle Jurassic consists mainly of marls. The Upper Jurassic formations are massive (over 100 m thick) and are made up exclusively of limestones. During Upper Jurassic and Lower Cretaceous the limestone deposits have been uplifted and resulted in a paleo-karst surface that hosts discontinuous bauxite deposits. Lower

Cretaceous sedimentation started with the deposition of fresh-water limestones (Hauterivian) followed by successive layers of marine limestones (Barremian), marls (Aptian), marine limestones (Aptian), glauconitic sandstone (Aptian-Albian) and ended with a package of red detritic deposits.

Subsequent positive epirogenetic movements and two main phases of magmatic activity (Upper Cretaceous – Paleocene and Badenian – Pliocene) completed the morphogenesis of the Piatra Craiului Mountains and the formation of the Pannonian basin at the east. The post tectonic cover of the Pannonian basin starts with the Senonian through the Paleogene, Neogene (Miocene and Pliocene) to the Quaternary. The Pliocene deposits of the Pannonian Basin develop on the north-western part of the area under study. They are predominantly pelitic (Bessarabian – Meotian) and psammitic (Pontian – Upper Pliocene).

The most important aquifer systems existing in the region are connected to the Pliocene deposits, and to the Lower Cretaceous – Upper Jurassic and Triassic limestone deposits respectively, all containing cold and thermal waters with varying hydrochemical properties (Tenu 1981). From a hydrogeological point of view, the area (maximum elevation range of 900 – 1020 m) is a heavy-rain area (~ 1000 - 13000 mm/year), with a snow cap that lasts for 2 - 3 months in the winter (Pascu 1983). The density of the hydrographical network is about 0.5 km/km^2. Due to the economic and balneological interest of geothermal springs (40 – 50 ^{0}C) two well known spas have been founded – Baile Felix and Baile 1 Mai (Oradea).

SAMPLING AND ANALYTICAL METHODS

Ninety water sources have been sampled. Deuterium content and global salt content were measured both in the underground sources (springs, drillings, wells) and in the surface sources (running water, precipitation), in order to include all the water types that might interact.

The Institute of Isotopic and Molecular Technology, Cluj-Napoca, performed all the analyses. The routine isotopic analyses were run on a Thomson THN 202D mass spectrometer, with a working precision of ±0.3‰. The uranium method was used to release hydrogen from water. All isotopic data are expressed in conventional δ notation as the permil deviation of D/H ratios with respect to the V-SMOW standard.

The global salt content was measured using a digital densimeter, and is expressed as the density difference of sample water relative to standard distilled water, at 25^{o}C. It is noted as Δd and expressed in units of mg/l. Major solutes within the groundwater samples (Li, Na, K, Mg, Ca, and Sr) were analysed using absorption spectroscopy.

RESULTS AND DISCUSSION

Figure 1 summarises the experimental data. All displayed values represent the mean values for one year of observation.

All types of groundwaters display δD values (-76.1‰ to -62.3‰) similar to the surface waters from the studied area (-76.5‰ to -50.7‰) (Table 1), suggesting that they are meteoric in origin. The δD values of the local precipitations vary between -104.7‰ and -45.9‰ during one year of observation. The Δd values range from 48.9mg/l to 1299.9mg/l for the groundwaters and from 47.5mg/l to 665.0mg/l for the surface waters. The

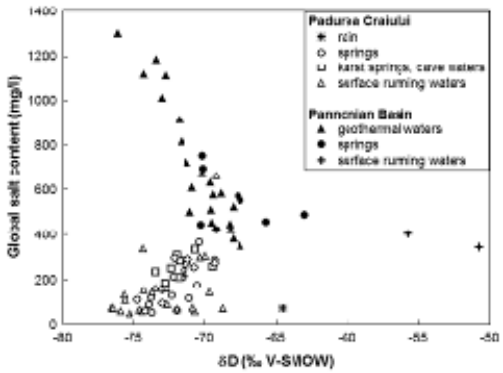

Fig. 1. Scatter plot of the δD values and the global salt content of the present free waters from the Padurea Craiului Mountains and the Pannonian Basin (Oradea - Felix).

Table 1. Summary of the distribution of the δD values, global salt content and major solutes of waters from the Padurea Craiului Mountains and Oradea - Felix.

	Mean value	*Min. value*	*Max. value*	*Standard deviation*
Padurea Craiului				
Springs (no. of obs. 22)				
δD (‰)	-72.0	-74.7	-69.3	1.5
δd (mg/l)	180.7	48.9	366.2	92.9
Karst waters (no. of obs. 8)				
δD (‰)	-71.8	-73.4	-69.4	1.3
δd (mg/l)	257.3	182.1	333.6	49.9
Surface waters (no. of obs. 25)				
δD (‰)	-72.9	-76.5	-68.7	2.4
δd (mg/l)	154.7	47.6	665.0	138.5
Precipitations (no. of obs. 14)				
δD (‰)	-66.8	-104.7	-45.9	20.0
δd (mg/l)	74.1	29.0	164.0	34.8
Oradea - Felix				
Geothermal waters (no. of obs. 21)				
δD (‰)	-70.6	-76.1	-67.5	2.3
δd (mg/l)	706.7	348.0	1299.5	288.8
Li (mg/l)	30.3	0.1	423.3	113.1
Na (mg/l)	28.5	9.5	76.4	19.8
K (mg/l)	9.6	2.6	17.2	5.4
Mg (mg/l)	27.1	1.1	59.6	13.9
Ca (mg/l)	153.13	70.45	245.75	53.1
Sr (mg/l)	2.7	0.3	5.9	1.8
Fossil waters (no.of obs. 2)				
δD (‰)	-35.4	-37.3	-33.5	2.7
δd (mg/l)	7204.8	5161.7	9248.0	2889.4
Li (mg/l)	3.1	1.2	5.0	2.7
Na (mg/l)	2532.9	2470.9	2595.0	87.7
K (mg/l)	70.2	46.4	94.0	33.7
Mg (mg/l)	14.0	5.1	22.9	12.6
Ca (mg/l)	62.2	13.4	111.0	69.0
Sr (mg/l)	1.4	1.1	1.7	0.4
Springs (no. of obs. 9)				
δD (‰)	-67.3	-70.2	-62.3	3.1
δd (mg/l)	579.1	423.3	822.0	145.1
Running waters (no. of obs. 2)				
δD (‰)	-53.2	-55.7	-50.7	3.5
δd (mg/l)	372.9	343.8	401.9	41.1

geothermal waters are characterized by much higher global salt content as compare to other groundwater sources from the study area, suggesting long-way underground circulation.

The higher deuterium content (-35.4‰) and higher global salt content (7204.8mg/l) correspond to two drillings from Oradea (Table 1). The chemical composition, characterized by high Na and K content, distinguish these waters from other groundwaters in the area. In addition, the correlation coefficients between δD and Δd are not significant. These findings are explained by a mixing phenomenon between a major component of fossil water and a minor component of fresh waters of meteoric origin.

Evidence of the meteoric origin is also based on a series of specific isotopic effects. For waters belonging to the meteoric cycle, temperature variations are the essential factor, which controls their isotopic composition. Both running waters and groundwaters show seasonal variation of the δD values, as well as of the global salt content. Due to the evaporation produced during warm seasons, which determines the enrichment both in deuterium and salts, a positive correlation between the δD values and the global salt content was expected for the running waters. As an example, for the Lesului Valley the correlation coefficient, *r*, is 0.72 (*n*=14). However, in many cases a low correlation coefficient or even a negative correlation was obtained, indicating relationships with phreatic waters.

The geothermal waters are less affected by the seasonal variation of temperature, and this suggests deep circulation. However, we could emphasize analogous seasonal variations of the δD values and the global salt content between the geothermal waters and water sources from Padurea Craiului, implying genetic relationships (Fig. 2). In many cases, a shift of 30 – 45 days could be observed in the variation sequences, pleading for a relatively rapid underground circulation.

Significant negative correlations between the δD values and Ca, Sr, and K contents of the geothermal waters have been found, suggesting similar leaching and transportation patterns for these elements. Mg also show negative correlations with the δD values, but less significant, while Li and Na display a slightly positive correlation. Significantly positive correlation coefficient between Ca, Sr, Mg, were obtained for most of the geothermal springs (0.77 to 0.86 (*n*=14)). This finding clearly indicates that the mineralization arises from the leaching of salts mainly from carbonate rocks.

CONCLUSIONS

The results of this study show that:

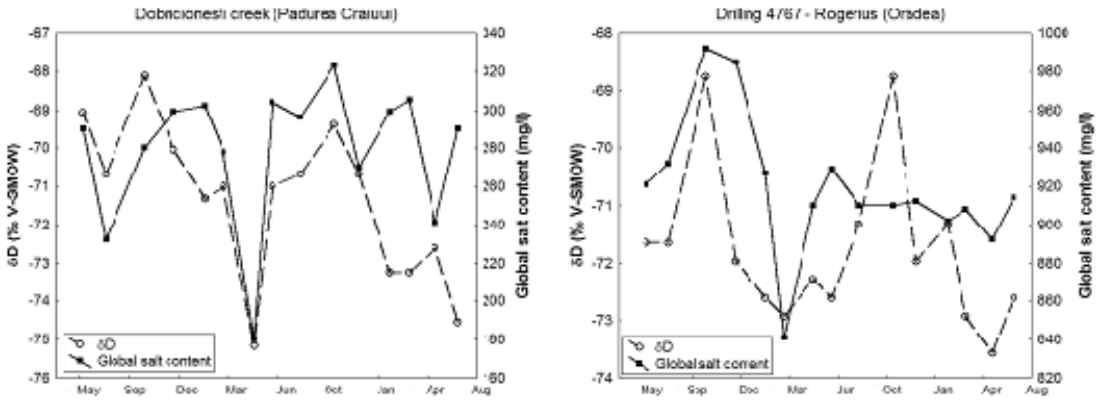

Fig. 2. Analogous seasonal variation of the δD values and the global salt content between surface water (Padurea Craiului Mountains) and geothermal water (Oradea).

(1) the majority of the groundwaters, belong to the meteoric cycle and therefore can be influenced by climatic changes and pollution factors;
(2) the mineralization of the groundwaters took place by means of an intense underground circulation, markedly on the fracture system developed within the carbonate deposits of the Padurea Craiului Mountains;
(3) the infiltration of local precipitation is considered the main source of recharge to the groundwater system;
(4) the high deuterium concentration and global salt content of the water from two drillings from Oradea can be explained by a mixing phenomenon between fossil water and fresh waters of meteoric origin;
(5) even though the water sources are spread over a relatively extensive area, the similarities in the evolution of their δD values and global salt content emphasise common genetic links. As underground circulation is relatively fast it follows that pollution of one source has a significant and rapid impact on the whole system.

ACKNOWLEDGEMENTS

Liviu Blaga is thanked for the access to his analytical data. The field work was partially funded by the Romanian National University Research Council (PN II, Programme: IDEAS).

REFERENCES

BLAGA, L., BLAGA, L. M., FEURDEAN, V., & BINDEA, C. 1981. Cercetari privind originea si dinamica apelor geotermale din zona Oradea – Felix - 1 Mai, Institute of Isotopic and Molecular Technology, Cluj-Napoca, Romania, *Technical report.*

INOVICI, V. BOROS, M., BLEAHU, M., PATRULIUS, D., LUPU, M., DIMITRESCU, R., & SAVU, H. 1976. Geologia Muntilor Apuseni. Ed. Academiei RSR, Bucuresti.

PASCU, M. 1981. *Apele subterane din Romania*. TEHNICA, B. (ed).

TENU, A. 1981. *Zacamintele de ape hipertermale din NV Romaniei*. Ed. Academiei RSR, Bucuresti.

The influence of soil and bedrock on trace metal concentrations and groundwater quality in northern Finland

Raija Pietilä[1]
[1]*Geological Survey of Finland, Northern Finland Office, P.O. Box 77, 96101, Rovaniemi FINLAND*
(e-mail: raija.pietila@gtk.fi)

ABSTRACT: Trace metal concentrations in groundwater in relation to local soil and bedrock were studied at twenty-six sites in the province of Oulu, Finland. The soil at the sites varies from coarse-grained sand to silty till. Soil samples were taken from all the genetic horizons of the podzol profile (A_0, A, B, C) to a depth of 1 to 2 meters. The trace metal concentrations of the samples were analyzed using three different digestion methods; total digestion (HF-$HClO_4$), partial digestion with Aqua Regia and digestion with NH_4Ac. Synthetic rainwater dissolution was also used for some of the samples. Groundwater samples were collected from springs and observation wells three times a year during 1995-1998 and 2006-2007. The effect of atmospheric wet fallout on pH, anions and the concentration of trace metals in the groundwater was estimated by analyzing rainwater and snowpack samples from the same sampling sites.

KEYWORDS: *groundwater, soil geochemistry, Oulu, Finland*

INTRODUCTION

Trace metal concentrations in groundwater and their relation to local soil and bedrock as well as seasonal changes in water quality in the province of Oulu, northern Finland (Fig. 1) were studied. Rural study sites were mainly chosen in order to rule out human or industrial impact on samples. Groundwater samples were collected three times a year during two separate time periods (1995-1998 and 2006-2007). The shallow springs (natural or captured) and wells represented mainly short groundwater residence time and samples from plastic pipes in the esker formations represents groundwater with long residence time.

STUDY AREA

Regional Geology

In a broad outline the bedrock of the study area is mainly composed of Archean granitoids and gneisses in the eastern part of the province. The western parts are characterized by Svecokarelian schists and gneisses, and granites and granodiorites in Oulu, Muhos and Vihanti areas. In the southern part there are granitoids, in Puolanka, quartzite and in the Kajaani and Vuolijoki areas the main bedrock is granite (Fig. 2). However, the composition of bedrock varies considerably within the areas. In the schist areas the presence of calcium- and magnesium-rich interlayers is reflected by elevated concentrations of these elements in the local soil. The major minerals in the granite gneiss areas where bedrock is highly resistant to weathering, especially in Pudasjärvi, are quartz, potassium feldspar, micas and sodium-rich plagioclases (Simonen 1980).

The topography rises towards the east from the coastal area in the west. Half of the study sites are situated in the esker formations and the other half in the basal till areas. The fine-rich tills are mainly composed of quartz, feldspars, amphiboles, chlorites and micas. The sand components are composed of mainly quartz and feldspars and poorly reflect the underlying bedrock (Räisänen *et al.* 1992).

ANALYTICAL METHODS

The water samples were analysed for pH, redox potential, dissolved oxygen, electrical conductivity, nitrate, nitrite, sulphate, chloride, fluoride, phosphate and

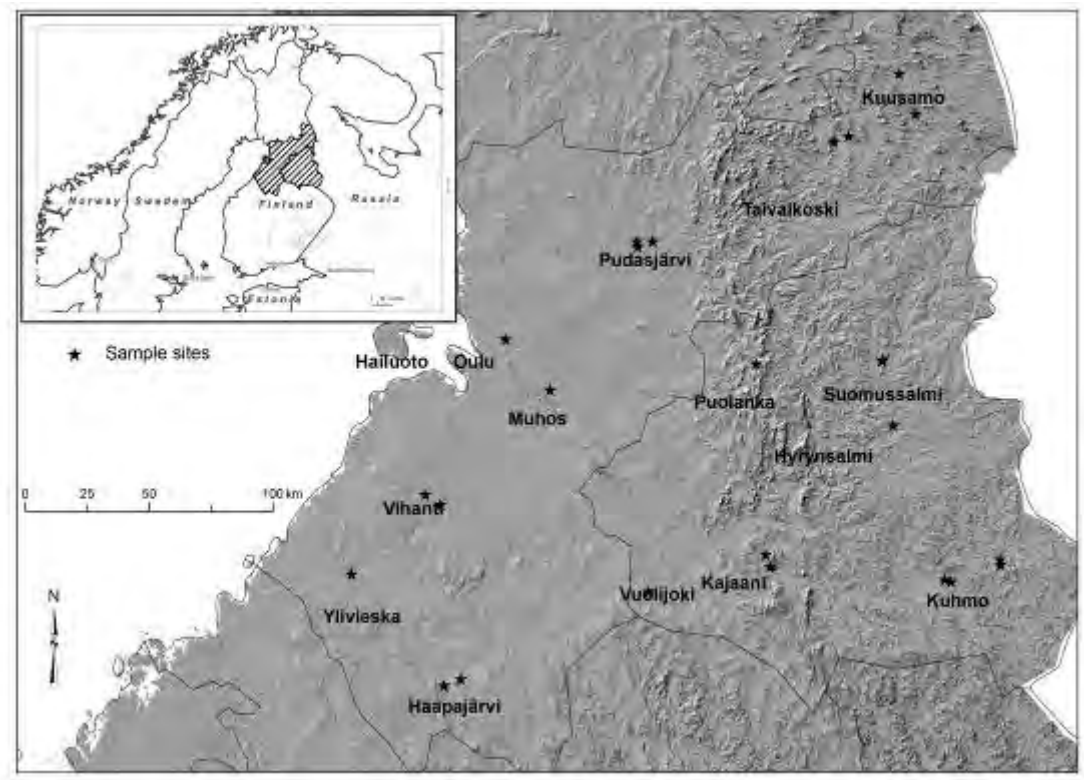

Fig. 1. Shaded relief map of the study area.

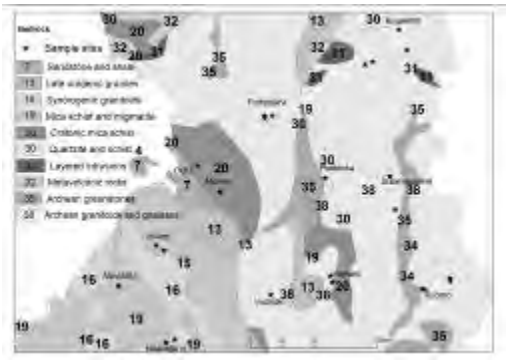

Fig. 2. Bedrock of the study area.

21 elements in the first sampling period. In the later sampling period there were more than 40 analyzed elements.

The podzol profile samples were taken from the groundwater catchment areas from humus (A_0) eluvial (A) and illuvial (B) horizons and the parent material (C). In coarse-grained sand areas the profile waspoorly developed and mainly 20 cm thick. the thickness in till areas ranged from 40 to 80 cm.

The soil samples were determined for pH, redox potential, electrical conductivity and 15 elements, using total digestion ($HF\text{-}HClO_4$), partial digestion (Aqua Regia) and with NH_4Ac.

CONCLUSIONS

Preliminary results indicate that the character of bedrock significally affects groundwater quality, especially in Haapajärvi, the south-western parts of the study area (Fig. 3). The arsenopyrite-bearing quartz dikes in mica schists are reflected by higher concentration of As both in local soil and groundwater samples. Arsenic in soil samples was found to be soluble in both weak acid and synthetic rainwater digestions. Mean As concentration of groundwater in the Haapajärvi (HaT in Fig. 4) site is 42 µg/l while the mean for the remainder of the province is less than 1 µg/l. In the eastern part of the province, the soils in the gneiss areas are depleted in most alkali metals

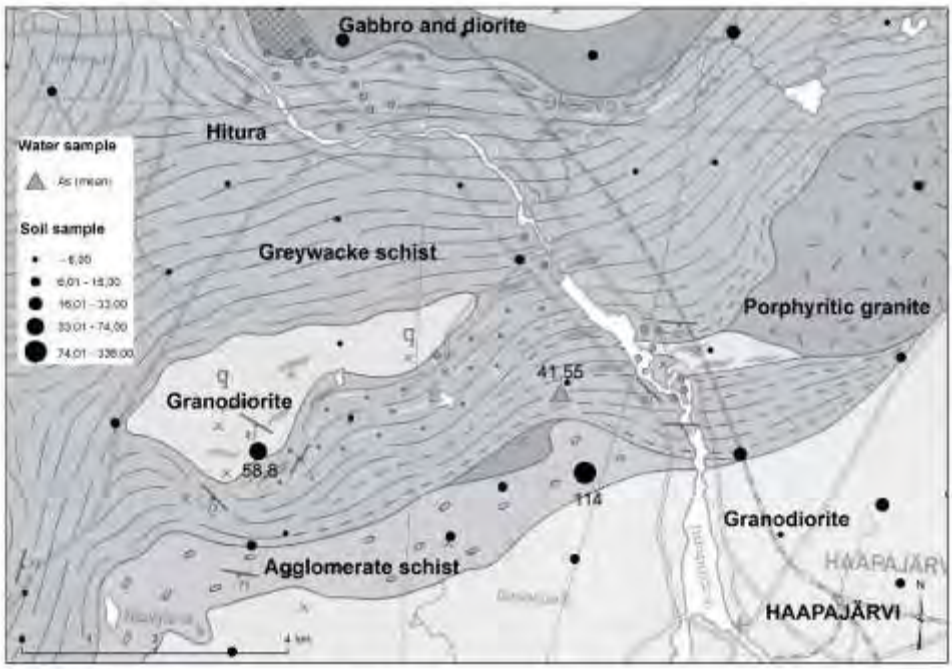

Fig. 3. Arsenic in soil and groundwater in Haapajärvi area

and elements including As, Cr, Fe, Mg, Ni, Pb, and V. The underlying geology is apparent in the groundwater chemistry of the area, which is slightly more diluted than the groundwaters near the coast, where mean concentrations of Ni, Pb, Cr, and Al are higher.

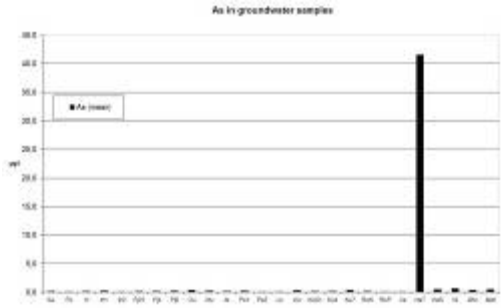

Fig. 4. Arsenic in groundwater.

REFERENCES

RÄISÄNEN, M.L., TENHOLA, J., & MÄKINEN, J. 1992. Relationship between mineralogy and physico-chemical properties of till in central Finland. *Bulletin of the Geological Society of Finland*, **64**, 25-58.

SIMONEN, A. 1980. The Precambrian in Finland. *Geological Survey of Finland, Bulletin*, **304**, 58.

Geochemistry of arsenic in the sediment-water interface of an alluvial aquifer, Bangladesh

Md. T. Rahman[1], Akira Mano[1], Keiko Udo[1], & Yoshinobu Ishibashi[2]

[1]Disaster Control Research Center, School of Civil and Environmental Engineering, Tohoku University, Sendai-980-8579 JAPAN (e-mail: liton2005@gmail.com)

[2]Dept. of Civil and Environmental Engineering, Tohoku Gakuin University, 1-13-1 Chuo, Tagajo, Miyagi, 985-8537 JAPAN

ABSTRACT: This paper is aiming to unearth the geochemical partitioning of Arsenic in the sediment-water interface with a view to explaining the mechanisms of the occurrence of high Arsenic (As) in the Holocene alluvial aquifer of the South-western Bangladesh. Observed relatively strong correlations of As with Fe, Al, HCO_3 and DOC in groundwater and also with Fe, Al, in sediment reflect the significant role of these elements in leaching As from the brown clay and the grey sand in the sediment-water interface. Sequential extractions followed by mineralogical investigation of the subsurface sediment revealed that Fe and Al minerals may not only be the principal source minerals in releasing As in the upper aquifers but may also be the adsorbent surfaces for As in the deeper aquifer. Potential As source mineral iron-pyrite was detected with XRD and TEM image successfully captured the Fe_2O_3 contents in the clay sediments. Vivianite and siderite are the two Fe minerals as suggested by the geochemical code PHREEQC that may control the GW Fe and As concentrations. Partition coefficient K_d was found to vary between 10 to 190 L/Kg. Low K_d computed for the upper aquifer suggests that leaching that has still been occurring may explain the As mobilization.

KEYWORDS: *arsenic, contaminated aquifer, leaching, adsorbent surface, mineralogy*

INTRODUCTION

High Arsenic (As) contamination detected in shallow sandy Holocene aquifers in different parts of Bangladesh has been recognized as a severe environmental catastrophe, since the early 1990s. About 45 million people who are heavily dependent on in collecting drinking water from these groundwater sources, are increasingly exposed to this elevated As pollution (Nickson *et al*. 2000; BGS & DPHE 2001; Anawar *et al*. 2002; Smedley 2003; Rahman *et al*. 2009).

Leaching and desorption of As from its associated mineral surfaces such as iron, aluminum and manganese oxides under the influence of the aquifer complex geochemistry, largely take part in its transport from sediment to aquifer pore-water. Adsorption has widely been considered as the retardation of As transport (Smedley 2003).

The objective of this paper is to evaluate the dominant geochemical mechanisms of the Holocene sandy aquifers so as to focus particularly the partitioning of As in the sediment-water interface.

STUDY SITE

Samples of groundwater and subsurface sediments were collected from one of the Arsenic hot spots located at a village named as Koyla (22^0 51' 03.1" N, 89^0 03 ' 50.9 "E, around 300 km from capital city Dhaka) under Kalaroa upazilla of Satkhira district of South-Western part of Bangladesh (Fig. 1). This site is situated on the river Betna and also not so far from a tributary, Kabodak of the Ganges River. The topographic surface of that area is very flat and the land elevation with

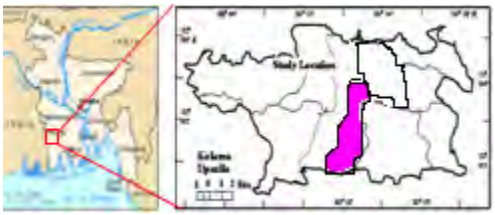

Fig.1. Location map of Study area, Kalaroa

respect to the mean sea level does not exceed even 5 m.

METHODOLOGY

Groundwater chemical analysis was done with ICP-MS to identify the major anions and cations. Sequential leaching (Koen 2001) coupled with mineralogical investigation was performed to get an account of the mineral compositions of the affected sediments. XRD (X-ray diffraction), SEM (Scanning Electron Microscope), TEM (Transmission Electron Microscope) were utilized for mineralogical study. Speciation analysis was performed and mineral saturation indices were calculated by using the geochemical code PHREEQC (USGS 1998). Sediment-water equilibrium distribution coefficient, K_d was computed from the ratio of adsorbed As that was found in sediment extraction with the As that was determined to be remaining as dissolved in the groundwater.

RESULTS AND DISCUSSIONS

The sequential extractions of As presented in Fig. 2 shows that significant amount of As can be liberated at oxalic extraction phase. This phase is relating with the Fe-mineral adsorption. Strong relationship of the oxalic extracted As and Fe shown in Fig.3 suggests that As should possibly have experienced with desorption together with co-dissolution during the Fe-mineral have undergone partial dissolution process. Fe mineral might be the most dominant one in controlling the As mobilization (Rahman *et al*. 2009a).

Considerable correlation of As with Fe (R^2= 53%), Al (R^2= 49%), HCO_3(R^2= 45%) and DOC (R^2= 42%) in groundwater (Fig. 4 and 5) suggests that reductive dissolution of Fe and Al hydroxides triggered by microbial activities might have been taken place in releasing As from sediment (Nickson *et al*. 2000; Rahman *et al*. 2009). Solid phase such as bulk mineralogical analysis by XRD, elemental analysis by XRF, elemental mapping by SEM and TEM could further reflect the wide-spread presence of the adsorbent minerals like iron oxy-hydroxide minerals (Rahman *et al.* 2009).

Roughly, 0.18% of the total mineral composition containing Fe_2O_3 in the brown clay was detected by XRD. Other minerals like quartz, K-feldspar, muscovite, microcline, mica, and pyrite were also identified by XRD data.

The very irregular mineral surfaces of the sediment grains that may suitably offer other anions or cations to be adsorbed

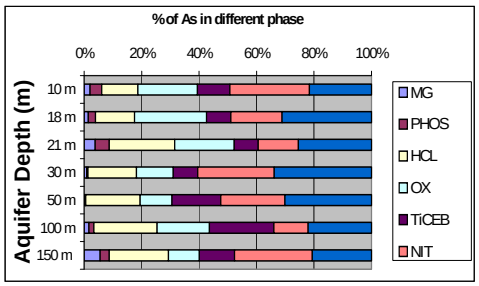

Fig. 2. Sequential extraction of Arsenic (MG-magnesium chloride, PHOS-sodium hypo phosphate, HCL-hydroclhoric acid, OX-oxalic acid, ToCEB- titanium chloride with EDTA, NIT- nitric acid).

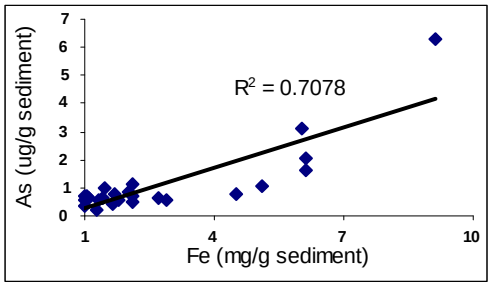

Fig. 3. Relationship between oxalic extracted As and Fe.

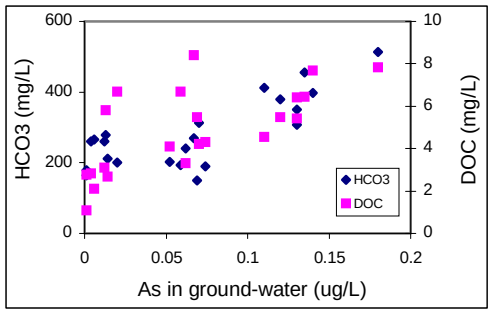

Fig. 4. Correlation of As with DOC and HCO_3 in groundwater.

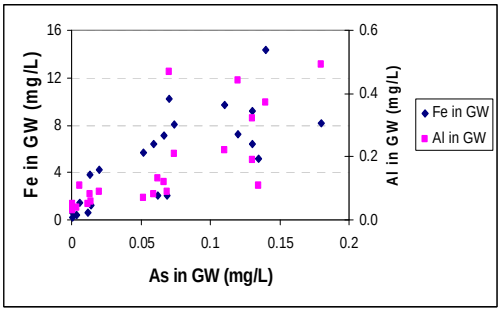

Fig.5. Correlation of As with Fe and Al in groundwater.

can clearly be recognized with this SEM image (Fig. 6).

Observations of the same clay sample in a very finer scale (500 nm) by TEM, may help to identify the potential Fe-oxyhydroxide surfaces attached on a sediment grain (Fig.6). Moreover, abundances of wide spread oxides that may have formed oxide minerals after binding with other elements such as Si, Fe and Al can easily be recognized from the right part of the TEM image (Fig. 7).

The variation of As in groundwater ranges between 1 to 180 µg/L and most of elevated concentrations were recorded for the upper shallow aquifers where mostly fine sandy sediments have frequently been noticed (Fig. 8). Oxalic extractable As in sediment has also been observed high in the fine sandy grains (8 µg/g) (Fig. 9). In contrast, the deeper aquifer was found to have contained low As in groundwater as well in sediment.

The partitioning of As in the aquifer solid-water interface can best be explained with the distribution coefficient, K_d (a ratio of solute adsorbed in sediment to that of dissolved in groundwater). Due to being simplistic in nature, K_d has long been well appreciated as well as applied by geochemical modelers.

In principle, smaller K_d values reflects the higher leaching potentiality of adsorbed As from the mineral surfaces in the sediment, whereas larger

K_d values suggest the possible sorption of As onto the Fe as well as other minerals.

The K_d was found to vary between 10 to 190 L/kg (Fig. 10). A high K_d was found

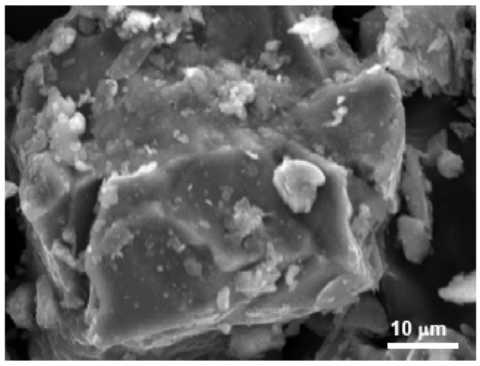

Fig. 6. Fe and Al minerals on sediment grain detected by SEM image.

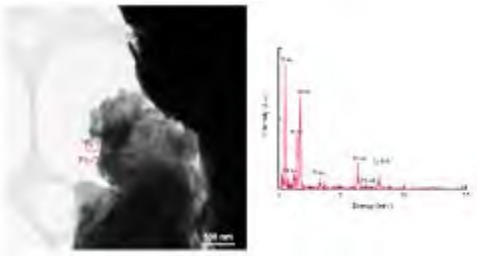

Fig. 7. Fe-oxidydroxide minerals on sediment grain detected by TEM.

for the deeper aquifer whereas a low K_d was computed for upper shallow aquifer. Also, the K_d was found to vary strongly with the variation of the aquifer parameters including pore water pH, Fe and Al contents of the sediments (Rahman *et al*. 2009). Having a larger amount of Fe, Al minerals, the deeper aquifer sediment may usually contain significant amount of adsorptive sites as compared to the upper aquifer and so the K_d of the deepar part was also high. Moreover, the mineral dissolution process in the shallower aquifer may have been occurring at a relatively higher rate compared to dissolution at depth. Due to this high dissolution, the potential sorption sites may have been diminishing significantly in number with time. Further more, As absorptive sites in the shallow aquifer may have already been occupied with other competing ions such as PO_4, HCO_3 (Rahman *et al*. 2009), These are the probable causes of the differences in As partitioning in the shallow as well as in the deeper aquifer. Thus, the As in the

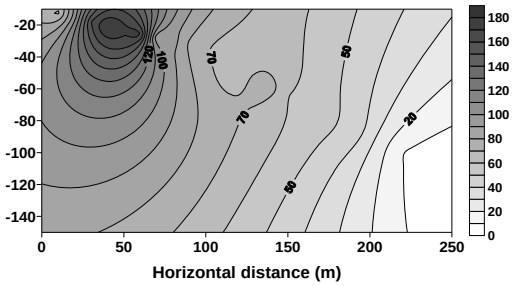

Fig. 8. Variation of Arsenic in groundwater.

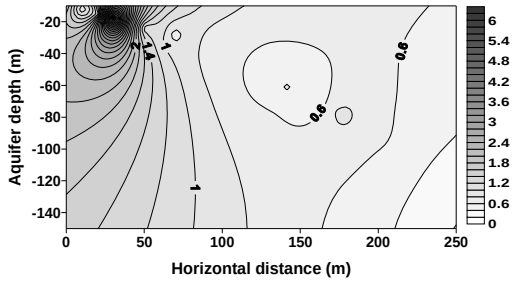

Fig. 9. Variation of Arsenic in aquifer Sediment.

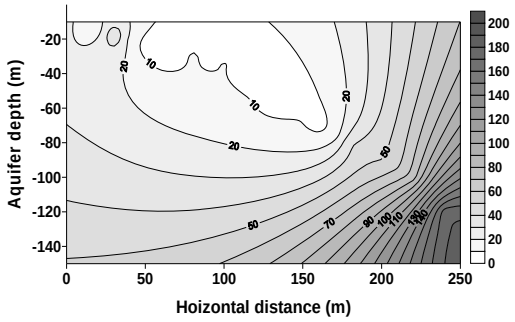

Fig. 10. K_d variation in the aquifer.

upper shallow aquifer can certainly be reductive dissolution of Fe and Al oxihydroxide mineral under the direct influence of the microbial degradation. Low K_d values computed in this study strongly support this view. Moreover, the strong correlation of As with Fe, Al, DOC, and HCO_3 also reflect the likely occurrence of reductive dissolution type geochemical phenomena in the studied aquifer. Mineralogical study, further, show the evidences of the presences of the Fe, Al oxide minerals.

CONCLUSIONS

Results of this present study can be summarized as:

(1) Arsenic in upper finer sediment has been releasing due to the microbial degradation driven by the dissolution of the Fe-Al minerals;
(2) computed low K_d values reflect the likely occurrence of As leaching reactions;
(3) the deeper aquifer may act as a sink for the leached arsenic, and
(4) due to the ion competition in groundwater parameters, leached As cannot be re-adsorbed and so high As predominates in the upper shallow aquifer

ACKNOWLEDGEMENTS

The financial support by the Grant in Aid for Scientific Research from the Japan Society for the Promotion of Science (B-18404009) is sincerely acknowledged.

REFERENCES

ANAWAR, H.M., AKAI, J., MOSTAFA, K.M.G., SAFIULLAH, S., & TAREQ, S.M. 2002. Arsenic poisoning in groundwater: Health Risk and geochemical sources in Bangladesh. *Environ. Int.* **27**: 597-604

BGS & DPHE. 2001. Arsenic Contamination of Groundwater of Bangladesh, Kinniburgh. In: D.G. & SMEDLEY, P.L. (ed.), Vol. 2: Final Report; *British Geological Survey Report* **WC/00/19**.

KEON, N.E., SWARTZ, C.H., BRABANDER, D.J., HARVEY, C., & HEMOND, H.F. 2001. Validation of an arsenic sequential extraction method for evaluating mobility in sediments. *Environmental Science and Technolology,* **35**, 2778-2784.

NICKSON, R.T., MCARTHUR, J.M., RAVENSCROFT, P., BURGESS, W.B. &, AHMED, K.Z. 2000. Mechanism of Arsenic Poisoning of Groundwater in Bangladesh and West Bengal. *Applied Geochemistry,* **15**, 403-413

RAHMAN, M.T., MANO, A., UDO, K., & ISHIBASHI, Y. 2009. Geochemistry of Arsenic in the Holocene Aquifer; South-Western Bangladesh. In: PARK, N.S. (ed.), *Advances in Geosciences*, Hydrological-Vol**,** World Scientific Publication, Singapore (Accepted)

PHREEQC USGS. 1998. http://wwwbrr.cr.usgs.gov/projects/GWC_coupled/phreeqc/index.html

SMEDLEY, P.L. 2003. Arsenic in groundwater South and East Asia. Welch. In: A.H. & STOLLENWERK, K.G. (ed.), *Arsenic in Groundwater Geochemistry and Occurrence*, Springer Science, New York, USA.

Groundwater as a medium for geochemical exploration in peatlands

Jamil A. Sader[1], Keiko Hattori[1], & Stewart M. Hamilton[2]
[1]*Unversity of Ottawa, Earth Sciences Department, Ottawa, ON, K1N 6N5 CANADA*
(e-mail: jamilsader@yahoo.com)
[2]*Ontario Geological Survey, Sudbury, ON, P3E 6B5 CANADA*

ABSTRACT: Shallow groundwater in peat displays chemical responses indicating the presence of underlying kimberlites in the Attawapiskat region in the James Bay Lowlands, Canada. The responses include high concentrations of Ni, Cr, Fe, Mg and REEs and elevated values of electrical conductivity, saturation index of CaCO3, and alkalinity. These chemical responses are produced by deep groundwaters reacting with kimberlites and upwelling into shallow groundwater. Several elements are conservative and are observed in peat groundwater down the horizontal hydraulic gradient. This study suggests that it is preferable to collect peat groundwater samples deeper into the saturated zone where waters are more reducing and are likely to have higher concentrations of metals. Oxidized groundwaters near the surface tend produce oxyhydroxides that can adsorb to peat and lower metal concentrations in peat groundwater.

KEYWORDS: *kimberlite, exploration, geochemistry, groundwater, peat*

INTRODUCTION

In regions where bedrock is hidden by thick sediments, surficial geochemical exploration has been used with a great deal of success. A variety of models and methods have been proposed to explain the migration of elements through the overburden to the surface from hidden kimberlites and other ore deposits (i.e., Hamilton *et al*. 2004a,b; Hattori & Hamilton 2008; Mann *et al*. 2005; McClenaghan *et al*. 2006). These models have focused on geochemical responses in mineral soil.

In many northern regions, peat bogs are widespread. Our study shows that peat groundwater can have geochemical responses consistent with its interaction with kimberlite rocks (Sader *et al*. 2007). The geochemical responses can be different from those in mineral soil. Therefore, exploration in peat bog terrains requires specific sampling methods**.**

GEOLOGICAL SETTING

The kimberlites in this study are located in the James Bay Lowlands and are in close proximity to the DeBeers Victor Mine. The kimberlites are mid Jurassic (~170 Ma) in age and have been emplaced into Paleozoic limestone (Webb *et al.* 2004). These kimberlites all have similar groundmass mineralogies consisting mainly of carbonate, spinel, and serpentine with lesser monticellite, mica, apatite, and perovskite (Kong *et al*. 1999) and they are all of volcaniclastic facies near ground surface. Varying thicknesses of clay and fine marine sediments of the Tyrell Sea (~ 4000 – 12000 years BP) and 1 to 4 m of peat overlie kimberlites (Fraser *et al*. 2005). Bioherms composed of coral and skeletal remains of other marine organisms sometimes outcrop.

METHODOLOGY

Fieldwork was conducted at Attawapiskat kimberlites (Yankee, Zulu, Alpha-1, Bravo-1, and X-ray), and at the Control location August 14-23, 2007 and October 14-18, 2007. Shallow piezometers were used to collect peat groundwater. At the Yankee and Zulu kimberlites piezometers were installed along transects between 25 to 50 m apart. Between 3 and 5 piezometers were installed at Alpha-1, Bravo-1, and X-ray. Piezometers were typically pushed into the peat 1.1 m with a loosely fitting plastic champagne cork at the end to prevent peat entering the pipe while it was

being pushed down. The pH, oxidation-reduction potential (ORP), electrical conductivity (EC), dissolved oxygen content (DO), temperature, and $CaCO_3$ alkalinity were measured on-site at the time of sampling for all piezometer, monitoring well, and borehole water samples.

Waters collected from piezometers and monitoring wells were analyzed for metals using an ICP-AES and ICP-MS at the Ontario Geological Survey. Anion contents were also determined at the Ontario Geological Survey using an ion chromatograph.

RESULTS AND DISCUSSION

Our results indicate that peat groundwater can be an effective medium for surficial geochemical exploration. The dilute, acidic peat groundwaters contrast well with groundwaters that have interacted with kimberlite.

Elevated Ca, $CaCO_3$-SI, alkalinity, and EC in peat groundwaters are good indicators of the upwelling of deep groundwater. The data are supported by measured groundwater levels that indicate upwelling (elevated water levels in piezometers and monitoring wells). These parameters are especially good indicators in peatlands because of high contrast between groundwaters that have interacted with rocks and dilute peat groundwaters.

We could identify groundwaters that have interacted with kimberlite rather than host limestone by identifying elevated concentrations of a suite of elements that are related to kimberlites. These elements include Mg, Ni, Cr, and REEs. For example, elevated Mg is found only where waters are discharging over the Yankee kimberlite even though Ca is elevated over the kimberlite plus where groundwater is discharging from the bioherm (Fig. 1). Select elements appear to be more chemically conservative in acidic peat groundwater and can sometimes be found down gradient of the kimberlite margin.

A "reduced chimney" is visible in the peat groundwater over both the Yankee and Zulu kimberlites, where elevated ORP responses correspond with low to non-detectable DO (Fig. 2). The "reduced chimney" model was first described by (Hamilton *et al*. 2004a, b). Elevated ORP and depletion of DO are due to the consumption of oxygen by ascending reduced ions from the kimberlite.

The depth of sampling is important. Deeper samples yield increased elemental concentrations. Our results also indicate

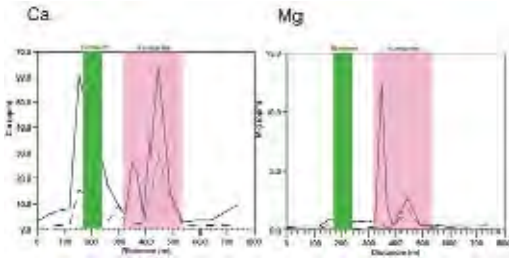

Fig. 1. Calcium exhibits a strong response over the kimberlite, but it shows elevated concentration near the bioherm. Magnesium, generally high in kimberlite rock, only shows responses over the kimberlite.

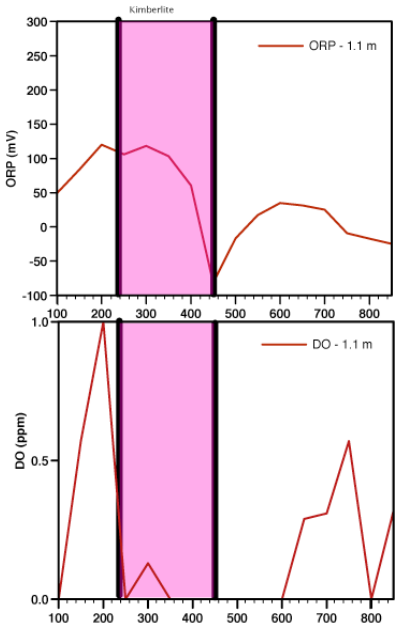

Fig. 2. The high ORP values and the corresponding low DO concentration in peat groundwaters along a transect at Zulu is an indication of reduced ions moving to the surface and oxidizing.

that absolute depth below surface is not the only important aspect to consider during sample collection. Samples that are collected deeper below the vadose/saturated boundary tend to be more reducing and have the potential to contain higher elemental concentrations (Fig. 3). Although piezometers were installed at a uniform depth into peat from the surface in this study, the water sampled from the piezometer was not necessarily from the same depth into the saturated zone. These variations can lead to imprecise results and misleading interpretations. A sample that is collected deep into the saturated zone will likely contain higher element concentrations relative to other samples along a transect where groundwaters are not collected as deep. This can erroneously indicate the presence of a buried kimberlite when none really exist.

CONCLUSIONS

This contribution can be summarized in the following points:

(1) Kimberlites can be detected in shallow peat groundwater, organic-rich environments using surficial geochemistry.

(2) Elements that are common to kimberlite rock are elevated in peat groundwater over buried kimberlite.

(3) The elevated concentrations of reduced ions that are migrating from a kimberlite produce a “reduced chimney” over the kimberlite.

(4) Unlike the protocol associated with the sampling of the upper B horizon, where reddish-brownish oxidized soil, sitting just below the more leached grayish soil, there are few visual signs in peat to indicate that sample collection is at the appropriate depth. Therefore we are reliant on geochemical and hydrogeological parameters in the field to guide us where best to collect a peat groundwater sample.

ACKNOWLEDGEMENTS

We thank NSERC Collaborative Research Development Program and DeBeers Canada for financial and in-kind support of this project. We also like to express our gratitude to the Ontario Geological Survey for providing us with invaluable field equipment.

Funding for this project was provided in part by an Ontario Graduate Scholarship (support for Jamil Sader’s Ph.D.) and a student research grant from the Society of Economic Geologists.

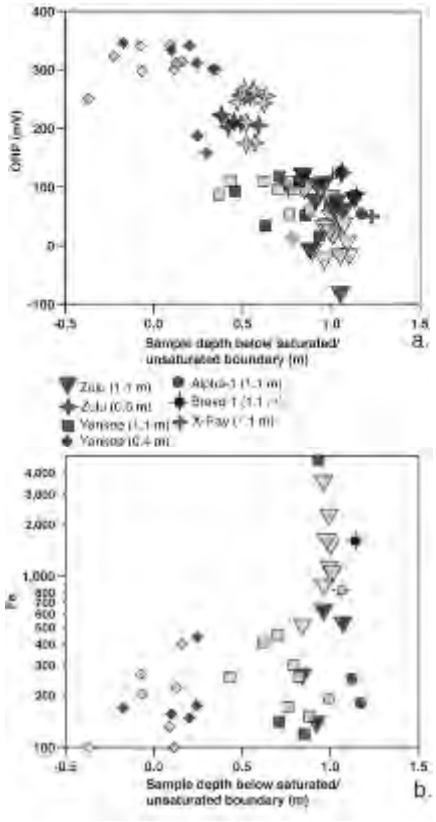

Fig. 3. Sample collection deeper into the saturated zone results in more reducing conditions (a) and increase in redox sensitive elements such as Fe (b).

REFERENCES

FRASER, C., HILL, P.R., & ALLARD, M. 2005. Morphology and facies architecture of a falling sea level strandplain, Umiujaq, Hudson Bay, Canada. *Sedimentology,* **52**, 141-160.

HAMILTON, S.M., CAMERON, E.M., MCCLENAGHAN, M.B., & HALL, G.E.M.. 2004a. Redox, pH and SP variation over mineralization in thick glacial overburden. Part I: methodologies and field investigation at the Marsh Zone gold property. *Geochemistry: Exploration, Environment, Analysis,* **4**, 33-44.

HAMILTON, S.M., CAMERON, E.M., MCCLENAGHAN, M.B., & HALL, G.E.M. 2004b. Redox, pH and SP variation over mineralization in thick glacial overburden; Part II, Field investigation at Cross Lake VMS property. *Geochemistry - Exploration, Environment, Analysis,* **4**, 45-58.

HATTORI, K.H. & HAMILTON, S. 2008. Geochemistry of peat over kimberlites in the Attawapiskat area, James Bay Lowlands, northern Canada. *Applied Geochemistry*, **23**, 3767-3782.

KONG, J., BOUCHER, D.R., & SCOTT SMITH, B.H. 1999. Exploration and geology of the Attawapiskat kimberlites, James Bay lowlands, northern Ontario, Canada. In: GURNEY, J.J., GURNEY, M.D., PASCOE, M.D., & RICHARDSON, S.H.J.D. (eds.), *Proc. 7th Int. Kimb. Conf. Red Roof Design.*

MANN, A.W., BIRRELL, R.D., FEDIKOW, M.A.F., & DE SOUZA, H.A.F. 2005. Vertical ionic migration; mechanisms, soil anomalies, and sampling depth for mineral exploration. *Geochemistry - Exploration, Environment, Analysis,* **5**, 201-210.

MCCLENAGHAN, M.B., HAMILTON, S.M., HALL, G.E.M., BURT, A.K., & KJARSGAARD, B.A. 2006. Selective Leach Geochemistry of Soils Overlying the 95-2, B30, and A4 Kimberlites, Northeastern Ontario. *Open-File Report - Geological Survey of Canada* No **5069**.

SADER, J.A., LEYBOURNE, M.I., MCCLENAGHAN, M.B., & HAMILTON, S.M. 2007. Low-temperature serpentinization processes and kimberlite ground water signatures in the Kirkland Lake and Lake Timiskiming kimberlite fields, Ontario, Canada; implications for diamond exploration. *Geochemistry - Exploration, Environment, Analysis*, **7**, 3-21.

WEBB, K.J., SCOTT SMITH, B.H., PAUL, J.L., & HETMAN, C.M. 2004. Geology of the Victor Kimberlite, Attawapiskat, northern Ontario, Canada: cross-cutting and nested craters. *Lithos*, **76**, 29-50.

Quantification of injection fluids effects to Mindanao Geothermal Production Field productivity through a series of tracer tests, Philippines

Benson G. Sambrano[1], Gabriel M. Aragon[2], & James B. Nogara[2]
[1]*Energy Development Corporation, Merritt Road, Fort Bonifacio, Makati City, Taguig PHILIPPINES*
(e-mail: sambrano.bg@energy.com.ph)

ABSTRACT: Tracer tests using napthtalene disulfonates were conducted in Mindanao Geothermal Production Field, Philippines in 2003 and 2006 to describe the extent of the re-injection fluids encroachment to the production sector and quantify its effects to wells performance and over-all field productivity. Modelling was done to predict the effects of RI fluids in terms of output and temperature declines in each production wells using the Icebox® software package. Majority of the production wells drilled in this sector indicated positive tracer response with % tracer recovery ranging from 2% to as high as 40%. These substantial amounts of injected fluid could lead to significant decrease in production temperature ranging from 13 to as high as 39°C. The timing of the temperature decline (thermal breakthrough) is highly dependent in the matrix porosity it could be as early as 2 years (porosity = 60 %) or as long as 15 years (porosity = 5 %) in the case of SK2D. The steam availability of the field has an average decline rate of 0.8 kg/month which is solely attributed to reservoir cooling. Changes in the reservoir management were implemented resulting to thermal recovery of the Marbel production sector and sustained overall Mindanao field productivity.

KEYWORDS: *Mindanao Geothermal Production Field, naphthalene disulfonates, Icebox® TRMASS, TRINV, TRCOOL, Marbel, Sandawa*

INTRODUCTION

Mindanao Geothermal Production (MGP) field is geographically divided into three sectors from the northwest to southeast, namely: Kullay-Matingao, Marbel and Sandawa. Steam is produced from Marbel and the Sandawa sectors. There are three injection sinks in the field, namely: Kullay Matingao and Kanlas (Fig.1).

Commercial production began in two-fold with Mindanao-1 (M1) in 1997 and followed by Mindanao-2 (M2) in 1999. M1 draws steam from the Marbel sector and M2 from the Sandawa sector. Geochemical monitoring of the well discharges after nearly a year of production in M1 indicated that injection returns were affecting Marbel sector. Two tracer tests were conducted to establish injection breakthrough from well MT2RD.

The first and second tracer tests used ~20 kgs of sodium flourescein dye in March 1998 and 1 curie of I^{131} in December 1998. The results of these tests are discussed in the reports of Malate *et al*. (1999) and Delfin *et al*. (1999).

The 2003 tracer tests were conducted in two wells by injecting 400 kg of *1,6* NDS into MT2RD on March 28, 2003 and

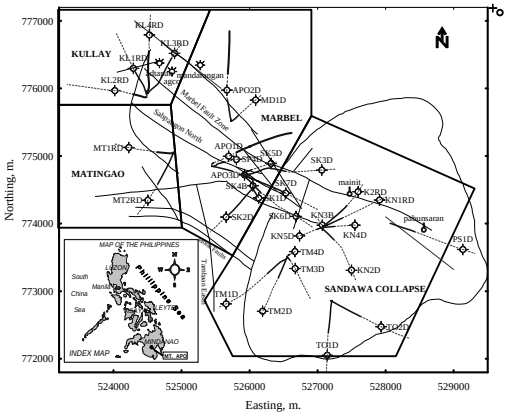

Fig. 1. Map of Mindanao geothermal production field (MGPF) showing the geographical boundaries. Philippine map (insert) shows the regional location of the geothermal project (Mt.Apo).

another 400 kg of *2,6* NDS into KL1RD on April 8, 2003. Subsequently in October 2006, 400 kg of *1,5* NDS and *1,3,6* NTS into MT1RD and KL4RD, respectively, and ~350 kg of *2,7* NDS into KN2RD, an injection well within Sandawa production sector. The tracer tests essentially evaluate the injected fluids coming from Matingao and Kullay due to high brine load injection into these sectors. This report presents an update of the tracer tests conducted in the Mindanao Geothermal Production Field.

STRUCTURAL CORRELATION

Detailed structural assessment by Pioquinto (1997) established that there are several structural routes connecting Matingao and Kullay injection sinks to the Marbel production sector. The preferential flow of the injection fluids from Matingao and Kullay was further enhanced due to high extraction rate concentrated at the Marbel production sector since majority of the production wells (mostly with high total mass flow, e.g. APO3D at 70 kg/s, SK2D at 72 kg/s and SP4D at 55 kg/s) were drilled and produced from this region.

The probable route and structures included are identified using the following hierarchical criteria: 1) direct and shortest structural connection, 2) interconnection of faults, 3) average breakthrough time of tracer which is directly correlated to tracer concentration and 5) the location of major and minor feed zones within the respective wells.

NAPHTHALENE DI-SULFONATES

Two injection wells are located inside the Matingao injection sink namely: MT1RD and MT2RD. The combined load of these injection wells averages 220 kg/s with > 120 kg/s being injected at MT2RD. The Matingao sector accepts almost 70% of the total brine effluent obtained from the Marbel production sector. Positive tracer responses were detected in the following production wells in order of decreasing tracer concentrations: SK2D, SK4B, SP4D, APO3D, APO1D, SK1D, SK5D, SK6D, SK7D, SK3D and APO2D after injecting 400 kg each of *1,5* and *1,6* naphthalene di-sulfonate (NDS) in MT1RD and MT2RD, respectively. The most probable passageways of injected fluid from MT2RD as it moves to production sector are shown in Figure 2.

In over a year of monitoring since March 2003, the wells that showed positive tracer responses for *2,6* NDS enumerated in order of decreasing tracer concentrations are APO1D, SP4D, SK5D, APO3D, SK4B, SK3D, SK2D, SK1D, SK7D, SK6D and APO2D. While the same wells in the Marbel production sector indicated *1,3,6* NTS tracer response except for SK2D, SK6D and SK7D. The tracer remains undetected in Sandawa production wells as of this writing.

Figure 3 summarizes the flow paths of the reinjected fluid coming from well KL1RD elucidated through the injection of *2,6*-naphthalene disulfonate.

Tracer injected (*2,7* NDS) in well KN2RD from within the Sandawa sector were observed in nearly all Marbel production wells except for SK3D at less than 1 per cent overall injected fluid returns. Well APO1D indicated the highest percentage returns at 0.7 % with respect to the *2,7* NDS tracer suggesting a structural flow path through Kinuhaan fault

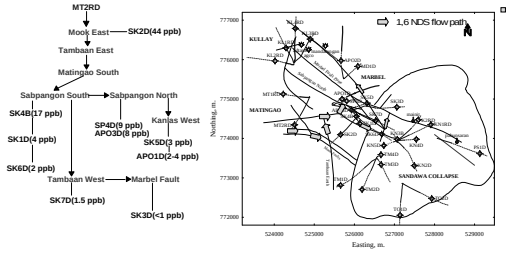

Fig. 2. Most probable flow paths of injected brine in MT2RD to the production sectors.

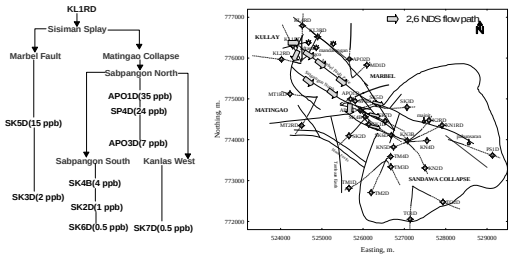

Fig. 3. Most probable flow paths of injected brine in KL1RD to the production sectors.

to Marbel Fault Zone reaching as far as well APO1D. Well SK2D indicated the least transit time of 3.5 months through Tabaco East Splay and Sabpangon South fault. Notably the tracer is undetected as of this writing in nearby Sandawa wells, namely KN3B, KN2D, TM1D and TM2D.

RESULTS AND DISCUSSION

Transit Time, Tracer Recovery and injection Fraction

The injection fractions were calculated using the following equation.

$$RI_{Frac} = (q \times Mr) / (100 \times Q) \quad (6)$$

Where: q = stable injection rate of injection well, M_r = % tracer recovered, and Q = stable production rate.

The profile of the tracer recovery curves (breakthrough curves) is best approximated and simplified using a single channel communication between the injection and production wells both for *1,6* and *2,6* NDS tracers.

The tracer breakthrough for *1,6* NDS injected in MT2RD (Matingao) is relatively faster and more pronounced compared to *2,6* NDS injected in KL1RD (Kullay). The earliest average breakthrough time is 4.7 months with a distance of 1100 meters and maximum tracer concentration of 44 ppb as given by well SK2D. While in *2,6* NDS, the earliest average breakthrough time is 11 months having a distance of 2400 m and maximum tracer concentration of 35 ppb as observed in well APO1D. The data seem logical because of the proportionate spatial differences of the two well pairs.

The total mass of tracer recovered for *1,6* NDS is about 48% or 192 kg out of 400 kg injected (combined mass tracer recovery on all wells affected by *1,6*). The residual 52% of the tracer injected possibly dispersed to the reservoir. The bulk of the tracer recovered was obtained in well SK2D amounting to 31% of the tracer mass injected (124 kg) or 65% of the total tracer recovered. Presence of direct structural connection between MT2RD and SK2D through Mook East and proximity of the two wells to each other explain this observation. Wells located at the margin of the Marbel production sector opposite to Matingao injection sink such as SK5D and SK6D gave minimal tracer recovery of < 2.0%. This implies that the tracer has vastly dispersed upon reaching the northeastern region of the reservoir.

Insufficient data sets were obtained for most of the wells monitored for *2,6* NDS. Data insufficiency is due to the generally longer transit time for *2,6* NDS requiring extended periods of monitoring. Wells APO1D and SP4D indicated a combined tracer mass recovery of about 30% or 120 kg *2,6* NDS out of 400 kg injected following the extended monitoring. Figure 4 shows the combined iso-contours of *1,6* NDS, *2,6* NDS maximum concentrations of both tracers in Mindanao geothermal field reflecting the spatial encroachment of both tracers to the production sectors which mimic the injected fluid coming from the two injection wells (MT2RD and KL1RD).

Cooling Prediction

Wells with direct communication and closer to the injection sinks have the highest predicted decline in temperatures like SK2D (32^{o}C), APO1D (13^{o}C) and SP4D (13^{o}C). The measured decline in temperatures for these wells based on silica geothermometer in 8 years of utilization is generally lower amounting to 3^{o}C. As mentioned earlier, the timing of decline is uncertain due to unknown porosity value and the 3^{o}C decline observed in these wells could possibly be the signal of the actual onset of thermal decline. Thus, further declines in the production temperatures are expected in the near future if the current injection scheme will be maintained.

In contrast, wells with low predicted reservoir temperature declines like SK5D and SK6D yielded higher actual values in 8 years of utilization. The actual temperature decline observed for SK5D and SK6D are 12^{o}C and 9^{o}C, respectively, but the maximum predicted temperature decline is about 1^{o}C in both wells. The faster decline rates observed for these two

wells cannot solely be attributed to injection returns but possibly to other reservoir and well-bore processes like interplay of feed-zones, formation of scales, e.g. calcite that blocks the contribution of the hotter feed, and movement of other neighbouring fluids that are relatively cooler but with comparable reservoir chloride to the wells involved.

CONCLUSIONS

- Positive tracer responses were noted in nine (9) production wells located inside the Marbel and three (3) production wells inside the Sandawa.
- Well SK2D has the highest decline value of around 39^{o}C followed by wells APO1D and SP4D with similar decline value of 13^{o}C. The timing of decline is greatly dependent on the actual porosity of the flow-channel where lower porosity value will prolong induction time for thermal decline.
- Temperature declines are also attributed to other reservoir and well-bore processes, e.g. interplay of feed-zones, scaling and inflow of other neighbouring cooler fluids.
- The *1,3,6* NTS injected in KL4RD validated the cold injection in-flow in APO2D which resulted to the continuous decline in the salinity of the well.
- Wells MD1D and SK5D are significantly affected by injected fluids from well KL4RD.
- Brine load reduction in well MT1RD should precede MT2RD since MT1RD has significantly affected well APO3D which has marginal production temperature at ~220^{o}C.
- Brine inflow towards the Marbel production sector from the in-field injection well, KN2RD resulted to abnormal temperature declines in SK3D, SK7D and SK6D which could not be attributed to Matingao and Kullay injection sectors.
- Tracer test in KN2RD suggests a permeability barrier rather than limited sector capacity which is evident by the positive tracer response of the Marbel production wells.
- Permanent utilization of the in-field Injectors may be detrimental in the long term as it affects the sustainability of the Marbel sector since it blocks the hot recharge towards this sector by creating a fluid barrier.

ACKNOWLEDGMENT

The authors wish to thank EDC for allowing the presentation and publication of this paper.

REFERENCES

ARASON, I. 1993. TRINV: Tracer Inversion Program. Orkustofnun

ARASON, I. 1993. TRMASS: A program to integrate observed data and give total recovered mass of tracer. Orkustofnun.

AXELSSON, G., BJORNSSON, G., & ARASON, I. 1993. TRCOOL: A program to calculate cooling of production water due to injection of cooler water to a nearby well. Orkustofnun.

AXELSSON, G. *et al.* 1994. Injection experiments in low temperature geothermal areas in Iceland. *Proceedings, World Geothermal Congress,* 1995, 1991-1996.

DELFIN, F.G. JR., MALATE, R.C.M., & ARAGON, G.M. 1999. Tracer tests and injection returns at MGPF. *PNOC-EDC Internal Report*, **1999**.

DELFIN, F.G. JR. & PIOQUINTO, W.P.C. 1999. Alternative analysis of reservoir permeability in the Mt. Apo geothermal project. *PNOC-EDC Internal Report,* **1999**.

GONZALEZ, R.C. *et al.* 1994. Mindanao 1 Geothermal Project: *Resource Assessment Update. PNOC-EDC Internal Report*, **1994.**

HERRAS, E.B. 2004. The Naphthalene Disulfonate Tracer Test in the Mahanagdong Field, Leyte. Proceedings, 25th Annual PNOC-EDC Geothermal Conference. 2005.

NOGARA, J.B. 2004. Tracer Tests Using Naphthalene Disulfonates in Mindanao Geothermal Production Field, Philippines. Proceedings, 25th Annual PNOC-EDC Geothermal Conference. 2004.

PIOQUINTO, W.P.C. 1997. Probable passageways of injection returns and proposed alternative pads of MGPF. *PNOC-EDC Internal Report.* **1997**.

Organic and inorganic surface expressions of the Lisbon and Lightning Draw Southeast oil and gas fields, Paradox Basin, Utah, USA

David M. Seneshen[1], Thomas C. Chidsey, Jr[2], Craig D. Morgan[2], & Michael D. Vanden Berg[2]

[1]*Vista Geoscience,130 Capital Drive, Suite C, Golden, CO, 80401 USA*
(e-mail: dseneshen@vistageoscience.com)
[2]*Utah Geological Survey, 1594 West North Temple, Salt Lake City, UT, 84114 USA*

ABSTRACT: Exploration for Mississippian Leadville Limestone-hosted oil and gas reservoirs in the Paradox Basin is high risk in terms of cost and low documented success rates (~10% based on drilling history). This study was therefore initiated to evaluate the effectiveness of low-cost, non-invasive, organic and inorganic surface geochemical methods for predicting the presence of underlying Leadville hydrocarbon reservoirs. Lisbon field was chosen for testing because it is the largest Leadville oil and gas producer in the Paradox Basin, and the recently discovered Lightning Draw Southeast field with nearly virgin reservoir pressure is also available for comparison. In comparison with Lisbon field, Lightning Draw Southeast field, San Juan County, Utah, is smaller, with more carbon dioxide, nitrogen and helium, and has productive intervals in the overlying Ismay zone of the Pennsylvanian Paradox Formation.

The main conclusion of this study is that hydrocarbon-based surface geochemical methods can discriminate between productive and non-productive oil and gas reservoir areas. Variables in surface soils that best distinguish productive and non-productive areas are ethane and *n*-butane and heavy (C_{24}+) aromatic hydrocarbons. Heavy metals (U, Mo, Cd, Hg, Pb) are possibly indirect indicators of hydrocarbon microseepage, but they are more difficult to link with the reservoirs.

KEYWORDS: *Lisbon, hydrocarbons, microseeps, metals, exploration*

INTRODUCTION

Previous work has shown the potential of remote-sensing techniques for identifying kaolinite-enriched, bleached redbed Triassic Wingate sandstones over productive parts of Lisbon field, San Juan County, Utah (Fig. 1) (Conel & Alley 1985; Segal *et al*. 1986). These studies used Landsat Thematic Mapper (TM) data to recognize the presence of kaolinite as well as reduced iron (i.e., bleached redbed sandstones). Other than this work, there are no published surface geochemical studies in the Lisbon field area. The Utah Geological Survey (UGS) therefore initiated this study to test the effectiveness of several conventional and unconventional surface geochemical methods in the Lisbon area. The main objective for testing these techniques is to find effective geochemical exploration methods to pre-screen large areas of the Paradox Basin for subsequent geophysical surveys and lease acquisition specifically for Leadville Limestone oil and gas reservoirs.

The premise behind surface geochemical exploration for petroleum is that light volatile hydrocarbons (i.e., C_1-C_5) ascend rapidly to the surface from a pressured reservoir as buoyant colloidal-size "microbubbles" along water-filled fractures, joints, and bedding planes (Klusman 1993; Saunders *et al*. 1999). In some cases, liquid C5+ hydrocarbons also ascend to surface along faults to produce oil seeps at surface. Partial aerobic and anaerobic bacterial consumption of the ascending hydrocarbons produces carbon dioxide and hydrogen sulfide that can significantly alter the chemical and mineralogical composition of overlying

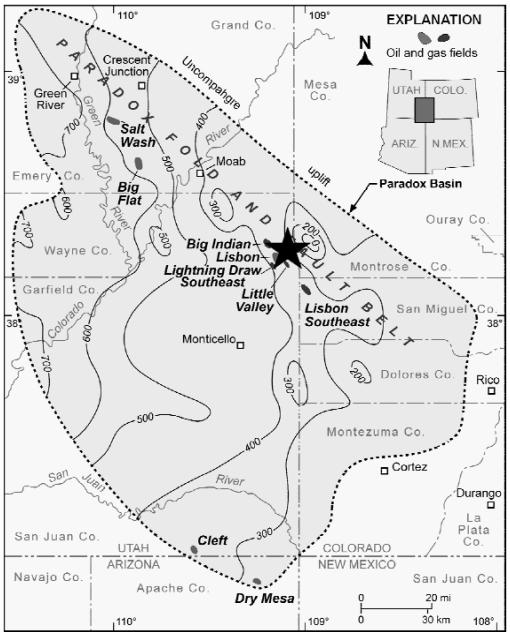

Fig. 1. Location of the Lisbon and Lightning Draw Southeast fields in the Paradox Basin of eastern Utah.

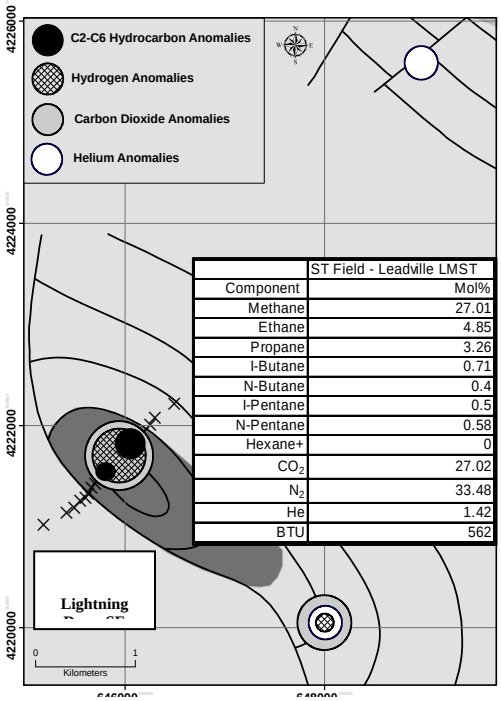

	ST Field - Leadville LMST
Component	Mol%
Methane	27.01
Ethane	4.85
Propane	3.26
I-Butane	0.71
N-Butane	0.4
I-Pentane	0.5
N-Pentane	0.58
Hexane+	0
CO_2	27.02
N_2	33.48
He	1.42
BTU	562

Fig. 2. Distribution of 395 to 470nm factor scores in soils over the Lisbon and Lightning Draw Southeast fields, which correspond to high correlation of 4- to 6-ring aromatic hydrocarbons.

sediments and soils (Schumacher 1996). Changes include decreased iron and potassium concentration and increased silica, carbonate, magnetic minerals and uranium.

Both direct and indirect methods were tested in the Lisbon area. Direct methods include the assessment of hydrocarbon compositional signatures in surface soils, outcrop fracture-fill soils and mosses, and 6-ft (2 m) deep free-gas samples. Indirect methods pertain to the major and trace element chemistry of soils to look for alteration effects resulting from hydrocarbon microseepage.

HYDROCARBON ANOMALIES IN SOILS

Soil samples were collected at 200 to 500 meter intervals over the Lisbon and Lightning Draw fields and analyzed for thermally desorbed C_1 to C_{12} alkanes by GC-FID and solvent-extractable C_6 to C_{36} aromatics by fluorescence spectrophotometry.

Aromatic hydrocarbon anomalies are evident in soils over both fields (Fig. 2). The anomalous 4-, 5-, and 6-ring aromatic hydrocarbons, which correspond with 395nm, 431nm and 470nm fluorescence peaks suggests the presence of heavy oil seeps at surface. Light alkanes (ethane and *n*-butane) are the most important variables for discriminating between the productive fields and down-dip water-legs.

FREE GAS ANOMALIES

Free gas samples were collected from 6-foot depth with a GeoProbe drill at 50-meter intervals over Lightning Draw Southeast. The samples were analyzed for C_1 to C_6 hydrocarbons by GC-FID and fixed gases (He, H_2, CO_2, CO, O_2, N_2, Ne, and Ar) by GC-TCD. The gas produced from the Leadville Formation is particularly rich in CO2 and He, and thus these are key variables for identifying microseepage (Fig. 3). Light alkanes (C_2-C_6), H_2 and CO_2 are anomalous over the Lightning Draw field, but He is only anomalous off-structure to the southeast and over the water-leg of Lisbon (Fig. 3).

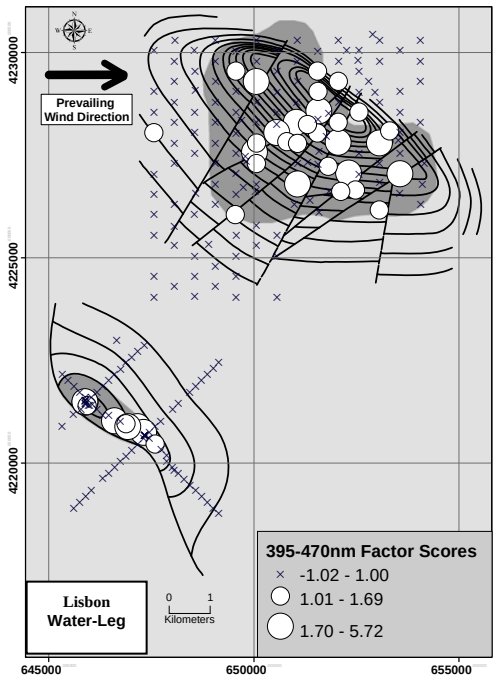

Fig. 3. Distribution of alkanes, H2, CO2 and the anomalies in 6-foot deep free gas over the Lightning Draw Southeast field.

HEAVY METAL ANOMALIES IN SOILS

Soil samples were analyzed for 53, aqua regia extractable elements by ICP-MS/ES. Cadmium, uranium and molybdenum are anomalous over part of the Lisbon field and most of the Lightning Draw Southeast field (Fig. 4). Mercury, lead and organic carbon are also anomalous over both fields.

DISCUSSION

Light alkane and heavy aromatic anomalies over the Lisbon and Lightning Draw Southeast fields suggest that both volatile and liquid hydrocarbons are ascending to surface from the Leadville Limestone reservoir. The free gas C_2 to C_6, CO_2 and H_2 anomalies over the crest of the Lightning Draw Southeast field also support the ascent of volatiles from the reservoir. In the case of Lightning Draw Southeast, however, there is also historic oil production from the stratigraphically higher Ismay Zone, and some of the hydrocarbon microseepage may therefore be partially or entirely sourced from this reservoir. The higher CO_2 in free gas over the field suggests that there is leakage also from the lower CO_2-rich Leadville Limestone reservoir. The lack of helium anomalies over the field is puzzling, but the anomalies on the margins of both fields may indicate leakage along faults related to salt collapse.

The heavy metal anomalies over both fields are interesting, but more difficult to explain in terms of leakage from the reservoir. The Cd-U-Mo anomalies over Lisbon can be explained by outcropping uranium mineralization in the Chinle Formation (Fig. 4), but there are no outcrops of Chinle exposed at Lightning Draw Southeast. An alternative explanation could be that uranium mineralization eroded from Morrison Formation deposits to the southeast (Fig. 4) is being "fixed" by the hydrocarbon microseepage at Lightning Draw Southeast. The anomalies would therefore be an indirect indication of hydrocarbon microseepage. The mercury and lead anomalies observed over both fields may be derived from the oil seeping to surface.

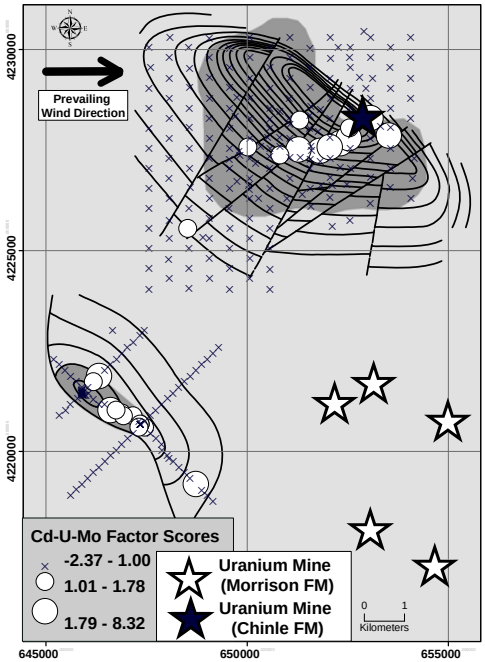

Fig. 4. Distribution of aqua regia extractable Cd-U-Mo factor scores in soils over the Lisbon and Lightning Draw Southeast fields

CONCLUSIONS

The main conclusion drawn from this study is that hydrocarbon- and fixed gas-based geochemical exploration methods in the Paradox Basin are cost-effective tools for pre-screening large areas to focus subsequent lease acquisition and seismic surveys for oil and gas exploration. Heavy metal anomalies are more difficult to link with the reservoir.

ACKNOWLEDGEMENTS

The Utah Geological Survey and the US Department of Energy are acknowledged for providing funding and logistical support for this study.

REFERENCES

CONEL, J.E. & ALLEY, R.E. 1985. Lisbon Valley, Utah uranium test site report. In: ABRAMS, M.J., CONEL, J.E., LANG, H.R., & PALEY H.N. (eds.), *The joint NASA Geosat test case project – final report: AAPG Special Publication*, *pt. 2,* **1**, 8-1 - 8-158.

KLUSMAN, R.W. 1993. *Soil gas and related methods for natural resource exploration*. Chichester, John Wiley & Sons, 483 p.

SAUNDERS, D.F., BURSON, K.R., &. THOMPSON, C.K., 1999. Model for hydrocarbon microseepage and related near-surface alterations: *AAPG Bulletin*, **83**, 170-185.

SCHUMACHER, D. 1996. Hydrocarbon-induced alteration of soils and sediments. In: SCHUMACHER, D. & ABRAMS, M.A. (eds.), *Hydrocarbon migration and its near-surface expression: AAPG Memoir,* **66**, 71-89.

SEGAL, D.B., RUTH, M.D., & MERIN, I.S. 1986. Remote detection of anomalous mineralogy associated with hydrocarbon production, Lisbon Valley, Utah. *The Mountain Geologist*, **23** (2), 51-62.

Aqueous geochemistry of Pit Lake at EL mine site, Manitoba, Canada: Implications for site remediation.

Nikolay V. Sidenko[1], Donald Harron[1], Karen H. Mathers[1], & J. Michael McKernan[1]

[1]*TetrES Consultants Inc., 603-386 Broadway, Winnipeg, MB, R3C 3R6 CANADA*
(e-mail: nsidenko@tetres.ca)

ABSTRACT: Geochemistry of the Pit Lake was studied to understand processes controlling migration of metals in order to make recommendations for rehabilitations of EL – mine site, Lynn Lake Manitoba. After the closure of Cu-Ni EL Mine in 1963, the former open pit and the shaft were apparently connected (by blasting the crown pillar). Subsequent flooding of the former shaft caused the formation of Pit Lake. Pit Lake was found to be meromictic with a thermocline and a chemocline coinciding at depth of ~20 m, where former open pit was connected to the shaft. The mixolimnion (0-20m) has lower pH (~5) and higher concentrations of Al, Cu and Zn, but lower concentrations of Ni, Fe and major ions in comparison with the monimolimnion (20-130 m). The chemistry of mixolimnion appears to be controlled by acidic runoff and seepage from the overburden. Within the monimolimnion, slow processes of neutralization and metal attenuation dominate over acid generation and release of metals. The monimolimnion of Pit Lake can therefore be considered as having potential for serving as a long-term repository for different sulfide wastes occurring around Lynn Lake.

KEYWORDS: *open pit lakes, metal leaching, mine waste, rehabilitation*

INTRODUCTION

Environmental assessments of open-pit mines include an understanding of geochemical processes, which control production of acidity and migration of metals (Davis & Ashenberg 1998, MEND 1991).

The El Mine site was located 3.5 km south of the Town of Lynn Lake, Manitoba (Fig. 1). The mine was operated between 1954 and 1963 using open pit and underground mining techniques. Copper-nickel ore was associated with gabbro, pyroxenites and peridotites. At mine closure, a crown pillar was apparently blasted, connecting the underground workings to the open pit. The workings and the pit started to flood in 1976 forming Pit Lake. Pit Lake was surrounded by piles of overburden in order to divert water from the open pit during the mining (Fig. 1). The overburden contains fragments of sulfides and has negative net neutralization potential, which causes acid generation and metal leaching (TetrES 2009).

The objective of this study was to understand the geochemistry of the Pit Lake in order to recommend effective options for site remediation.

METHODS

Bathymetry of Pit lake was studied using sonar. Sampling of the water column was preformed with a Kemmerer sampler on August 18 and September 20, 2008. Temperature, pH, redox potential and conductivity were measured immediately after sampling using meters calibrated against standard solutions. Samples were field filtered through 0.45 mm filter and divided into two aliquots, for analyses of metals and major ions. The aliquot for metals was preserved with nitric acid to pH<2. All samples were kept at temperature near 4^{o}C until delivered and analyzed by ALS laboratory, Winnipeg. Saturation indexes were calculated using the WATEQ4f computer program (Ball & Nordstrom 1999). The activities of the Fe redox couple were calculated from measured Eh.

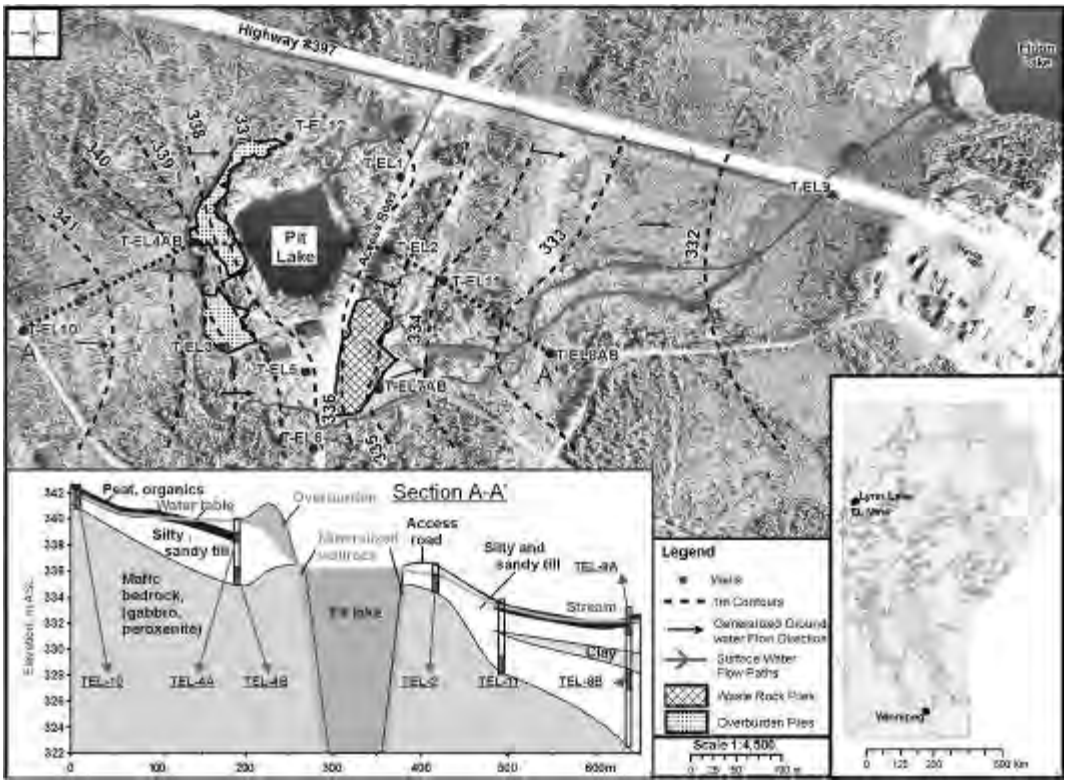

Fig. 1. Surface- and groundwater flows at former EL mine, Lynn Lake, Manitoba.

RESULTS AND DISCUSSION

Bathymetry shows that the shape of Pit Lake resembles of a funnel with the an upper surface diameter of ~110 m and the diameter of the "neck" of ~50 m. The depth from the surface of the lake to the "funnel neck" is approximately ~20 m (the approximate position of the former crown pillar) and the total depth of the lake is ~130 m. Lake outflow is controlled by a culvert at elevation 236.4 m above sea level. Field investigation indicates that the lake is fed by surface runoff and seepage of groundwater through the overburden and fractured walls of the pit (Fig. 1).

Depth profiles of physical and chemical properties of Pit Lake indicate that the lake is divided into two zones with a boundary at the depth at ~20 m. The upper zone (mixolimnion) is characterized by variable temperature, redox and pH compared to lower zone (Figure 2). Lower zone (monimolimnion) is anoxic, and has relatively stable temperature, redox conditions and pH. Concentrations of total dissolved solids (TDS) increase with depth and have an inflection point near the boundary between the zones (~20 m). Calculations of water density from different temperature and TDS across water column indicate that the lake does not have a complete turnover. Therefore, the lake can be classified as meromictic with a thermocline and a chemocline coinciding at the depth ~20 m, which are controlled by the morphology of the lake.

Concentrations of major ions (Ca, Mg, K, Na sulfate and bicarbonate) are similar to profile of TDS and increase with depth (Fig, 2). Iron concentrations sharply increase near the thermocline and remain constant below, indicating anoxic conditions at the monimolimnion, deeper than 20 m (Fig. 2). Thermodynamic calculation shows that the water column is close to ferrihydrite saturation indicating that redox conditions in Pit Lake are likely controlled by $Fe^{2+}/Fe(OH)_3$ couple (Fig. 3).

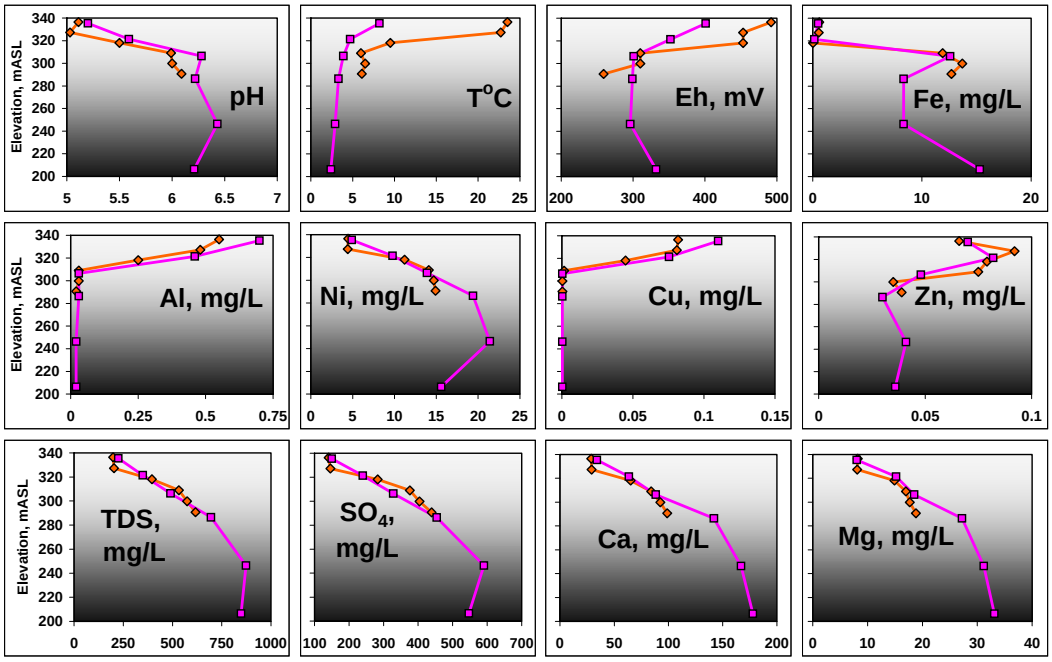

Fig. 2. Depth profiles of physical and chemical parameters in Pit Lake, August (diamonds) and September (boxes).

Aluminum concentrations are greater in the mixolimnion and negatively correlate with pH. Pit Lake is slightly supersaturated with respect to amorphous Al-hydroxide (Fig. 3). This fact indicates that concentrations of aluminum appears to be controlled by the solubility of $Al(OH)_3$, which is pH-sensitive. Concentrations of Ni are four times lower in the upper zone of the lake than in the lower zone. By contrast, significantly more Cu and Zn are found in the mixolimnion compared with the monimolimnion. Such distinction in the behaviour of elements that originated from the oxidizing sulfides can be explained by different rates of metal release or attenuation in two zones of the lake. The lower zone (monimolimnion) likely represents the chemistry of Pit Lake after the flooding of EL mine, with some later changes associated with adsorption of metals onto the Fe-hydroxides and neutralization resulting from dissolution of Ca and Mg pyroxenes, amphiboles and basic pagioclase (Jambor 2003). Metal affinity for Fe-hydroxides decreases in the order Cu>Zn>Ni (Walton-Day 2003). Therefore, Cu and Zn were likely more easily scavenged from solution than Ni in the monimolimnion. The upper zone (mixolimnion) receives acidic runoff and seepage from the overburden, which lower pH and causes Cu, Zn and Al to be more mobile than in the lower zone. The mixolimnion was diluted with respect to Ni since Pit Lake was formed.

CONCLUSIONS

(1) Pit lake at the former El Mine is a meromictic lake with a thermocline and a chemocline coinciding at the depth ~20 m, where former open pit was connected to the shaft.

(2) The chemistry of mixolimnion (0-20m) appears to be controlled by acidic runoff and seepage from the overburden, which contains fragments of sulfide minerals.

(3) Below the chemocline, slow processes of neutralization and metal attenuation dominate over generation of acid and release of metals. Pit Lake, can therefore be considered as a potential long-term repository for different sulfide wastes occurring around the site and the town of Lynn Lake.

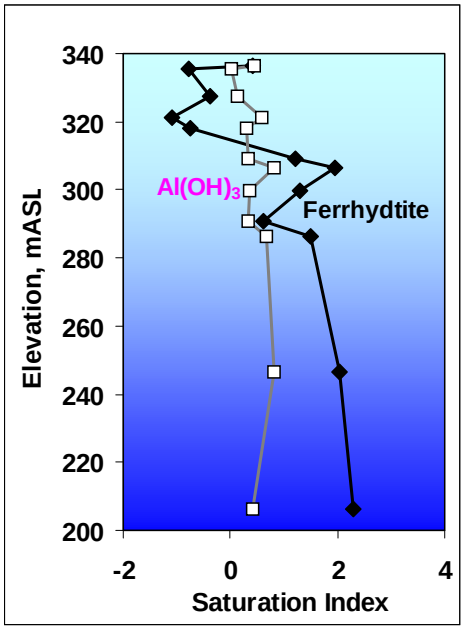

Fig. 3. Saturation indices of Fe (diamonds) and Al (boxes) and hydroxides in Pit Lake.

ACKNOWLEDGEMENTS

This study was funded by Division of Science, Technology Energy and Mines of Manitoba Province.

REFERENCES

BALL, J.W. & NORDSTROM, D.K. 1991. User's manual for WATEQ4f, with revised thermodynamic data base and test cases for calculating speciation of major, trace, and redox elements in natural waters. *US. Geological Survey Open-File Report* **91-183**.

DAVID, A. & ASHENBERG, D. 1988. The aqueous geochemistry of Berkly Pit, Butte, Montana, USA. *Applied Geochemistry, **4**, 23-36.*

JAMBOR, J.L. 2003. Mine waste mineralogy and mineralogical perspectives of acid-base accounting. In JAMBOR, J.L., BLOWES, D.W., & RITCHIE, A.M.I. (eds.), *Environmental aspects of mine waste, Mineralogical Association of Canada Short Course*, **31**, 117-147.

MEND 1995. Review of in-pit disposal practices for the prevention of acid drainage – case studies. *MEND Report **2.36.1**.*

TETRES CONSULTANTS INC. 2009. *Environmental Site Assessment for EL-Mine Site, Lynn Lake, Manitoba.* Report to Manitoba Mines Branch, Winnipeg.

WALTON-DAY, K. 2003. Passive and active treatment of mine drainage. In: JAMBOR, J.L., BLOWES, D.W., RITCHIE, & A.M.I. (eds.), *Environmental aspects of mine waste, Mineralogical Association of Canada Short Course*, **31**, 117-147.

The case for logratio based grain-size normalization of sediment

Robert C. Szava-Kovats[1]
[1]*Inst. Of Ecology and Earth Sciences, University of Tartu, Lai 40, Tartu, 51005 ESTONIA*
(e-mail: robszav@ut.ee)

ABSTRACT: Normalization of sediment is performed to mitigate the confounding effects of grain-size and mineralogical differences on the distribution of contaminants, such as heavy metals. Normalization has typically entailed linear regression analysis of a contaminant by a normalizing agent, either an element or compound. This method fails to recognize the inherent risk of statistical analysis of "raw" compositional data. Reanalysis of published data with a multivariate log-ratio approach reveals that the assumption that the normalizing agent maintains a linear relationship with clay content is nebulous. Furthermore, relationships between contaminants and normalizing agents are likely confounded by spurious correlation with other components. Therefore, the traditional approach to normalization is suspect and may lead to erroneous interpretations. Log-ratio methods are recommended.

KEYWORDS: *grain-size, normalization, compositional data, trends, principal component analysis*

INTRODUCTION

The ability of sediments to adsorb contaminants makes sediment analysis an effective tool with which to assess and monitor contamination in marine environments. This ability is largely a joint function of grain-size distribution and mineralogy. Normalization is a common approach to compensate for grain-size and mineralogical differences in sediment (Horowitz 1991). Normalization often entails regression analysis of a contaminant against a 'conservative' element, (e.g. Al, Li, Fe) – one thought to represent the clay-sized fraction and/or presumed to have no anthropogenic input – or some other compound, such as organic carbon. The normalizing agent is usually selected based on the strength of the correlation with the contaminant (e.g. Aloupi & Angelidis 2001).

This approach, however, fails to consider the inherent nature of 'compositional data', i.e. all components are restricted to positive values with the sum of all components totalling 100%. These restrictions make suspect statistical analysis based on "raw", untransformed data. Log-ratio transformations, developed by Aitchison (1982), rid compositional data of these constraints and allow statistical analysis within Euclidean space.

We examine grain-size normalization by means of multivariate log-ratio techniques. Specifically, published data are reanalyzed to explore the relationship between normalizing agents and grain-size composition, and to compare the log-ratio method with the traditional approach of heavy metal normalization.

DATA SOURCES

The data for this reanalysis comes directly or has been derived from two published studies of marine sediments: the Gulf of Trieste (Covelli & Fontolan 1997) and the Aegean Sea (Aloupi & Angelidis 2001). The former study provides grain-size data and measurements of Al_2O_3, Fe_2O_3, CaO, MgO, as well as total and organic carbon, from which non-organic carbon – expressed as CO_2 – was calculated. The latter study provides potential normalizing agents: $CaCO_3$, organic C, Al_2O_3, Fe_2O_3, Mn, and Li, and heavy metal concentrations, of which we examine Zn. Both datasets also contain a component, "other", the remainder of the composition. Instrumental analysis for major elements in both studies was preceded by a so-

called "total" (hydrofluoric-nitric-perchloric-hydrochloric) digestion.

MATHEMATICAL METHODS

The constraints on compositional data create induced correlations on the components in a composition: a change in the value of any component must be compensated by corresponding changes in other components. However, log-ratio transformation rids compositional data of these constraints, thus enabling components to vary independently. For a detailed description, readers are referred to Aitchison (1982) or Buccianti *et al.* (2006).

Grain-size and geochemical trends in this reanalysis were calculated from the first component derived from a Principal Component Analysis (PCA) of covariance matrices resulting from *centered log-ratio* transformation (van Eynatten 2004; Szava-Kovats 2008). Given a *d*-part composition, $\boldsymbol{x}=[x_1, \ldots, x_d]$, the log-ratio transformation to composition $\boldsymbol{y}$ is

$$y_n = \ln (x_n/x_G) \quad n = 1, \ldots, d \qquad (1)$$

where x_G is the geometric mean of the *d* components of $\boldsymbol{x}$. The retransformation from $\boldsymbol{y}$ to $\boldsymbol{x}$ is

$$x_n = \exp(y_n)/\sum[\exp(y_1), \ldots,\exp(y_n)] \qquad (2)$$

The first PC provides a set of *d*-dimensional loadings, which can be transformed by *(2)* into a compositional data array, $\boldsymbol{L}$, and a PC score, *S*, for each $\boldsymbol{y}$. The first PC expressed as compositional data is calculated by the perturbation operation

$$\boldsymbol{x} = C[g_1 L_1^S, \ldots , g_d L_d^S] \qquad (3)$$

where *g* is the geometric mean for a given component and *C* is the closure operation to sum to 100%. The compositional trends of each component of the first PC is calculated from *(3)* as a continuous function of *S*. The percentage of the total variance expressed by the first PC is a measure of goodness-of-fit.

GRAIN-SIZE TRENDS (GULF OF TRIESTE)

The fist PC accounts for 83.6% of the total variability. Linear log-ratio analysis often features markedly non-linear trends when transformed into compositional data (Fig. 1). As the clay content increases from 0, the trend reveals a rapid decline in sand, compensated largely by an increase in the silt fraction. Once the clay content approaches 40%, the sand content becomes exhausted and the silt fraction then begins to decrease with increasing clay. The log-ratio approach realistically models a theoretical transition from a high to low-energy environment (Szava-Kovats 2008). The chemical composition trend sees Al_2O_3 and Fe_2O_3 increasing concurrently with increasing clay content, whereas CaO, MgO and CO_2 exhibit a similar decrease. Organic C displays a slight increase and "other" – dominated by SiO_2 and alkali metals – shows an initial rise followed by a decline.

This set of chemical trends suggests carbonates dominate the coarser fractions and Al-silicates dominate the finer grained fractions. However, the Al-Fe trend is non-linear, which, combined with the decline in "other", suggests replacement of coarser-grained Al-silicates by clay minerals with increasing clay. Because clay minerals have surface areas orders of magnitude greater than silt or sand, the absorption potential of sediment is governed largely by clay content. Thus, a normalizing agent, such as Al, may not necessarily reflect the true absorption capacity. In this example, not only is the trend non-linear, but sediment with very little clay contains considerable amounts of Al.

ZN NORMALIZATION (AEGEAN SEA)

The authors of this study divided their dataset into harbour and offshore sediments, assuming that the latter are contaminant-free, and used Li as the normalizing agent. All samples were compared to the regression equation based on the offshore sediments, which indicated considerable Zn contamination – with some samples >3 times background

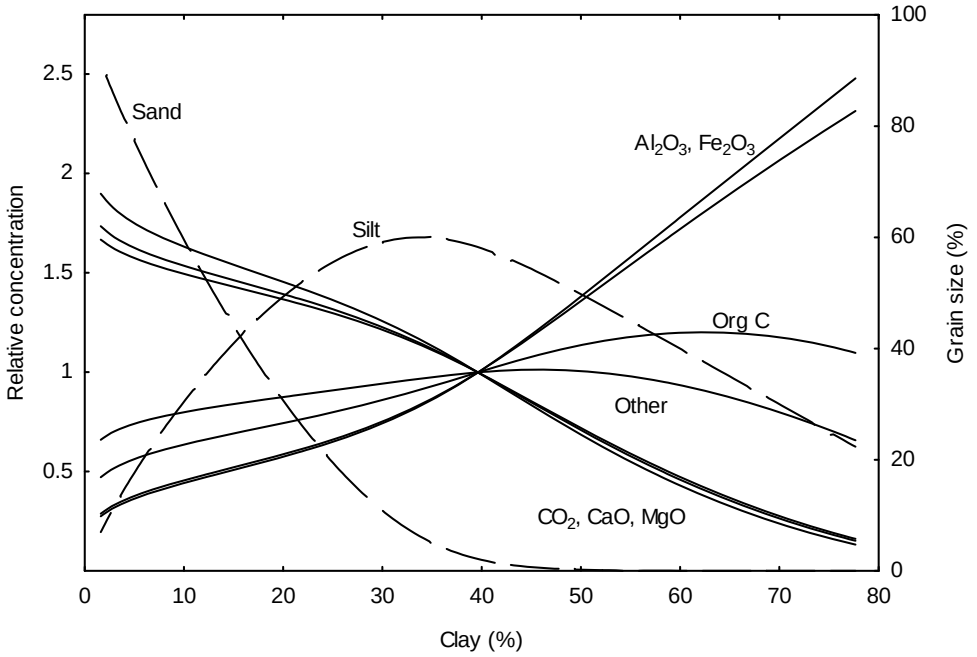

Fig. 1. Log-ratio-based normalization trends for Gulf of Trieste sediments. Grain-size fractions measured in %, chemical components scaled to relative abundance.

concentration – in most of the harbour samples (Fig. 2). Analysis of the complete dataset results in a significantly different regression fit and subsequently a vastly different interpretation.

Normalization was performed with the log-ratio method on both the entire dataset and the offshore subset. Biplots of the factor loadings show little difference between the two analyses (Fig. 3). The first PC accounts for no less than 75% of the variance and the loadings of the individual components are similar. Although the original study was based on Li normalization, the log-ratio PCA suggests greater affinity of Zn with organic C. More importantly, the similarity of the two sets of factor loadings indicates that the relationship among Zn and the other components changes little by limiting the analysis to offshore samples. In other words, the only genuine difference among the two datasets is the location of central tendency, and that the visual distinction between harbour and offshore samples in the Zn-Li scatterplot is largely an artefact of the effects of other components.

Log-ratio analysis reveals that, although the harbour samples display elevated Zn content, the degree of enrichment is considerably lower than suggested by the traditional regression method. The log-ratio analysis calculates the enrichment

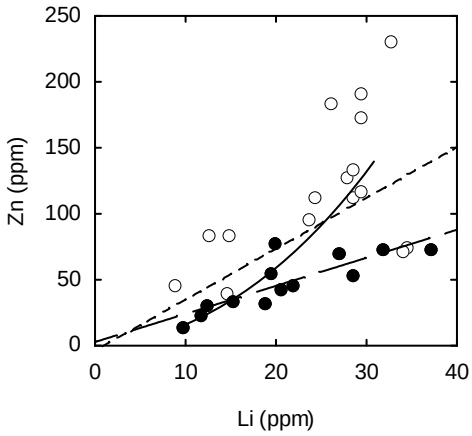

Fig. 2. Scatterplot of Zn and Li for Aegean Sea sediments. Open circles, harbour samples; full circles, offshore samples. Short dashed trend, regression for complete dataset; long dashed trend, regression for offshore samples; solid trend, log-ratio trend for all samples.

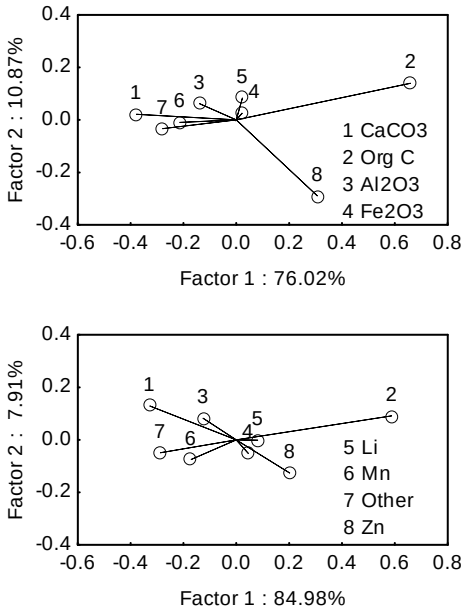

Fig. 3. Biplots of log-ratio factor loading for Aegean Sea sediments. Upper plot, complete dataset; lower plot, offshore samples. Percentages indicate variance accounted for by factor.

in the harbour samples as averaging about 40% greater than the offshore samples, whereas the traditional approach suggest the harbour samples average twice the background.

CONCLUSIONS

The traditional approach to grain-size normalization – simple linear regression of "raw" data – is likely to result in dubious interpretation:
(1) the normalizing agent and the clay content in sediment is unlikely to have a linear relationship,
(2) the relationship between potential contaminants and normalizing agents can be confounded by other, unaccounted for components,
(3) a log-ratio approach is recommended for grain-size normalization.

ACKNOWLEDGEMENTS

This research was funded by Estonian Science Foundation Grant no. 7016.

REFERENCES

AITCHISON, J. 1982. The statistical analysis of compositional data. *Journal of the Royal Statistical Society*, **44**, 139-177.

ALOUPI, M. & ANGELIDIS, M.O. 2001. Geochemistry of natural and anthropogenic metals in the coastal sediments of the island of Lesvos, Aegean Sea. *Environmental Pollution*, **113**, 211-219.

BUCCIANTI, A., MATEU-FIGUERAS, G., & PAWLOWSKY-GLAHN, V. (eds.). 2006. *Compositional data analysis in the geosciences: from theory to practice*. Geological Society, London.

COVELLI, S. & FONTOLAN, G. 1997. Application of a normalization procedure in determining regional geochemical baselines. *Environmental Geology*, **30**, 34-45.

HOROWITZ, A.J. 1991. *A primer on Sediment – trace element chemistry.* Lewis Publishers Ltd., Chelsea, MI.

SZAVA-KOVATS, R.C. 2008. Grain-size normalization as a tool to assess contanination in marine sediments: Is the <63 µm fraction fine enough? *Marine Pollution Bulletin*, **56**, 629-632.

VAN EYNATTEN, H. 2004. Statistical modelling of compositional trends in sediments. *Sedimentary Geology*, **171**, 79-89.

Sponsors

Symposium bags sponsor

ACME Analytical Laboratories Ltd.

Platinum sponsors

SGS

Anglo American

Gold sponsors

AREVA

Newmont – The Gold Company

Barrick

TGI3 Canada

Canada

Silver Standard

maxwell DATASHED

Actlabs

FREEWEST – Freewest Resources Canada Inc.

Silver sponsors

ODM – Exploring Heavy Minerals

Thermo Scientific

Innov-X Systems – Innovative XRF Technologies

APEGNB / APEGNB

OZ

xstrata zinc

Adex

Bronze sponsors

PotashCorp – Helping Nature Provide

International Association of Geochemistry – IAGC – Est. 1962

New Nouveau Brunswick – Natural Resources and Energy

Department of Geology, University of New Brunswick

IAG